The Binding Behavior of Daptomycin on the Bacterial Membranes

Dissertation

zur

Erlangung des Doktorgrades (Dr. rer. nat.)

der

Mathematisch-Naturwissenschaftlichen Fakultät

der

Universität Bonn

vorgelegt von

Xinliang Liu

aus

Shandong, P. R. China

Bonn 2018

Angefertigt mit der Genehmigung der Mathematisch-Naturwissenschaftlichen
Fakultät der Rheinischen Friedrich-Wilhelms-Universität Bonn

1 Gutachter: Prof. Dr. Ulrich Kubitscheck
2 Gutachter: Prof. Dr. Hans-Georg Sahl
Tag der Promotion: 06. July 2018
Erscheinungsjahr: 2018

Acknowledgments

This dissertation would not have been possible without many remarkable people.

First and foremost, I would like to express my sincere gratitude to my supervisor, Prof. Ulrich Kubitscheck for giving me the opportunity to pursue my dream of a Ph.D., for his continuous help and support, for having always encouraged me and maintained confidence in me. It was really difficult for me to know where to start, he guided me in building the idea from a blur picture to a focused one. I must admit that for many times I have put his patience to the test, but he has been constantly available to me for advice and suggestions. Ulrich's patience, enthusiasm, tremendous scientific interest have always guided my studies at Bonn. I am truly grateful to be Ulrich's student.

I would like to express my appreciation to Dr. Katharina Scherer. My gratefulness is beyond expression for her. She played a key role in conducting my measurements and coordinating the whole project. She has always been there every time I needed help both in the lab and in my life. Without her generosity in sharing her ideas and resources, this project might not have come to fruition.

I would like to express thanks to Prof. Dr. Hans-Georg Sahl and his research group, especially Dr. Fabian Grein for generously providing bacteria, antibiotics and valuable encouragement and discussions on my results.

I would like to thank Dr. Jan Peter Siebrasse for inspiring suggestions during the meetings and providing help throughout my studies.

I would like to thank all my present and former colleagues for their help in the lab and letting me enjoy my time there. Special thank to our former group member Dr. Jan-Hendrik Spille who taught me the methods of super-resolution imaging.

I am grateful to Prof. Dr. Hanns Häberlein and Dr. Thomas Sorkalla for helping me with the FCS measurements and all the discussions on the results.

I would like to thank Abonl Goel for reading through my thesis and checking the grammer.

My sincere thanks also go to CSC (Chinese Scholarship Council) for its financial support.

Last but not least, I would like to express my gratitude to my parents and my sister for supporting me spiritually throughout my study in Germany and my life in general. A very special thanks to my girlfriend Xiaoqi, thanks for being with me all these years.

Author's Declaration

I hereby declare that the work submitted here is the result of my own investigation. Furthermore, I have not used anything other than the resources and sources stated and where I have taken sections from these works in terms of content or text, I have identified this appropriately.

Bonn, 9th May 2018

_____

Xinliang Liu

Abstract

Daptomycin (DAP) is a cyclic anionic lipopeptide antibiotic that kills gram-positive bacteria via cell membrane distortion. It is currently approved for treatment of complicated infections caused by gram-positive bacteria, including methicillin-resistant *Staphylococcus aureus*, vancomycin-resistant *S. aureus*, coagulase-negative *staphylococci*, penicillin-resistant *streptococci* and vancomycin-resistant enterococci. Recent studies showed that the bactericidal activity of DAP on the target membrane is dependent on Ca^{2+}. DAP is also associated with membrane depolarization in the presence of phosphatidylglycerol (PG). Therefore, in this study, we aimed to investigate the binding behavior of DAP on the membrane of *S. aureus* cells as well as the specific interaction of DAP with target molecules.

We first used highly inclined and laminated optical sheet (HILO) microscopy to visualize DAP location on the membrane of *S. aureus* cells. Then, we quantitatively analyzed DAP distribution on *S. aureus* cell membranes and its correlation with cell size and aggregate formation in a time- and concentration-dependent manner. We observed septum binding for the concentrations lower than the minimum inhibitory concentration (MIC) of DAP and for the concentration around the MIC until 10 min of incubation. However, overall membrane binding of DAP occurred at longer incubation times and higher DAP concentrations. This result was further supported by the super-resolution imaging of the localization of single DAP molecules on the membrane of *S. aureus*. We found that DAP accumulation correlated negatively with cell size but positively with aggregate formation.

Thus, we further examined the colocalization of 5(6)-TAMRA-X, SE-labeled DAP (DAP-TMR) with the FtsW-GFP fusion protein and lipid II. FtsW is a bacterial cell division protein, which is positioned at the septum. For the short incubation interval, DAP-TMR localized to the septum and was colocalized with FtsW-GFP. For incubation times, DAP bound to the complete cell membrane but the distribution of FtsW-GFP remained unaffected. Furthermore, in cells stained with a BODIPY FL conjugate of vancomycin (Van-BDP FL), considerably less binding of DAP-TMR occurred, indicating that Van-BDP FL prevented the binding of DAP and that lipid II might be the target molecule of DAP.

Finally, we used fluid supported lipid bilayers to study the binding behavior of DAP on membranes with different lipid compositions. Bilayers were prepared on coverslips by vesicle fusion. The neutral phosphatidylcholine phospholipids were used as the matrix to which PG or/and bactoprenol lipids (C_{55}-PP, C_{55}-P, lipid II) were added. PG as well as the three bactoprenol lipids enhanced the binding of DAP. Surprisingly, addition of PG in bactoprenol-containing membranes significantly strengthened DAP binding, indicating that the bactoprenol lipids affect the binding of DAP and that the combination of PG and bactoprenol lipids is critical for the bactericidal mechanism of DAP. This explains the preferential binding of DAP to the septum. Our findings describe a new model for the mechanism of action of DAP.

Keywords: Daptomycin; fluorescence microscopy; septum binding; colocalization; DOPC bilayers; bactoprenol lipids

Table of Contents

List of Figures

List of Abbreviations

℃	Degree centigrade
µL	Micro liter
µg/L	Microgram per liter
µM	Micromoles per liter
alanyl-PG	APG
arginyl-PG	ArPG
cationic antimicrobial peptides	CAMPs
calcium- dependent antibiotic	CDA
cytidine diphosphate	CDP
circular dichroism spectroscopy	CD spectroscopy
cardiolipin	CL
undecaprenol-phosphate	C_{55}-P
undecaprenyl pyrophosphate	C_{55}-PP
diacylglycerol	DAG
daptomycin	DAP
daptomycin-resistance	DAPr
diacylglyceryl-N,N,N- trimethylhomoserine	DGTS
dimethylformamide	DMF
1, 2-dioleoyl-sn-glycero-3-phosphocholine	DOPC
1,2-di-(9Z-octadecenoyl)-sn-glycero-3-phospho-(1'-rac-glycerol)	DOPG
electron-multiplying charge-coupled device	EMCCD
European Medicines Agency	EMEA
United States Food and Drug Administration	FDA
fluorescence correlation spectroscopy	FCS

fluorescence ratio	FR
green fluorescent protein	GFP
N-acetylglucosamine	GlcNAc
glycophospholipids	GPLs
hetero-VISA	hVISA
highly inclined and laminated optical sheet	Hilo
L-kynurenine	Kyn
lysyl-phosphatidylglycerol	LPG
lipopolysaccharide	LPS
lipoteichoic acid	LTA
minimal inhibitory concentration	MIC
multiple peptide resistance factor	mprF
methicillin-resistant *S. aureus*	MRSA
methicillin-susceptible *S. aureus*	MSSA
N-acetylmuramic adid	MurNAc
numerical aperture	NA
nuclear magnetic resonance	NMR
non-ribosomal peptide synthetases	NRPSs
ornithine lipids	OLs
penicillin-binding proteins	PBPs
phosphatidylcholine	PC
phosphatidyl-(N,N)-dimethylethanolamine	PDME
phosphatidylethanolamine	PE
phosphoenolpyruvate	PEP
phosphatidylglycerol	PG
peptidoglycan	PGN

phosphatidyl-(N)-methylethanolamine	PME
phosphatidylserine	PS
regions of increased fluidity	RIFs
region of interest	ROI
Staphylococcus aureus	*S. aureus*
sulfonolipids, or sphingolipids	SLs
transmission electron microscopy	TEM
total internal reflection fluorescent microscopy	TIRF
uridine diphosphate	UDP
UDP-N-acetylglucosamine	UDP-GlcNAc
UDP-N-acetylmuramyl-pentapeptide	UDP-MurNAc-pentapeptide
universal point accumulation imaging in the nanoscale topography	uPAINT
undecaprenyl pyrophosphate phosphatase	UppP
undecaprenyl pyrophosphate synthase	UppS
vancomycin-intermediate *S. aureus*	VISA
vancomycin-resistant enterococci	VRE
vancomycin-resistant *S. aureus*	VRSA

1. Introduction

1.1 A brief history of antibiotics

The field of antibiotics has been explored extensively in academia and presented many breakthroughs as well as difficulties in the global evolutionary and human history scales [1]. The discovery and use of antibiotics were turning points that revolutionized medicine in many respects, thereby saving countless human lives and enabling spectacular successes in genetic engineering, molecular biology, and other sequencing-related fields. .

The concept of a "magic bullet", which could selectively target only the disease-causing microbes but not its host, was first introduced by P. Ehrlich around 1900. Following this concept, the anti-syphilis drug salvarsan (arsphenamine) was discovered via a systematic screening program in 1909. Later, in the early 1930s, the first sulfonamide drug named prontosil (sulfamidochrysoidine) was discovered and used clinically to treat a wide range of bacteria [2]. At the same time, penicillin was discovered by A. Fleming in 1929, and its clinical use began in the early 1940s [3]. In the meantime, "antibiotic" was first used as a noun by S. Waksman in 1941 to describe any small molecule produced by a microbe that antagonizes the growth of other microbes [4]. Thus, the discovery of these first three antimicrobials, salvarsan, prontosil, and penicillin, marked the beginning of the antibiotic era, and was followed by the discovery of several new antibiotics in the 1950s. The period in the succeeding 10-15 years was indeed the golden era of discovery and medicinal use of novel antibiotics [5]. Human beings derived countless benefits from these antibiotics in the treatment and control of infectious, neoplastic, and viral diseases.

1.2 Bacterial membrane components

Bacterial cell membranes, which not only surround and protect the cytoplasm but also play a key role in bacterial cell structure, have been well studied since the 1950s [6]. Bacterial membranes are structurally similar to eukaryotic cell membranes, except that bacterial membranes consist of saturated or monounsaturated fatty acids and usually do not contain sterols. Bacterial membrane composition varies with the

bacterial species, and also changes in response to environmental factors, such as temperature, pH, salinity, and osmolarity [7,8].

The major lipid components identified and studied are diacyl-based glycerophospholipids containing two fatty acids and variable heads, such as phosphatidylethanolamine (PE), phosphatidylglycerol (PG), phosphatidylcholine (PC), cardiolipin (CL), lysyl-phosphatidylglycerol (LPG) and phosphatidylserine (PS) [9]. In some bacteria, phosphatidyl-(N)-methylethanolamine (PME) and phosphatidyl-(N, N)-dimethylethanolamine (PDME) act as intermediates during PC synthesis [10,11]. PG has been demonstrated as the second most plentiful lipid and has an essential function in bacterial membranes [9]. The head group of PG can be modified by transfer of amino acids to form LPG, alanyl-PG (APG) or arginyl-PG (ArPG) [12,13]. Most of the modified PGs have been reported in gram-positive bacteria, including *Staphylococcus aureus*, *Listeria monocytogenes*, *Lactococcus plantarum* and *Bacillus subtilis* [14,15,16], and a few modified PGs have been reported in some gram-negative bacteria such as *Rhizobium tropici* and *Pseudomonas aeruginosa* [17,18,19]. PS is rarely found in bacterial membranes, as it is an intermediate in PE biosynthesis [20,21]. Generally, PE, PG and CL comprise a large portion of the bacterial membrane phospholipids. *Escherichia coli*, the standard model used for studying bacterial membrane lipids, contains these three major phospholipids in its cell membrane: 70-80% PE, 20-25% PG, and 5% CL [22].

In addition to these main membrane lipids, other varieties of lipids are synthesized by different types of bacteria. For instance, some bacteria contain membrane lipids that lack the phosphate group but contain the diacylglycerol (DAG) backbone, such as diacylglyceryl-N,N,N-trimethyl-homoserine (DGTS) [23,24], and glycophospholipids (GPLs) [25]. Some bacteria contain bacterial membrane lipids without a DAG backbone, such as ornithine lipids (OLs), sulfonolipids, or sphingolipids (SLs) [26,27,28]. Although the synthesis pathways or locations of these membranes are different, they serve different but equally important functions.

Bacteria are classified into two major categories based on the structural differences in their cell walls via a special technique called Gram staining, devised by the Danish bacteriologist H. C. J. Gram in 1884 [29]. In this technique, the staining characteristics of bacteria are denoted as positive or negative, depending on whether the bacteria

retain the stain when observed under a microscope. Here, bacteria are stained with the crystal (or gentian) violet dye, washed with a decolorizing solution, and counterstained with safranin or fuchsine. Bacteria that retain the crystal violet dye are called gram-positive bacteria, whereas the ones that do not retain crystal violet and are stained red or pink are classified as gram-negative bacteria [29]. This property of stain retention is associated with the outer layer of bacterial cells. Gram-positive bacteria do not have an outer cell membrane but have a thick layer of peptidoglycan (PGN), which absorbs the Gram stain. In contrast, gram-negative bacteria possess an outer membrane and cannot retain the crystal violet stain after the decolorization step; alcohol used in this stage degrades their outer membrane making the cell wall more porous and incapable of retaining the crystal violet stain. Furthermore, their PGN layer is considerably thinner and is sandwiched between an inner cell membrane and the outer membrane, causing them to take up the counterstain (safranin or fuchsine) and appear red or pink. Despite their thicker PGN layer, gram-positive bacteria are more susceptible to antibiotics than gram-negative bacteria are, owing to the absence of the outer membrane.

Gram-positive bacteria differ from gram-negative bacteria in several ways. First, unlike gram-positive bacteria, gram-negative bacteria contain an outer membrane [30], gram-positive bacteria only possess a single lipid membrane (also called plasma membrane) surrounded by a cell wall composed of a thick layer of PGN and lipoteichoic acid (LTA) [31]. In some gram-negative bacteria, the PGN layer is considerably thicker than that generally present in other gram-negative bacteria, thus enabling them to withstand the turgor pressure exerted on the plasma membrane. Bacterial cell membranes are composed of 40 % phospholipid and 60 % protein. As gram-positive bacteria lack the outer membrane to hold extracellular proteins, all these structural and enzymatic proteins are present in or near the cell membrane; some proteins are embedded or inserted into the membrane, located on the membrane, or covalently attached to the PGN [32]. Thus, many different types of proteins are associated with the cell membrane.

Gram-negative bacteria are surrounded by two membranes, the inner membrane (also called plasma membrane) and the outer membrane. The inner and outer membranes differ in their phospholipid composition and organization [33]. The outer membrane,

present outside the rigid cell wall and composed of lipopolysaccharide (LPS), phospholipids, and proteins, is a distinguishing feature of gram-negative bacteria. It provides the bacterium with a hydrophilic surface, owing to the presence of LPS molecules. The LPS of a gram-negative bacterium is composed of three different parts: lipid-A, the core polysaccharide comprising the inner and the outer cores, and the O-specific polysaccharide chains projecting outward [34]. Several proteins are located in the outer membrane and are involved in several important functions, such as adherence, nutrient acquisition, signaling, and protection of cells from the environment [35,36]. Most of the outer membrane proteins can be divided into two classes, lipoproteins and β-barrel proteins [37]. Generally some porin proteins provide hydrophilic trans-membrane channels that enable the transport of small hydrophilic solutes through the outer membrane, whereas the outer membrane acts as a strong permeability barrier to macromolecules and hydrophobic compounds; therefore, gram-negative bacteria are relatively resistant to many antibiotics [38]. In addition, as a phospholipid bilayer, the lipid portion of the outer membrane is impermeable to charged molecules.

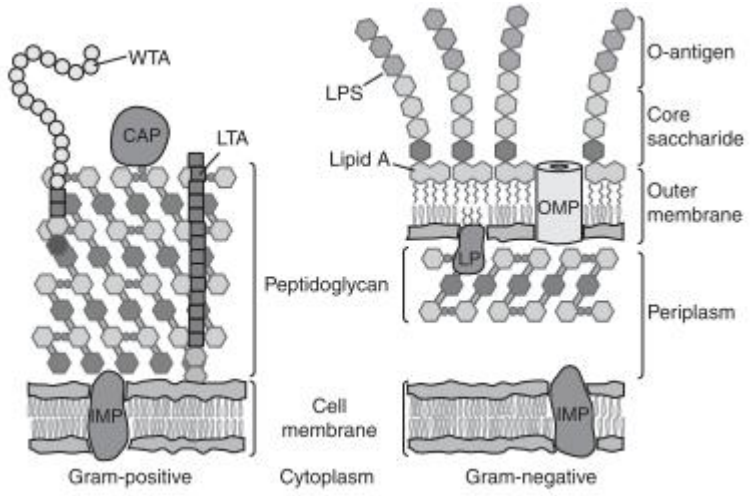

Figure 1: Differences in the cell membranes of gram-positive and gram-negative bacteria. Picture adopted from Silhavy et al. 2010 [39].

Fig. 1 shows the differences in the cell membranes of gram-positive and gram-negative bacteria. Both have a cell wall composed of peptidoglycan (PGN): in gram-positive bacteria, the wall is thick, whereas in gram-negative bacteria, the wall is thin. Moreover, an outer membrane containing lipopolysaccharides and lipoproteins surrounds the cell wall in gram-negative bacteria. Porins are cell membrane proteins

that allow transport of substances through the outer membrane of gram-negative bacteria. In gram-positive bacteria, LTA anchors the cell wall to the cell membrane.

Bacterial plasma membranes are critical structures that play vital roles in multiple cellular processes [40,41,42]. As hydrophobic films, they provide a physical barrier to separate the aqueous cytoplasm from the environment. They provide selective permeability to allow substrate uptake and product release. They also prevent the loss of essential interior compartments through leakage but allow the import and export of specific ions and molecules, to maintain a stable chemical environment required for the biological processes of the living cell. In addition, bacterial plasma membranes support several different crucial cell processes, including cell division, differentiation, protein secretion, and supplementary protein functions, and are the sites for synthesis of cell wall constituents. To understand their role in the formation of the cell wall constituents, it is essential to understand cell wall formation. As an example, the involvement of the plasma membrane in the synthesis of cell wall PGN in gram-positive bacteria has been briefly described in Fig. 2.

1.3 Bacterial cell wall biosynthesis

PGN, the major constituent of the bacterial cell wall, is composed of long glycan chains cross-linked by peptide bridges [43]. It forms a large elastic meshwork that covers the entire cell to provide the strength and rigidity to cell walls in both gram-positive and gram-negative bacteria. Thus, PGN serves to protect the cell from damage, bear the stress from the osmolarity of the cytoplasm, and maintain the characteristic cell shape. PGN biosynthesis is a multistep process containing three different stages, each involving a series of enzyme-catalyzed reactions (Fig. 2) [44,45]. Briefly, the first stage occurs in the cytoplasm and involves the synthesis of the soluble activated nucleotide precursor UDP-N-acetylmuramyl-pentapeptide (UDP-MurNAc-pentapeptide) and UDP-N-acetylglucosamine (UDP-GlcNAc) [46]. Here, the Mur ligases catalyze the synthesis of the peptide moiety [47]. The pentapeptide in this synthesized sugar-peptide moiety is critical for the cross-linking of fully modified strands in the final step [48]. In the second stage, two kinds of bactoprenol lipids, lipid I and lipid II, are synthesized on the cytoplasmic membrane. The phospho-MurNAc-pentapeptide moiety of UDP-MurNAc-pentapeptide is linked to the membrane anchor undecaprenyl-phosphate (C_{55}-P) by the translocase MraY, yielding lipid I (C_{55}-PP-

MurNAc-pentapeptide). Then, GlcNAc from UDP-GlcNAc is added to lipid I by the transferase MurG, resulting in the formation of lipid II (C_{55}-PP-GlcNAc-MurNAc-pentapeptide), which is the basic building block for direct formation of the cross-linked PGN in bacteria [45]. Once synthesized, lipid II is further modified and subsequently translocated across the cytoplasmic membrane with the help of a specific protein (translocase or flippase, such as FtsW) to the periplasm [49,50]. Thereafter, in the third and final stage of PGN biosynthesis, lipid II is incorporated into the polymerized disaccharide moieties to form a PGN network at the exterior surface of the cell [51,52]. This process is achieved mainly by the activity of penicillin-binding proteins (PBPs) and transglycosylation and transpeptidation reactions to form the glycosidic and peptide bonds of the PGN, respectively [53,54]. The lipid carrier, C_{55}-PP, is released by the transglycosylase reaction and then flipped back across the bacterial membrane after dephosphorylation to enter a new synthesis cycle (Fig. 2).

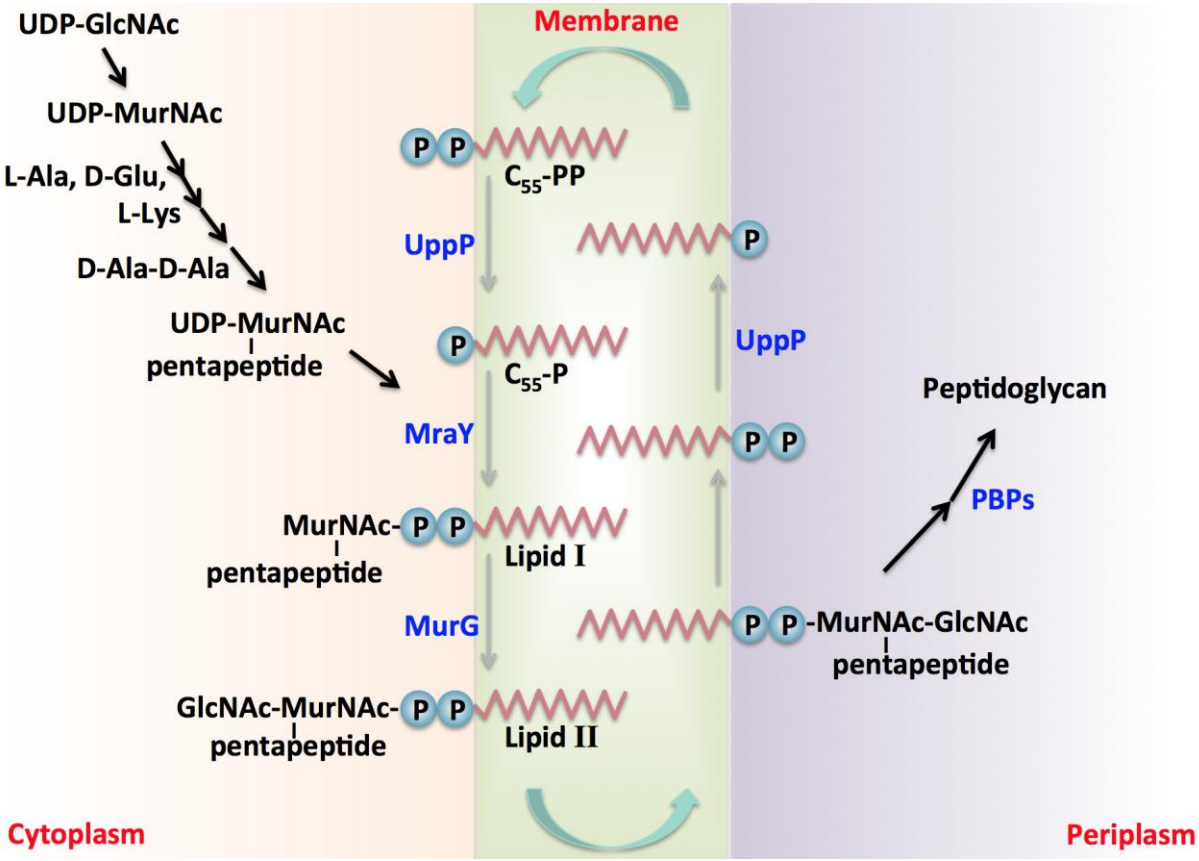

Figure 2: Schematic representation of peptidoglycan biosynthesis. Synthesis starts in the cytoplasm with the conversion of uridine diphosphate-N-acetylglucosamine (UDP-GlcNAc) to the final soluble precursor UDP-N-acetylmuramyl-pentapeptide (UDP-MurNAc-pentapeptide), catalyzed by the sequential action of enzymes. In the membrane-linked steps, lipid I and lipid II

are successively formed at the inner face of the membrane by MraY and MurG. Finally, lipid II is translocated across the membrane and incorporated in the growing peptidoglycan network through the activity of penicillin-binding proteins (PBPs). C_{55}-PP and C_{55}-P represent undecaprenyl pyrophosphate and undecaprenyl phosphate, respectively.

C_{55}-P, also called bactoprenol, is an important lipid in the cytoplasmic membrane. It plays a crucial role in PGN biosynthesis and is involved in the synthesis of other cell wall polymers [55,56,57]. Several pathways of the C_{55}-P metabolism via phosphatases and kinases have been demonstrated in bacteria (Fig. 3) [58,59,60].

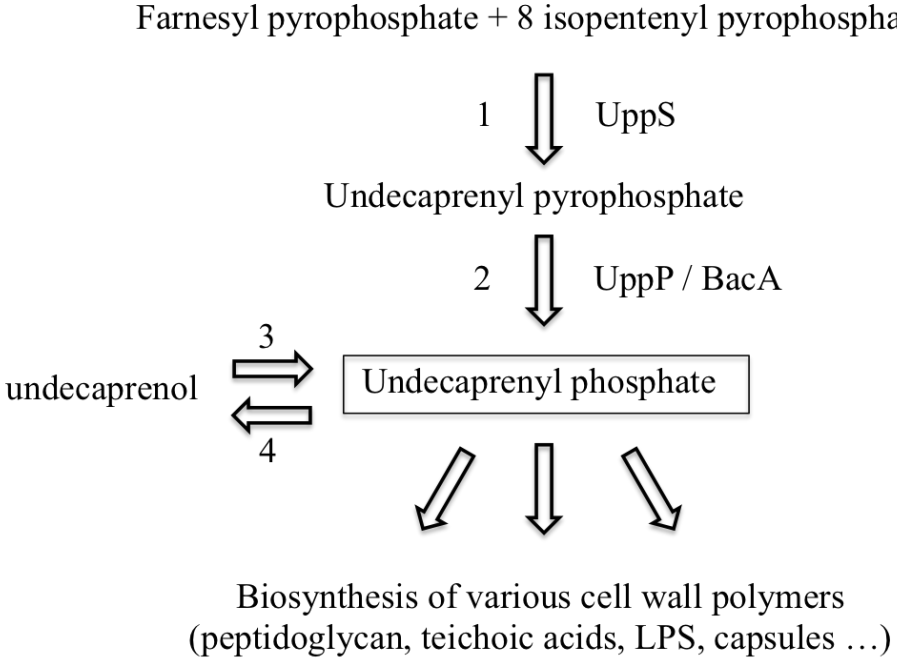

Figure 3: Metabolism of undecaprenyl phosphate (C_{55}-P) in bacteria. Steps 1-4 are catalyzed by undecaprenyl pyrophosphate synthase (UppS), undecaprenyl pyrophosphate phosphatase (UppP), undecaprenyl phosphokinase, and undecaprenyl phosphate phosphatase, respectively. Figure from A. Bouhss et al., 2008 [61].

The precursor for C_{55}-P, undecaprenyl pyrophosphate (C_{55}-PP), is synthesized by undecaprenyl pyrophosphate synthase (UppS) [62]. The recycling of C_{55}-P (dephosphorylation of C_{55}-PP to C_{55}-P, further re-phosphorylation, and dephosphorylation again to C_{55}-P) during PGN biosynthesis enables the cell to transport newly synthesized hydrophilic sugar-peptide moieties from the aqueous environment of the cytoplasm, across the hydrophobic membrane, to the exterior periplasm for further growth of the three-dimensional PGN network.

1.4 Daptomycin

1.4.1 History, structure and biosynthesis

Brief history and discovery

Daptomycin (DAP), the naturally occurring fermentation product of *Streptomyces roseosporus*, is an antimicrobial lipopeptide with potent *in vitro* bactericidal activity against most gram-positive bacteria, including multiple antibiotic-resistant and -susceptible strains [63,64,65].

DAP was initially discovered by Eli Lilly & Company in the early 1980s, but the clinical trials were shelved in 1991 owing to the adverse effects and potential toxicity problems [66,67]. Cubist Pharmaceuticals Inc. licensed the global rights for DAP from Eli Lilly & Company in 1997 and clinical trials recommenced in 1999 [68]. After intensive clinical trials, the United States Food and Drug Administration (FDA) and the European Medicines Agency (EMEA) approved DAP in September 2003 and January 2006, respectively for the treatment of complicated skin and skin structure infections (cSSSI) associated with methicillin-susceptible and methicillin-resistant *S. aureus* (MSSA and MRSA respectively), *Streptococcus pyogenes*, *Streptococcus agalactiae*, *Streptococcus dysgalactiae* subsp. *equisimilis*, and *Enterococcus faecalis* (vancomycin-susceptible only) [69]. Since 2007, it is distributed in Europe by Novartis. Since its introduction in clinical practice in 2003, DAP was approved as the key antibiotic for effective treatment of a variety of infections caused by gram-positive bacteria, such as skin and soft tissue infections, uncomplicated bacteremia, and right-sided endocarditis [70]. Moreover, the bactericidal activity of DAP was shown to be equal to or even higher than that of vancomycin, linezolid, and quinupristin-dalfopristin [64]. DAP efficaciously reduces bacterial growth in a concentration-dependent manner [71,72].

Structure

DAP is an acidic cyclic lipopeptide antibiotic [73]. Structurally, DAP consists of a highly lipophilic 10-amino acid fatty acid side chain linked to the N- terminal tryptophan of a 13-member peptide which is cyclized by an intramolecular ester bond to form a core 10-membered ring with a 3-residue side chain [67] (Fig. 4). DAP has

different stereochemically distinct amino acid residues: D-aspartate at position 2, D-alanine (D-Ala) at position 8, and D-serine at position 11. The amino acid residues with L-stereochemistry are the normal isomeric forms of amino acids found in proteins. Furthermore, DAP contains three uncommon amino acid residues, ornithine at position 6, 3-methylglutamate at position 12, and kynurenine at position 13. DAP contains two aromatic residues (Trp-1 and Kyn-13) that are intrinsically fluorescent [137]. Kynurenine is responsible for forming the ester bond with threonine that completes the cyclic structure [74]. Owing to this unique structure, DAP exhibits a novel mechanism of action [75].

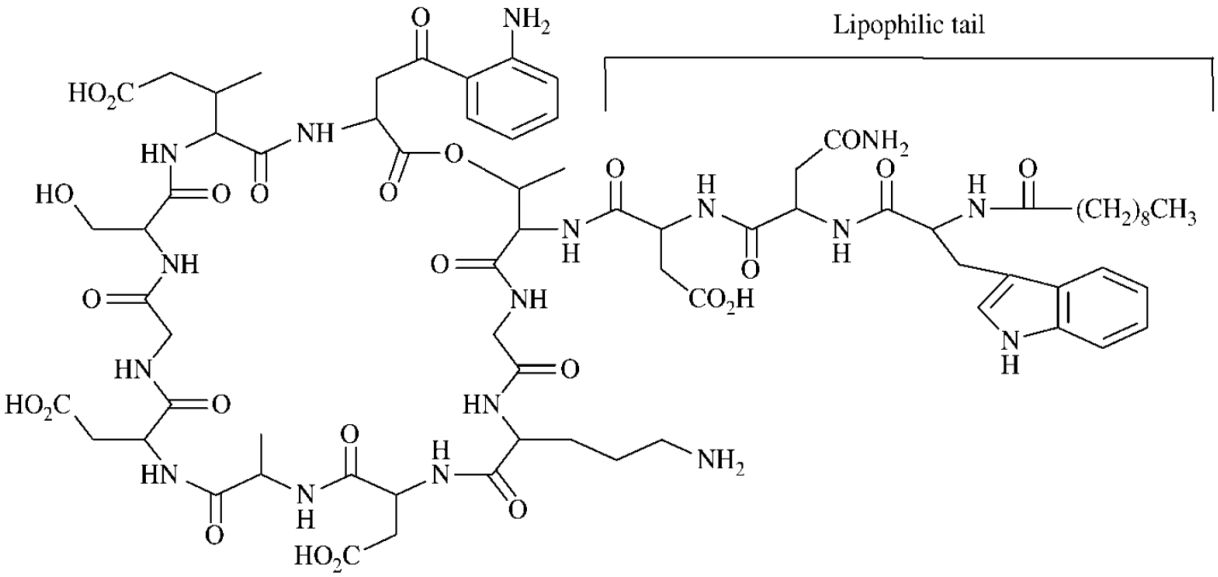

Figure 4: Chemical structure of daptomycin. Picture adopted from Cubicin, 2003 [69].

The chemical name of DAP is N-decanoyl-L-tryptophyl-D-asparaginyl-L-aspartyl-L-threonylglycyl-L-ornithyl-L-aspartyl-D-alanyl-L-aspartylglycyl-D-seryl-threo-3-methyl-L-glutamyl-3-anthraniloyl-L-alanine ε1-lactone. DAP has a chemical formula of $C_{72}H_{101}N_{17}O_{26}$ and a molecular weight of 1620.67 g/mol [69].

Biosynthesis

DAP, the first approved lipopeptide antibiotic, is a natural secondary metabolite produced via n-decanoic acid-directed fermentation in *Streptomyces roseosporus* [76]. During the fermentation, *Streptomyces roseosporus* produces a complex combination of lipopeptides called the A21978C complex, which includes several lipopeptide structures. Generally, the analogs of A21978C contain chains consisting of 13 D- and

L-amino acids, linked by an ester bond between the carboxyl group of L-kynurenine13 (Kyn) and the hydroxyl group of L-Thr4 to form a 10-macrolactone ring with three exocyclic residues [77]. Antimicrobial activity requires at least 4-8 carbons in the fatty acyl side chain, with longer chains showing higher antimicrobial activity. The lipopeptides of the A21978C complex have different long-chain fatty acid tails, and these fatty acyl moieties are connected to the N-terminal of the tryptophan residue at position 1 of the amino acid chain, and enable distinction between the different types of A21978C complex components [74,78].

During the fermentation of *Streptomyces roseosporus* the three major components, A21978C1-3 with branched 11-, 12-, or 13-carbon chain fatty acids, are produced [79]. The A21978C complex is unique to *Streptomyces roseosporus*, but other similar compounds can also be found in the A21978C complex, such as the calcium-dependent antibiotic (CDA) in *Streptomyces coelicolor* [80,81] and members of the A54145 family in *Streptomyces fradiae* [73,82].

DAP is the N-decanoyl analog of the A21978C lipopeptide factor C1 and commonly contains a straight lipid side-chain with only 10 carbon atoms to form the n-decanoyl tail of the molecule.

Generally, ribosomes are considered the protein builders and protein synthesizers of a cell; they link one amino acid at a time and build long polypeptide chains [83]. However, some important antibiotic lipopeptides such as DAP, vancomycin, cyclosporin, and β-lactams are not produced by ribosomes but are biosynthesized by the large enzyme complexes called non-ribosomal peptide synthetases (NRPSs) [84]. Typically, NRPS is composed of three catalytic domains, adenylation (A), condensation (C), and thiolation (T) domains; these domains work collectively to recognize specific amino acids and constitute them in the correct sequence during one cycle of this non-ribosomal peptide biosynthesis [85]. Often, a fourth subunit is responsible for the catalytic release of the mature non-ribosomal peptide from the enzyme complex.

In *Streptomyces roseosporus*, DAP is synthesized by a large NRPS via a thiotemplate mechanism [86,87]. A 128 kb region of *Streptomyces roseosporus* DNA was verified to contain the DAP biosynthetic gene cluster (*dpt*) containing the tandemly arranged

genes *dptA*, *dptBC*, and *dptD*, which encode the three catalytic subunits of NRPS (Fig. 5). Each subunit contains two to six modules and is responsible for one step of particular amino acid incorporation into the non-ribosomal peptide [88].

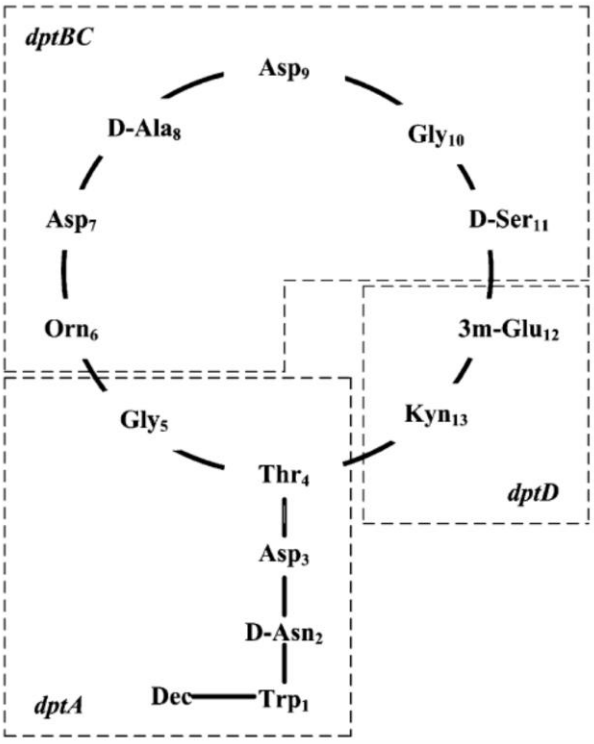

Figure 5: Biosynthesis of the daptomycin precursor. Picture adopted from Nakhate et al., 2013 [89].

Other neighboring genes are also likely to be involved in the constitution of DAP. The genes *dptE* and *dptF* located upstream of the NRPS genes show sequence similarities to the genes encoding acyl-CoA ligase and acyl carrier protein, respectively. Their products are probably involved in the acylation of the first amino acid, N-terminal tryptophan (Trp), required to initiate DAP biosynthesis. Other contiguous downstream genes, including *dptG*, *dptH*, *dptI*, and *dptJ*, also have important functions in the biosynthesis of daptomycin. *dptG* is predicted to regulate the expression or export of antibiotics, and *dptH* may be involved in enhancing the efficiency of DAP production by clearing misincorporated substrates that block the pathway. *dptI* probably functions in conjunction with formation of the non-proteinogenic amino acids L-3-methylglutamic acid *in vivo*. The *dptJ* gene may encode the tryptophan 2,3-dioxygenase, which is involved in the conversion of Trp to Kyn [90,91].

The scientists at Eli Lilly developed a DAP production process by feeding decanoic

acid during fermentation [92]. Feeding other fatty acid structures during fermentation experiments resulted in production of different lipophilic tails of the core structure [93]. However, DAP is formed as the main product when decanoic acid fed during fermentation [74,78]. After chemical and enzymatic modification, DAP showed rapid in vitro antimicrobial activity against selected gram-positive bacteria [67].

The understanding of the NRPS structure, DAP synthesis strategy, and the cloned *dpt* gene cluster not only provides an opportunity to study the biosynthesis of DAP and other lipopeptides, but also offers a chance to explore new and better methods to build novel lipopeptide antibiotics by pathway engineering [94,95].

1.4.2 Putative mode of action

1.4.2.1 Action mechanism of general antibiotics

Development of antibiotics for the treatment of bacterial infections has revolutionized medical care and has remarkably reduced human morbidity and mortality. To be effective against bacteria, antibiotics should basically fulfill the following three conditions: the antibiotic must be specific to one or more susceptible targets in the cell; the dose of the antibiotic must be sufficient; and the antibiotic must not be inactivated or modified [96,97]. Moreover, the antibacterial drug should show selective toxicity towards bacteria but not its host organism; namely, it should act on a unique target present in bacterial special structures or involved in their metabolic processes. On the basis of this criterion of selective toxicity, many antibacterial drugs function by targeting components of the bacterial cell. Antibiotic actions occur via the following five major mechanisms: i) interference with cell wall synthesis, ii) inhibition of protein synthesis, iii) interference with nucleic acid synthesis, iv) breakdown of the cell membrane structure or function, and v) inhibition of a metabolic pathway [98]. Fig. 6 illustrates examples of the most common targets of antibiotics, antibiotic drugs, and their mode of actions.

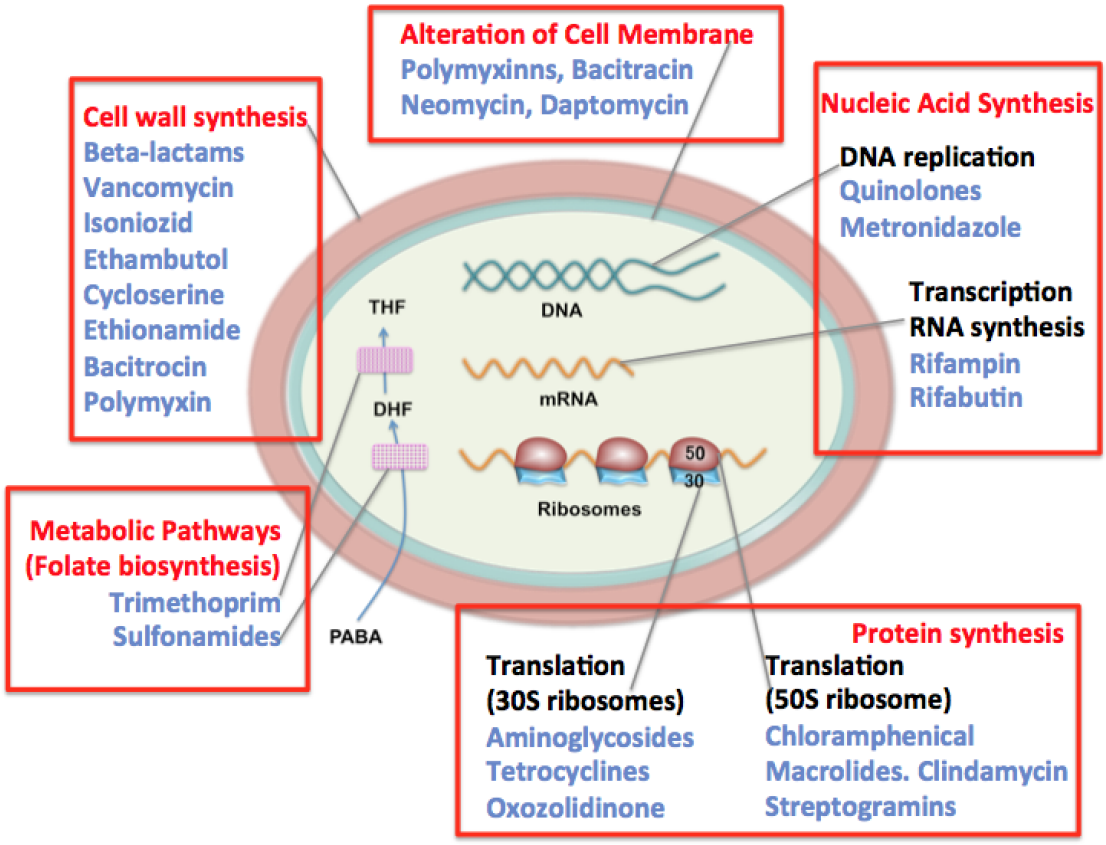

Figure 6: General antibiotic action mechanisms and target sites of several antibiotic representatives. Sketch adopted from Chakraborty et al., 2012 [99].

As we have briefly described the biosynthesis of the cell wall (PGN) and the function of cell membrane components in PGN formation in the earlier sections, we describe the mechanism underlying antibiotic-induced inhibition of cell wall biosynthesis as an example. As mentioned earlier, bacterial cell wall is mainly composed of PGN, which is synthesized via a complex pathway that occurs in the cytoplasm and the periplasm [43]. As PGN synthesis proceeds via several steps involving multiple enzyme-catalyzed reactions, the enzymes in each step can be targeted and inhibited by several classes of antibiotics (Fig. 7), thereby resulting in rapid cell lysis and death [100,101]. The main reactions and the enzymes involved in PGN synthesis, and the corresponding inhibitors are as follows:

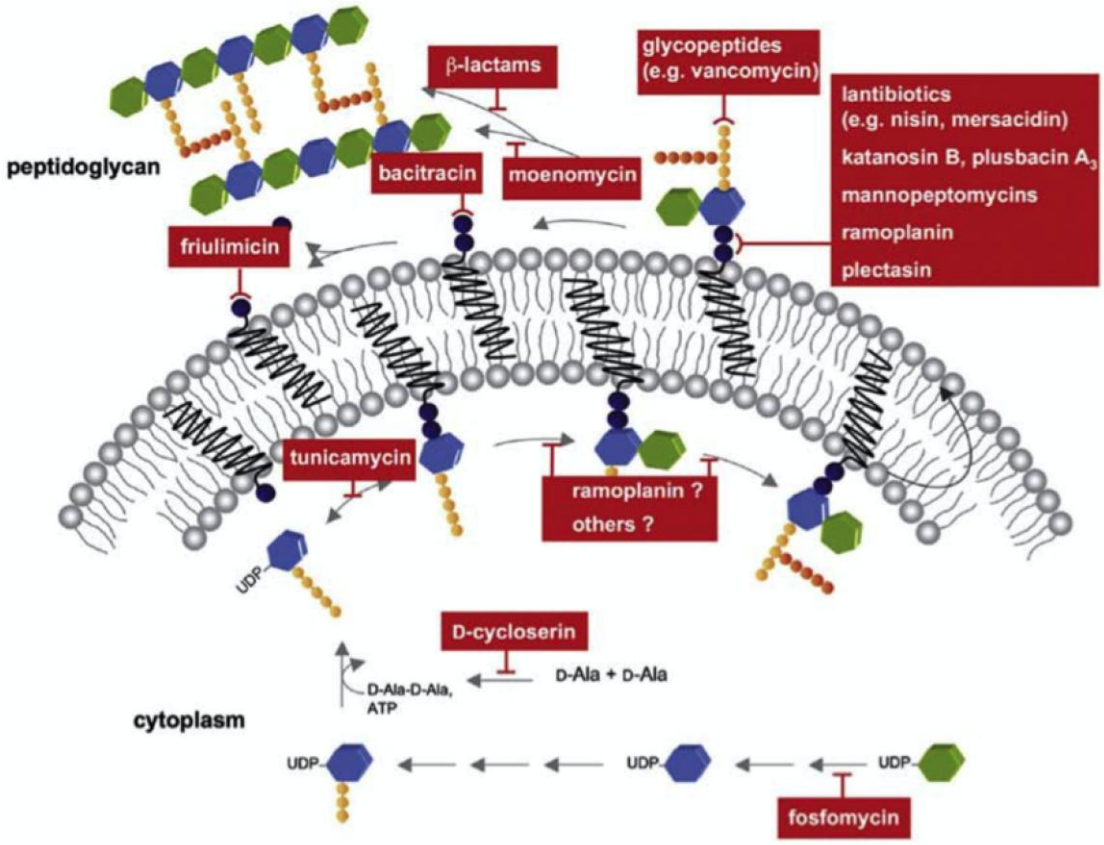

Figure 7: Inhibition sites for main antibiotics in the peptidoglycan biosynthesis pathway. Picture taken from Schneider and Sahl, 2011 [101].

i) Formation of UDP- MurNAc from GlcNAc. PGN synthesis begins in the cytoplasm with the formation of UDP-MurNAc from UDP-GlcNAc and phosphoenolpyruvate (PEP) by the enzyme UDP-GlcNAc enolpyruvate transferase (MurA) [102]. MurA is the target of fosfomycin, which is a broad-spectrum antibiotic and is structurally similar to both glycerophosphate and PEP. When the catalytic site of MurA is exposed during formation of a binary complex with UDP-GlcNAc, fosfomycin binds to MurA covalently, causing irreversible MurA inactivation [103,104].

ii) Attachment of a pentapeptide to MurNAc. A pentapeptide containing the five amino acids, L-Ala, D-isoGlu, L-Lys, and the D-Ala–D-Ala dipeptide, is added to UDP-MurNAc in four sequential steps to form UDP-MurNAc-pentapeptide [105,106]. Here, two enzymes, D-Ala racemase and D-Ala ligase, which convert L-Ala to D-Ala and create a peptide bond between two D-Ala residues respectively, are effectively targeted and inhibited by cycloserine [107,108].

iii) Attachment of UDP-MurNAc-pentapeptide to C_{55}-P and formation of lipid I. The final cytoplasmic precursor UDP-MurNAc-pentapeptide is transferred to C_{55}-P, a carrier lipid, by the membrane-bound phospho-MurNAc-pentapeptide translocase (MraY), thus forming lipid I (C_{55}-PP-MurNAc-pentapeptide). In this step, the MraY-catalyzed reaction can be targeted by tunicamycin, which belongs to the uridyl peptide antibiotic family [109]. Tunicamycin causes competitive and reversible inhibition for the MraY substrate but does not affect the rate of polyprenyl phosphate binding [110]. Besides, C_{55}-P plays a crucial role in membrane-associated biosynthesis steps and cell wall teichoic acid biosynthesis as well as supports polysaccharide transport across the cytoplasmic membrane in the later step. Therefore, blocking this lipid carrier could inhibit PGN synthesis. The lipopeptide antibiotic amphomycin binds to the substrate of C_{55}-P for the inhibition of this step [111,112].

ix) Formation and translocation of lipid II. Another UDP-GlcNAc is linked to the MurNAc moiety of lipid I to form lipid II (C_{55}-PP-GlcNAc-MurNAc-pentapeptide) by the membrane-associated transferase MurG. After further modification, the newly synthesized lipid II is translocated across the cytoplasmic membrane for the final PGN assembly. Two protein transporters, FtsW and MurJ, are responsible for the translocation of lipid II across the membrane [113]. Of all the molecules involved in cell wall biosynthesis, lipid II, the key building block of PGN biosynthesis, is undoubtedly the most directly targeted molecule by several classes of antibiotics. In this stage, some lantibiotics function via multiple mechanisms, such as by binding to lipid II, disrupting membrane integrity through pore formation, or blocking transglycosylation [114]. After flipping of lipid II to the outside of the cytoplasmic membrane, the glycopeptide moiety of lipid II is released and linked to an existing substrate strand of PGN by transglycosylase. Moenomycin, a glycolipid antibiotic, binds and inactivates this enzyme inhibiting this step of PGN synthesis [115,116].

v) Covalent cross-linking of PGN strands. Adjacent PGN strands are cross-linked to form the final polymer on the extracellular side of bacterial cells. This process is catalyzed by PBPs, which catalyze both transglycosylation reactions of the disaccharide units MurNAc-GlcNAc and transpeptidation (cross-linking) of PGN peptides [117]. The latter reaction leads to the formation of the interpeptide bridges between the D-Ala–D-Ala residues of peptide chains and the pentaglycine residues.

The D-Ala at the C-terminal end of the pentapeptide is removed in the process [51]. This enzymatic reaction is the target of the glycopeptide antibiotic vancomycin, which binds to the D-Ala–D-Ala residues of PGN strands, thereby inhibiting the transglycosylation and transpeptidation reactions [118,119]. These reactions are also inhibited by penicillin, ampicillin, and other β-lactam antibiotics, which bind to the transpeptidase active site of PBPs by mimicking the structure of D-Ala–D-Ala residue of the PG pentapeptide [120].

vi) Recycling of the lipid carrier C_{55}-P. C_{55}-P is converted back to its pyrophosphatase from C_{55}-PP, which is released by the transglycosylase reaction, and then flipped back across the membrane to repeat the C_{55}-P-mediated transport cycle [121]. Bacitracin retains C_{55}-PP outside the bacterial membrane, thus inhibiting the function of this lipid carrier and the subsequent PGN synthesis [122,123].

1.4.2.2 Action mechanism of DAP

DAP with its distinctive structure shows effective bactericidal activity against most gram-positive bacteria [124]. Nevertheless, the precise biological mechanism underlying DAP action remains poorly understood. Several studies have reported different action mechanisms of DAP, and many research groups have attempted to elucidate these proposals. Briefly, the main proposed action modes can be categorized into two major types: inhibition of cell wall macromolecule synthesis (specifically PGN and LTA), and interference with the normal membrane function.

Inhibition of PGN or/and LTA synthesis

In Chapter 1.2 and 1.4.2.1, we have depicted the complex pathway of PGN biosynthesis. Several early studies have reported the inhibition of PGN formation by DAP. Allen and colleagues first proposed that DAP could inhibit PGN biosynthesis in *S. aureus*. They showed that DAP inhibited the formation of the PGN precursor, UDP-MurNAc-pentapeptide [125]. However, they later observed an inhibition of LTA biosynthesis and suggested this pathway as the target of DAP [126]. Boaretti and colleagues reported that DAP binds irreversibly to the bacterial cell membrane, suggesting that DAP cannot be involved in the synthesis of PGN precursor molecules in the cytoplasm [127]. They also claimed that LTA is the primary target for DAP [128]. However, the hypothetical inhibition of LTA biosynthesis was not consented by

Laganas and colleagues [129]. Their investigation suggested that LTA biosynthesis was not the primary target. Later, they also identified the effect of DAP on growth-arrested cells, in which all the macromolecular biosynthesis pathways were blocked. Their results showed that DAP inhibited all macromolecular synthesis in *S. aureus*, *Enterococcus faecalis*, and *Enterococcus hirae* without kinetic or dose specificity for LTA. DAP remained bactericidal in the absence of ongoing LTA synthesis. Hence, the bactericidal activity of DAP does not occur via inhibition of LTA synthesis in these pathogens.

Interference with normal membrane function

Many researchers believe that DAP functions primarily by disturbing the normal membrane function of the bacterial cell. Silverman et al. used fluorimetric and flow cytometric assays to demonstrate that DAP exerts rapid bactericidal activity in association with the dissipation of the cell membrane potential [75]. Cotroneo and colleagues suggested that DAP might promote the formation of small and discrete pores in the cell membrane of *S. aureus* [130]. They also showed that DAP altered the cell wall morphology by abnormal septation events. Furthermore, Pogliano and colleagues reported the colocalization of DAP-induced curved membrane patches and the bacterial protein DivIVA, which is involved in cell wall synthesis via recruitment of other cell division enzymes, thus demonstrating DAP-mediated alterations in cell morphology [131].

Researchers at Cubist Pharmaceuticals Inc. suggested that it is indeed unclear whether DAP activity occurs via one fundamental mechanism [132]. Collectively, although the exact mechanism underlying DAP action is under debate since many years, all these findings and the proposed action modes led to a general consensus and the currently accepted hypothesis that DAP effects its rapid bactericidal activity primarily by disrupting the normal cytoplasmic membrane function [133,134,135].

The prevalent model for the mechanism of action involves a calcium-dependent insertion of the lipophilic tail of the DAP molecule into the bacterial target membrane without entering the cytoplasm of the cell [136]. This mechanism is only effective against gram-positive bacteria because DAP is unable to penetrate the outer membrane of gram-negative bacteria [67]. However, DAP may insert into the

membrane via two different mechanisms. The first hypothesis claims that calcium-bound DAP forms oligomers on the bacterial cell membrane [75], whereas the other theory suggests that calcium-bound DAP oligomerizes to form loose micelles before insertion into the cell membrane [133]. In the presence of calcium ions, insertion of DAP into the cell membrane is considered to generate an ion conducting channel and disrupt the functional integrity of the bacterial membrane, ultimately resulting in cell death. This mechanism is in agreement with both the hypothesis for cell membrane insertion.

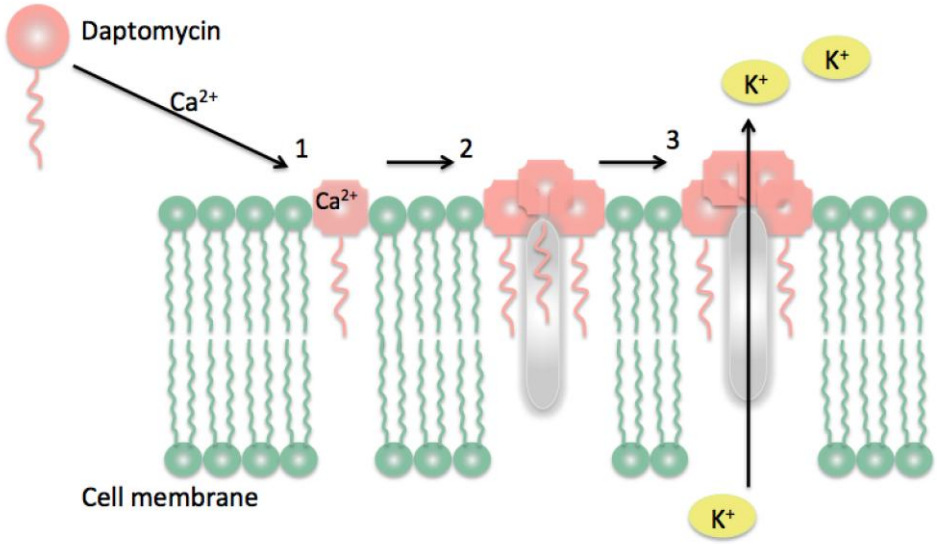

Figure 8: Hypothetical mechanisms of action of daptomycin (DAP) suggested by Silverman et al.. Step 1: DAP insertion into the cytoplasmic membrane in the presence of calcium; step 2: DAP oligomerization and disruption of the membrane; step 3: the efflux of potassium ions, membrane depolarization, and cell death. Picture adopted from Silverman et al., 2003 [75].

The hypothesis that calcium-bound DAP oligomers are formed on the bacterial cell membrane is illustrated in Fig. 8. It shows that DAP binds Ca^{2+} and then inserts into the bacterial membrane headgroups in the first step. During this step, the presence of calcium induces a conformational change in DAP to increase its amphipathicity and to increase its interaction with neutral or acidic membranes [137]. Then DAP oligomerizes in the membrane, thus disturbing membrane integrity. This is followed by rapid membrane depolarization and intracellular potassium ion leakage, which subsequently causes cell death due to the widespread cessation of DNA, RNA, and protein synthesis. Notably, DAP treatment does not cause cell lysis in *S. aureus*,

suggesting that this hypothesis does not depend on cell lysis [130]. Furthermore, large molecules are not released from the cytoplasm [138].

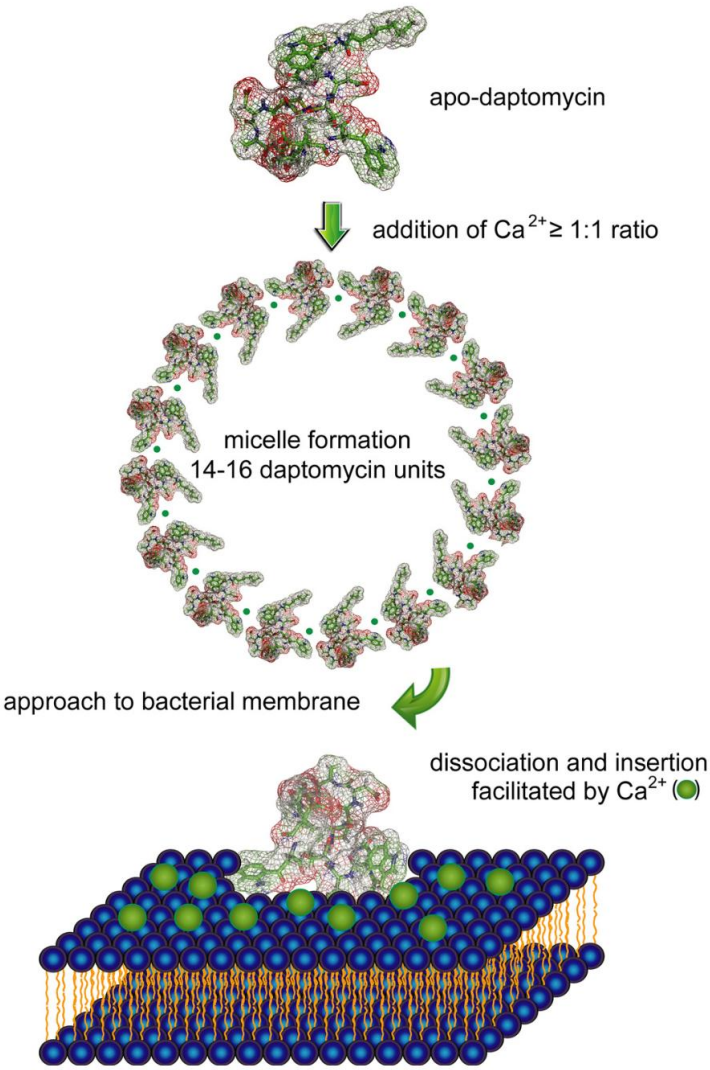

Figure 9: Hypothetical mechanism of action of daptomycin (DAP) suggested by Robbel et al.. DAP forms micelles after addition of Ca^{2+} in the solution. The complex approaches the membrane and dissociates in close proximity of the lipid bilayer. DAP subsequently inserts into the membrane, ultimately leading to cell death. Picture adopted from Robbel et al., 2010 [76].

The second hypothesis, mostly based on nuclear magnetic resonance (NMR) studies [133,137,139], states that DAP forms micelles with 14-16 subunits in the presence of a minimum of 1:1 calcium to DAP molar ratio in solution to become competent for membrane insertion (Fig. 9). These micelles are vehicles to deliver DAP to bacterial cell membranes at high local concentrations. To enable interaction with the bacterial membrane, the micellar DAP structure dissociates and individual DAP molecules are

inserted into the membrane. This insertion is facilitated by calcium, which binds strongly to the PG headgroups, and may be accompanied by a second conformational transition to generate larger pores [137]. In the final step, potassium efflux and membrane depolarization, lead to cell death.

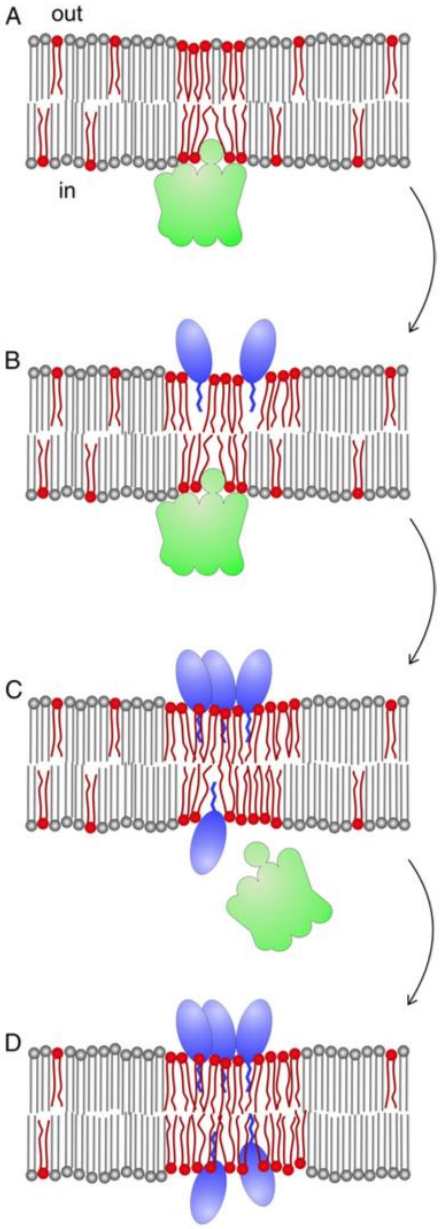

Figure 10: Hypothetical mechanisms of action of daptomycin (DAP) suggested by Müller et al.. (A) Peripheral membrane proteins MurG and PlsX localize to regions of increased fluidity (RIFs) indicated by a high concentration of fluid lipids (red). (B) DAP inserts into such regions and induces bilayer distortions. (C) DAP forms oligomer on the membrane stimulated by calcium ions. More fluid lipids are attracted. DAP molecules flip through the bilayer to the inner leaflet, causing membrane proteins to be displaced from the RIFs. (D) DAP blocks access to fluid lipids in the

inner leaflet, thus increasing membrane rigidity. Picture adopted from Müller et al., 2016 [140].

In addition to these two main mechanisms underlying DAP bactericidal activity, Müller and colleagues recently proposed a new DAP action mechanism involving inhibition of cell envelope synthesis by interfering with fluid membrane microdomains [140]. Using the model organism *Bacillus subtilis* and different assays, including proteomics, ionomics, and fluorescence light microscopy, they revealed that DAP does not lead to membrane pore formation or rapid K^+ leakage and membrane curvature, but acts on the cell membrane by causing the clustering of fluid lipids, which in turn increases membrane rigidity and causes delocalization of the peripheral membrane proteins MurG and PlsX, which are involved in PGN and phospholipid synthesis. The novel DAP action mechanism proposed on the basis of these findings is shown in Fig. 10. Once DAP reaches the bacterial cell membrane, it inserts its short lipid tail between the fatty acyl chains of phospholipid molecules, and its large peptide ring structure causes strong disturbance in the regular fatty acid packing of the cell membrane. Ca^{2+}-dependent DAP oligomerization leads to further distortion of the membrane bilayer. Owing to its bulky structure, DAP localizes to the regions of increased fluidity (RIFs) and restricts the chain flexibility of lipids. Moreover, DAP has been shown to flip from one membrane leaflet to the other. Therefore, DAP has a dramatic effect on the fluid lipid order/disorder balance of the bacterial cell membrane.

1.4.2.3 The function and effect of Ca^{2+} and lipids

Although many aspects of DAP mechanism are subject to an ongoing debate, all the studies are consistent with the notion that the antibacterial activity of DAP is dependent on the presence of calcium ions (Ca^{2+}) [141,142]. The DAP molecule is an anionic molecule with one basic and four acidic amino acids. After binding to Ca^{2+}, the Ca^{2+}-DAP complex can act as a cationic peptide and interact with negatively charged phospholipids by an electrostatic attraction [135]. Ca^{2+} neutralizes the negative charges of the DAP molecule and the anionic phospholipid heads (e.g., PG) of the cell membrane to promote the membrane insertion, and bridges the gap between them [137,143]. Moreover, investigations based on NMR and CD showed that the presence of Ca^{2+} leads to oligomerization and micelle formation [144,145]. Other divalent cations may enable the insertion of DAP into membrane bilayers; however, studies have

demonstrated that Ca^{2+} can bind better and stronger to DAP, compared to other divalent cations such as Mn^{2+}, Mg^{2+}, Cu^{2+}, and Ni^{2+} [139,146].

In addition to calcium, lipids, especially those with negatively charged headgroups, are also critical for the interaction between DAP and lipid membranes. Lipid compositions of bacterial membranes are highly variable; however, PG, CL, and PE generally account for a large portion of the phospholipids of bacterial membranes.

The rapid activity of DAP on bacterial membranes has been investigated in numerous studies with both cells and artificial model membranes. Early studies using artificial model membranes supplemented with PC, and sometimes cholesterol, have shown that in the presence of Ca^{2+}, DAP can act spontaneously on the lipid bilayer in the absence of any bacterial protein or other cell surface components [147,148]. However, CD spectroscopy demonstrated that the effect of DAP is considerably lower when binding to pure PC membranes, whereas profound conformation changes occur in membranes containing both PC and PG [137]. Because PG and CL are abundant anionic phospholipids present in bacterial membranes, their depletion could reduce the net negative charge of the membrane, thus affecting the function of DAP [149]. The key role of PG in DAP action is also supported by studies with bacterial cells. Fluorescently labeled daptomycin-Ca^{2+} complexes interact preferentially with PG-enriched membrane regions in *B. subtilis* cells [150]. Furthermore, changes in membrane lipids and fluidity have been demonstrated to affect the DAP susceptibility [151,152]. For instance, an MRSA strain with increased carotenoid production was reported to show reduced susceptibility against DAP and other cationic antimicrobial peptides [153]. Moreover, many of the mutations that alter cell membrane composition have been shown to prominently affect the susceptibility to DAP [150]. *S. aureus*, for example, is one of the susceptible bacterial species containing large amounts of PG in their cell membrane, and mutations that decrease the amount of PG result in the reduced susceptibility [154,155]. In addition, PG is the immediate precursor of CL, which has been demonstrated to cause more active membrane binding of DAP with around 10% content in model membranes [156]. Although several lines of evidence show the involvement of CL in the interaction of DAP and bacterial membrane, its precise role in the action mechanism is not well defined. For example, Zhang and coworkers reported that CL inhibits membrane permeabilization in the liposome

model, and they claimed that CL might mediate DAP resistance by competing for it with PG [156]. Tran et al. also provided the evidence to support a similar effect *in vivo* [157].

Despite significant evidence of DAP activity against the cell membrane in susceptible bacteria, the cell wall has also been considered a target site of DAP [158,159]. As described in Chapter 1.2 and 1.3.2, cell membranes are involved in PGN synthesis and C_{55}-P is a key lipid carrier that anchors in the membrane. It can be bound with antibiotics like fruilimicin and MX-2401 [160,161]. As DAP is structurally related to fruilimicin and MX-2401, it can bind to C_{55}-P, resulting in the inhibition of PGN synthesis [162,163].

1.4.3 Resistance against antibiotics

1.4.3.1 Role of antibiotics resistance

With the development and widespread use and misuse of antibiotics, several bacterial species of human and animal origin have developed numerous mechanisms for resistance to an increasing number of antibiotics [164,165,166]. Such bacterial resistance should be a concern for many reasons. First, the increase in antibiotic resistance is closely associated with the use of antimicrobial agents in clinical practice. For example, a microorganism/bacterium might be initially sensitive to one antimicrobial/antibacterial agent but can later adapt gradually and develop resistance to these type of agents. The extensive use of antibiotics in clinical practice is causing an increase in resistant bacteria. Bacterial resistance can limit treatment options, compromise effective therapy, and subsequently result in treatment failure [167,168]. In addition, with the continued use of various antibiotics in prolonged therapy, microorganisms could develop resistance mechanisms to multiple drugs (multidrug resistance) [169]. Multiple resistance mechanisms, which are hard to control and complicate the treatment, are becoming the norm and increase both human morbidity and financial costs in hospitals [170,171]. Finally, the spread of resistant bacteria is another noticeable problem, especially for infection control within healthcare institutions and other communities [172,173]. Antimicrobial resistance has resulted in an enormous clinical and financial burden on health care systems, and has undoubtedly become a global health concern [174,175].

A complete understanding of the molecular mechanisms of antibiotic resistance would allow us to develop new approaches and control strategies to further reduce the spread of resistant bacteria and their evolution and may eventually enable to overcome most of the antibiotic resistance in the health care system.

Many excellent reviews describe antibiotic discovery, modes of action, and mechanisms of resistance over the past decades [176,177,178]. With the evolvement of bacterial resistance to antibiotics, new resistance mechanisms are constantly being described. Although a wide range of biochemical and physiological mechanisms may be involved in resistance and the manner of acquisition of resistance may vary among bacterial species, the main and classic antibiotic resistance mechanisms in bacteria are summarized in Fig. 11.

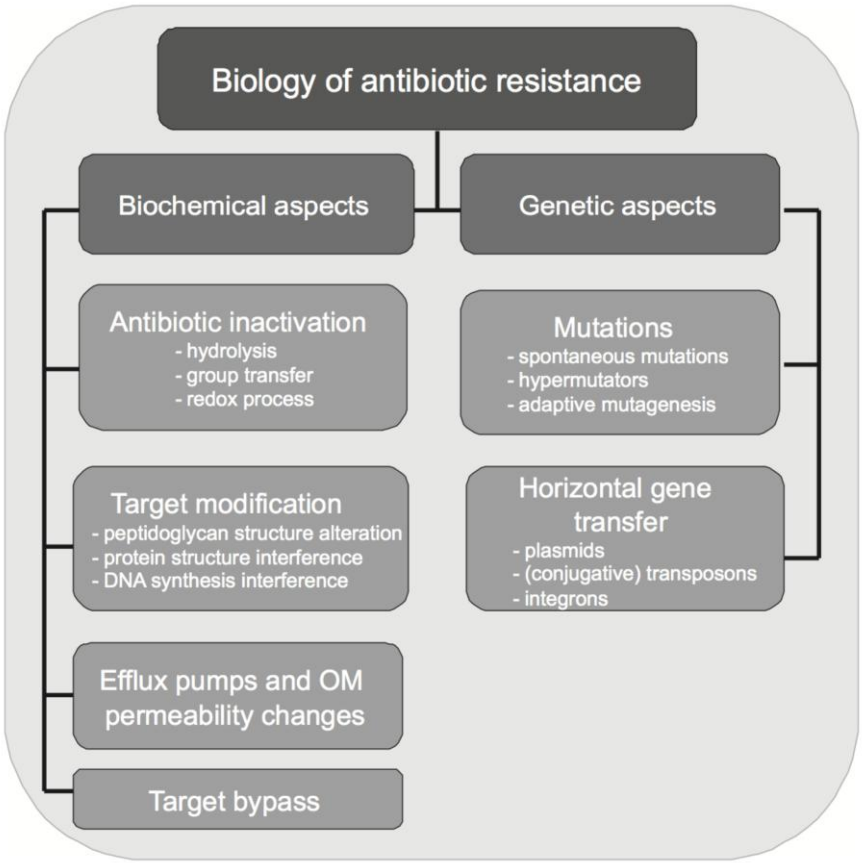

Figure 11: Biochemical and genetic aspects of antibiotic resistance mechanisms in bacteria. Picture adopted from Senka et al., 2008 [179].

1.4.3.2 Mechanisms of DAP resistance

DAP is a calcium-dependent cyclic lipopeptide antibiotic with potent bactericidal

activity in vitro against a wide variety of clinically important gram-positive bacteria, including multidrug-resistant organisms, such as MRSA, penicillin-resistant *Streptococcus pneumoniae*, glycopeptide-intermediate *S. aureus*, coagulase-negative s*taphylococci*, and vancomycin-intermediate *S. aureus* (VISA) [64,65,180]. DAP also maintains clinical activity for the treatment of infections caused by vancomycin-resistant enterococci (VRE) [181,182].

Although most gram-positive bacteria are susceptible to DAP, several studies have reported the emergence of DAP-resistance (DAPr) strains during prolonged treatment in several important gram-positive bacteria, such as *S. aureus*, *Enterococcus faecalis*, and *Enterococcus faecium* [183,184]. These strains with reduced susceptibility to DAP could consequently lead to clinical treatment failures; thus, it is important to understand the mechanism of DAP resistance to reduce its occurrence and enhance the understanding of the mechanism of interaction between DAP and its target. Moreover, the clinical failures caused by DAPr have also been mentioned during treatment for vancomycin resistant *Enterococcus faecium* [185], vancomycin resistant *Enterococcus faecalis* [186] and *Enterococcus durans* [187]. On the basis of phenotypic observations and DNA sequencing, several research groups have proposed to elucidate the mechanisms of DAP resistance in bacteria. Serial passages with increasing concentration of DAP rarely led to resistance in the strains of *staphylococci*, *enterococci*, and *pneumococci* [188]. Moreover, experiments with chemical-induced mutagenesis did not show any resistance [154]. Some phenotypes associated with DAPr, such as thickened cell walls, enhanced surface charge, changes in cell membrane fluidity and phospholipid synthesis, cross-resistance to host defense cationic peptides, have been identified by many research groups [152]. Although the mechanisms seem to be diverse, complex, and are not yet completely defined, the studies have provided important insights and shown that bacterial resistance is related to activation of the inherent bacterial self-defense processes and adaptation in cell wall homeostasis and membrane phospholipid metabolism [189,190]. Genomic studies have demonstrated the involvement of single point mutations in increasing DAP resistance in *S. aureus* [191]. Laboratory studies have identified several mutations associated with reduced susceptibility in several genes, such as *mprF*, *yycG*, *rpoC*, and *rpoB*.

The mprF (multiple peptide resistance factor) gene was found by transposition mutagenesis in many resistant *S. aureus* strains [154]. This gene encodes the bifunctional membrane enzyme MprF (also known as phosphatidylglycerol lysyltransferase) that couples lysine to PG to form lysyl-phosphatidylglycerol (LPG) using lysyl-tRNA as a co-substrate in the inner leaflet of the membrane, and it also provides translocase activity to subsequently transfer LPG to the outer membrane leaflet [192]. The mutant enzyme found in resistant strains showed gain-in-function that led to an increase in the LPG content and the acceleration of its flipping [193]. As LPG is positively charged, it was considered to be a major contributor of the alteration of surface charge that results in the reduction of the binding sites for the Ca^{2+}-bound DAP in bacterial membranes [194]. The *mprF* deletion mutants showed increased susceptibility to DAP and other CAMPs [195,196], whereas an insertion in the *mprF* gene resulted in increased susceptibility to cationic peptides in *S. aureus* [197].

The *yycFG* gene encodes the YycFG response regulator system, which is a critical two-component regulatory system for cell wall metabolism and biofilm formation [198]. *YycFG* mutations have been reported in many DAPr strains [154,199]. Studies in *S. aureus* have shown that enhanced expression of YycFG leads to increased PGN biosynthesis whereas its depletion results in cell death [200].

The *rpoC* and *rpoB* genes encode RNA polymerases [154]. The effect of mutations in *rpoB* and *rpoC* on DAP susceptibility is not completely clear; however, alterations in both RpoB and RpoC have been implicated in increased DAP minimal inhibitory concentration (MIC) via serial passage experiments [154]. Whole-genome sequencing studies confirmed that hetero-VISA strains with *rpoB* mutations showed reduced susceptibility to DAP, compared to that observed in the parent MRSA strain. Moreover, *rpoB* mutation-induced resistance was accompanied by thickening of the cell wall and reduction of the cell surface negative charge [201]. Besides, Watanabe and coworkers indicated that *rpoB* mutation is one of the main contributors to vancomycin resistance in *S. aureus* [202]. Therefore, although *rpoB* is not a regulator gene, its mutation changes the transcription profile of the cell drastically, compared to that by other regulatory mutations [203,204].

The three components of the LiaFSR system are a transmembrane protein (LiaF), which is encoded by *liaF* and acts as a specific inhibitor of LiaR-dependent gene

expression [205]; a membrane bound bifunctional histidine-kinase (LiaS), which acts as a phosphatase in uninduced conditions and prevents LiaR phosphorylation to maintain the system in the "off" state [206]; and a response regulator (LiaR), which regulates the expression of a gene cluster (*liaIHGFSR*) that is involved in cell membrane stress response against attack by antibiotics and antimicrobial peptides [150,207]. The studies in *B. subtilis* showed that the membrane-anchored LiaF could negatively regulate the LiaRS system [205], hence, it is predicted that *liaF* mutations may reverse the inhibitory effect of LiaS, thus activating the LiaFSR system. The activation of this system may influence cell-envelope homeostasis by affecting the transcription of several genes that can help mitigate the damage caused by an antibiotic. For instance, this system is activated by DAP, which in turn reduces bacterial DAP susceptibility [150,163].

2. Aims of the thesis

DAP is a reliable antibiotic in the combat against clinical pathogens, as it displays strong bactericidal activity against high inoculum MRSA resulting in rapid cell death. Nevertheless, the precise mechanism of DAP action remains controversial. Despite different views, all the studies suggest that cell membrane and Ca^{2+} are involved in DAP action mechanism. Understanding the precise DAP mechanism requires an understanding of the target of DAP. It is therefore essential to study the binding behavior of DAP and to define its target binding site in bacterial membranes. Furthermore, this knowledge may help to elucidate the precise mode action of DAP as well as suggest approaches to reduce bacterial DAP resistance in clinical use.

The primary goal of this thesis was to gain more insights into the bactericidal mechanism of action of DAP using different types of fluorescence imaging techniques. Therefore, this research focused on the following objectives:

1. Investigation of the binding behavior of DAP to *S. aureus* cells using highly inclined and laminated optical sheet (HILO) microscopy. A fluorescent derivative, 5(6)-TAMRA-X, SE-labeled DAP (DAP-TMR) that retains antimicrobial activity was used for imaging. Additionally, the super resolution imaging method termed universal point accumulation imaging in the nanoscale topography (uPAINT) was used to study the binding of DAP to *S. aureus* at the single-molecule level.

2. Examination of the colocalization of DAP-TMR with the cell division protein FtsW and lipid II. Dual-color imaging was used to acquire images from two fluorescence channels. FtsW was expressed as a GFP fusion protein (FtsW-GFP) and nascent lipid II was labeled using BODIPY FL fluorescent vancomycin (Van-BDP FL).

3. Study of the specific interaction of DAP with selected lipid components. Fluid supported lipid bilayers, which were prepared on coverslips by fusion of very small unilamellar vesicles (VSUVs), were used to study the binding behavior of DAP dependent on the lipid composition of the membrane. PG and/or the bactoprenol lipids (C_{55}-P, C_{55}-PP, and lipid II) were integrated into neutral DOPC bilayers for investigating the specific binding of DAP. In addition, fruilimicin,

bacitracin, and oritavancin, which can specifically bind to C_{55}-P, C_{55}-PP, and lipid II respectively, were used to evaluate the specificity of DAP binding.

3. Materials and methods

3.1 Bacteria

3.1.1 Bacterial strains, media and growth conditions

The *S. aureus* strain used in this thesis was the MSSA strain RN4200. To study the colocalization of DAP with a cell division protein, we constructed *S. aureus* RN4220 strains expressing a C-terminal GFP fusion to FtsW by modifying its native chromosomal locus. Both strains were kindly provided by Dr. Fabian Grein from the Institute for Pharmaceutical Microbiology, University Hospital Bonn.

Glycerol stocks were used for long-term storage of the bacterial strains. An overnight culture was mixed 1:1 with sterile glycerol (v/v) and stored at -80 ℃. Prior to each experiment, the frozen bacterial strains were revived by streaking out on solid agar plates and incubating overnight at 37 ℃.

Unless otherwise noted, *S. aureus* were cultured either in Luria Bertani (LB) medium or in tryptic soy broth (TSB) at 37 ℃ with gentle agitation. The formula of the LB medium is described in Table 1. For growth experiments, cells were grown in LB medium at 37 ℃ until an optical density at 600 nm (OD_{600}) of 0.3 was reached; these cells were used in the subsequent steps.

Table 1. The formula of the Luria Bertani medium

1 % NaCl	5.0 g
1 % tryptone	10.0 g
0.5 % yeast extract	5.0 g
dH_2O	added to1 L
For agar plates	17 g agar per 1 L medium

3.1.2 Sterilization of media, equipment, and bacterial cultures

The maintenance of sterile conditions is necessary to work safely with bacterial samples.

Heat-stable culture media, solutions, buffers, plastic vials, and pipette tips were sterilized in a steam autoclave (Labortechnik AG, Oberschleißheim, Germany) at 121 ℃ for 20 min. Heat-sensitive solutions were filtered using cellulose acetate membrane filters (Millipore, Renner, Darmstadt, Germany). Glassware was incubated in a sterilizator (Kelvitron® T; Heraeus, Langenselbold, Germany) at 180 ℃ for 4 h. Bacterial cultures and contaminated labware were autoclaved at 134 ℃ for 30 min.

3.1.3 Measurement of optical density of liquid cultures

The cell density of bacterial suspensions was determined by measuring OD_{600} using a spectrophotometer, against the respective suspending medium as a blank.

3.1.4 Determination of the MIC of DAP

MIC is defined as the lowest antibiotic concentration that prevents visible turbidity after 18 h of incubation at 37 ℃. MIC was determines using 96-well polypropylene microtiter plates (TPP, Techno Plastic Products AG, Switzerland) containing LB medium supplemented with 1 mM $CaCl_2$ in a standard serial dilution assay accord-ing to the broth microdilution guidelines established by the Clinical and Laboratory Standards Institute (CLSI) [208]. A culture of *S. aureus* was grown to an OD_{600} of 1 and subsequently diluted to 1×10^5 cells/mL. Then, 50 µL of the bacterial suspension was mixed with 50 µL of DAP in LB medium (serial dilutions were performed to obtain 20, 15, 10, 5, 3, 2, 1.5, 1, 0.5, 0.25 µM solutions). The inoculated microtiter plate was incubated for 10 min at room temperature (RT) on a microtiter shaker (Titertek; Flow Laboratories, Germany). Positive controls contained 50 µL of inoculum and 50 µL of LB medium without antibiotic. The MIC was determined after 18 h of incubation at 37 ℃ without agitation. The results were recorded as mean values of at least two independent experiments performed in duplicate. $CaCl_2$ was added to all cultures to a final concentration of 1 mM, unless indicated otherwise.

3.1.5 Effect of Ca^{2+} on DAP activity

A culture of *S. aureus* was grown overnight in LB medium-containing flask at 37 ℃ on a rotating shaker at 250 rpm. The culture was then diluted 250-fold using fresh LB medium and incubated at 37 ℃ to an OD_{600} of 0.3. From this, aliquots were diluted 1000-fold using fresh LB medium in 250-mL flasks supplemented with: 1) no

antibiotic (control), 2) 2 μM DAP and 1 mM Ca^{2+}, 3) 0.5 mM DAP and 1 mM Ca^{2+}, 4) 2 μM DAP and 0.1 mM Ca^{2+}, 5) 2 μM DAP and 0.1 mM EDTA. Then samples were incubated at 37 ℃ with shaking at 250 rpm. The OD_{600} was measured during cell growth at every 30-min interval for a total period of 210 min.

3.2 Reagents

3.2.1 Chemicals and solvents

The reagents and chemicals used in this work and their respective suppliers are listed in Table 2. All the chemicals were of analytical grade or better.

Table 2. Chemicals and solvents used in this study

Chemical/Solvent	Manufacturer
BODIPY FL NHS ester	Lumiprobe
5(6) - TAMRA - X, SE	AnaSpec
Alexa fluor 546	Invitrogen
Nile red	Sigma-Aldrich
Agarose	Merck
Agarose low melt	Applichen
Agar	Invitrogen
Diethylether	Merck
Triton X-100	Merck
D-Serine	Sigma-Aldrich
Calcium chloride	Carl Roth
Zinc chloride	Carl Roth
Sodium chloride	Sigma-Aldrich
β-Cyclodextrin	Sigma-Aldrich
Glycerol	ICN Biomedicals Inc
Sodium hydroxide	Merck
Dimethyl sulfoxide (DMSO)	Sigma-Aldrich
Methanol	Merck
Ammonium Hydroxide	Sigma-Aldrich
Chloroform	Merck
Dimethylformamide (DMF)	Merck
Ethylene glycol-bis(2-aminoethylether)-	Sigma-Aldrich

N,N,N′,N′-tetraacetic acid (EGTA)	
Tryptone	Sigma-Aldrich
Yeast extract	Carl Roth
Tween-80	Calbiochem
Hellmanex II	Hellma
Sulfuric acid	Merck
Hydrogen peroxide	Sigma-Aldrich
Tryptone soya broth	Thermo Scientific

3.2.2 Antibiotics

When required, the appropriate antibiotic(s) was (were) added to either growth medium or solutions listed in Table 3. DAP, friulimicin and bacitracin were dissolved in sterile water. Oritavancin was dissolved and diluted in the presence of 0.002% Tween-80 (vol/vol). The solutions were filter-sterilized, aliquoted and stored at -20 ℃.

Table 3. Antibiotics used in this study

Antibiotic	Supplier / Source
Daptomycin	Novartis
Vancomycin-BODIPY FL	Molecular Probes
Friulimicin	University of Bonn, AG Sahl
Bacitracin	University of Bonn, AG Sahl
Oritavancin	University of Bonn, AG Sahl

3.2.2.1 Labeling of DAP

DAP was fluorescently labeled by coupling 5(6)-TAMRA-X, SE or BODIPY FL NHS ester to the amino group of DAP (Fig. 12). DAP was dissolved in dimethylformamide (DMF) to obtain a 3 mM stock solution and stored at -20 ℃. 5(6)-TAMRA-X, SE and BODIPY FL NHS ester were dissolved in DMSO at a concentration of 16 mM and 26 mM, respectively. Then, 1.5 µL of 5(6)-TAMRA-X, SE or BODIPY FL NHS ester were added per 10 µL of DAP stock solution and incubated for 1 h at room temperature with gentle agitation. After incubation, 100 µL of ice-cold diethyl ether was added to the mixture, and the mixture was immediately

incubated on ice to enable precipitation. After 3-5 minutes, precipitates were observed at the bottom of the tube; then, the mixture was centrifuged at 13000 rpm for 5 min. The supernatant was carefully removed, the tube was rested for ~5 minutes to allow evaporation of the remaining ether, and the pellet was resuspended in methanol. Labeled and non-labeled DAP were separated by preparative thin-layer chromatography (TLC) using Rick solvent (chloroform/methanol/Aqua dest./ammonium hydroxide [88:48:10:1 (v/v)]). The bands corresponding to the labeled DAP were scratched from the TLC plates (Fig. 13), then extracted from the silica using distilled water.

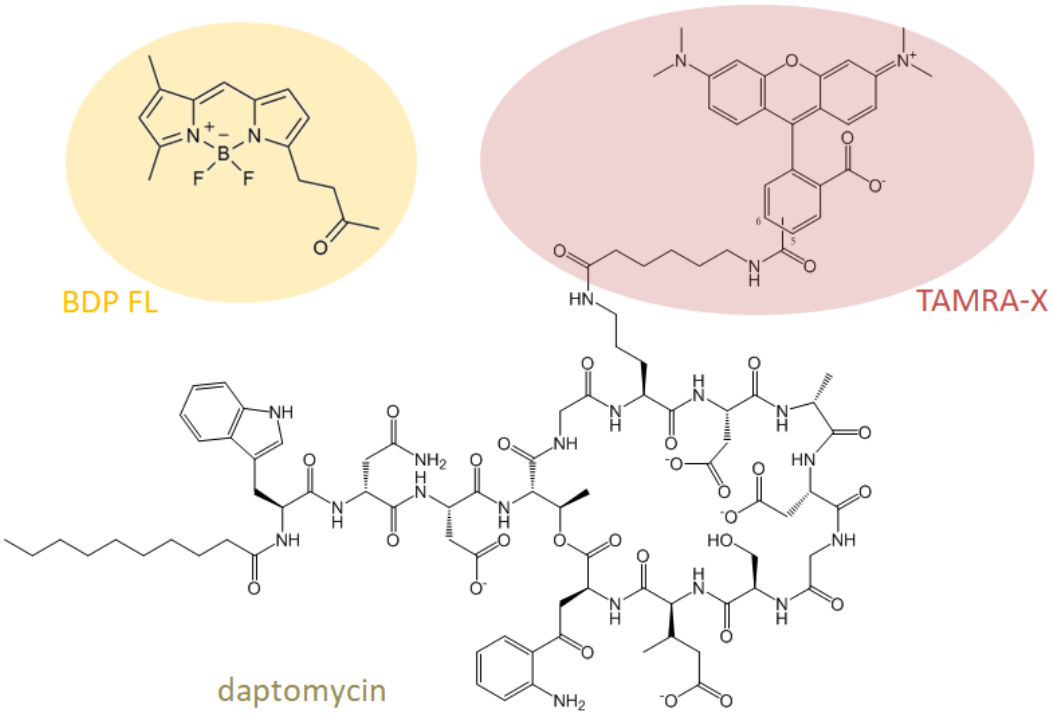

Figure 12: Structures of fluorescently labeled daptomycin (DAP) derivatives used in this study. The ornithine residue has a single free amino group, which was labeled with the fluorophores 5(6)-TAMRA-X, SE or BODIPY FL NHS ester to form DAP-TMR and DAP-BDP FL, respectively.

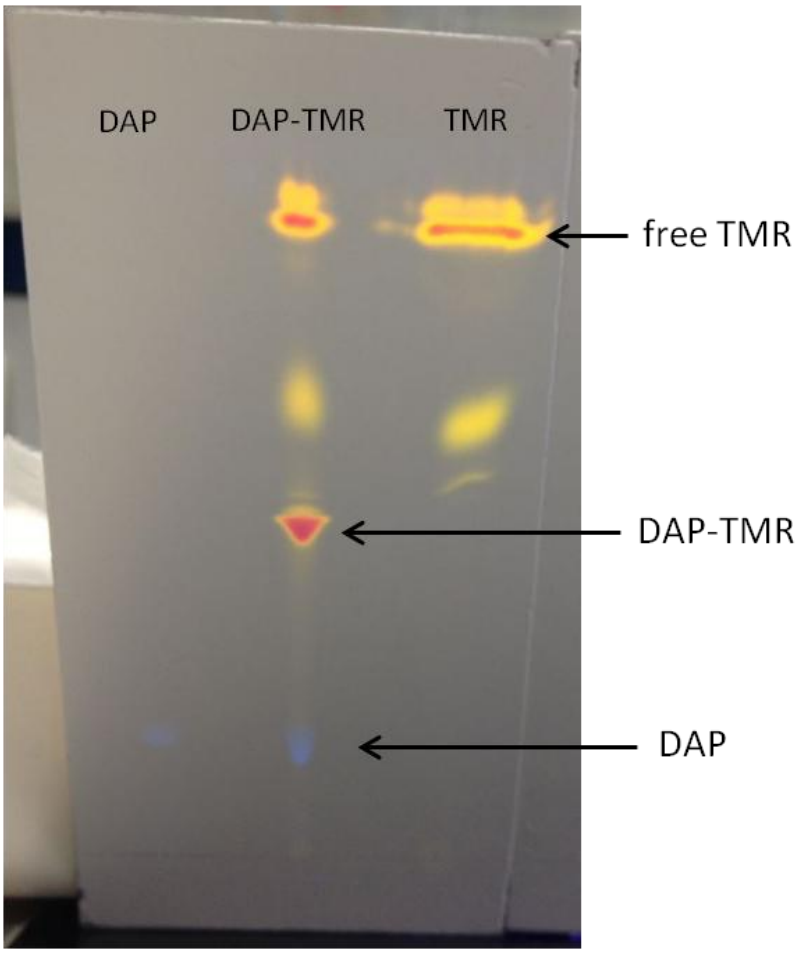

Figure 13: Photograph of a thin-layer chromatographic purification of 5(6)-TAMRA-X, SE-labeled daptomycin (DAP-TMR). The plate was illuminated by a UV lamp in order to visualize the DAP band duo to the intrinsic fluorescence of kynurenine residue.

3.2.2.2 Antibacterial activity testing for DAP-TMR and BODIPY FL-labeled DAP

DAP-TMR and BODIPY FL-labeled DAP (DAP-BDP FL) were tested for their antibacterial activity by broth dilution assays as described in section 3.1.4. Serially diluted labeled DAP solutions (20, 15, 10, 8, 5, 3, 2, 1.5, 1 and 0.5 μM) with 1 mM calcium in LB broth were tested. Growth inhibition was evaluated visually by turbidity. Growth controls without the antibiotic were prepared for comparison.

3.2.2.3 Van-FL labeling of *S. aureus*

A BODIPY FL conjugate of vancomycin (Van-BDP FL) was used to label cell walls of *S. aureus*. A culture of *S. aureus* RN4200 was grown overnight in tryptone soy broth (TSB) containing 0.125 M of D-serine [209]. For fresh culture, 20 μL the

overnight culture was added to 5 mL TSB and 0.125 M D-serine, yielding a 1/250 dilution, and the culture grown to an OD_{600} of 0.25. Cells were then washed and resuspended in the same volume of pure TSB medium, and incubated for 5 min at room temperature to allow D-Ala incorporation into the cell wall. Cells were then incubated with 2 μM Van-BDP FL for not longer than 5 min. The cells were washed to remove excess Van-BDP FL and incubated with a mixture of 0.1 μM DAP-TMR and 1 μM unlabeled DAP in the presence of 1 mM Ca^{2+}. Cells were washed again and immobilized on an agarose pad and observed by fluorescence microscopy.

3.2.3 Lipids

The phospholipids used in this study and their suppliers are listed in Table 4. All the lipids were dissolved in chloroform in phosphate-free tubes and stored at -20 ℃.

Table 4. Phospholipids

Lipids	Supplier / Source
DOPC: 1,2-dioleoyl-sn-glycero-3-phosphocholine; 18:1 phosphatidylcholine	Avanti Polar Lipids, Alabaster, USA
DOPG: 1,2-dioleoyl-sn-glycero-3-[phosphor-rac(1-glycerol)] sodium salt; 18:1 phosphatidylglycerol	Avanti Polar Lipids, Alabaster, USA
TopFluor PC	Avanti Polar Lipids, Alabaster, USA
C_{55}-P	Larodan Fine Chemicals AB
C_{55}-PP	Larodan Fine Chemicals AB
Lipid II	University of Bonn, AG Sahl

3.2.3.1 Preparation of fluid supported bilayers

Fluid supported bilayers were prepared on coverslips by fusion of VSUVs (average diameters of 18-25 nm), which were generated by detergent extraction with cyclodextrin [210]. Neutral DOPC was used as a matrix to which 0.1 mol% or 0.2 mol% of PG or/and bactoprenol lipids (C_{55}-P, C_{55}-PP, and lipid II) respectively, were added. TopFluor PC was used to visualize lipid membranes by fluorescence microscopy and gauge the mobility of the supported lipid bilayers. Twelve types of bilayers with different lipid components were prepared in this work. The types and

the corresponding volumes obtained from their stock solutions are listed in Table 5. The preparation of fluid supported bilayers is described in the next section.

Lipid vesicle preparation

The lipids from chloroform stock solutions were mixed in the appropriate molar ratios in clean glass vials, and the solvent was removed under a nitrogen stream. For fluorescence recovery after photobleaching (FRAP) measurements, 0.1 mol% TopFluor PC was included prior to evaporation. The dried thin lipid film was resuspended in 2 mL Triton X-100-HEPES buffer (20 mM HEPES, 150 mM NaCl, 2 mM Triton X-100). For vesicle preparation, 200 µL lipid detergent solution was thoroughly mixed with 200 µL of cyclodextrin-HEPES buffer (20 mM HEPES, 150 mM NaCl, 4 mM cyclodextrin) by vortexing for 2 min. The vesicles were generally used within 1 h of preparation.

Supported bilayer formation on glass

The vesicle fusion method was used to spread VSUVs onto a glass coverslip to form homogeneous lipid bilayers; the bilayer formation occurs within a few minutes. Here, 400 µL VSUV solutions were pipetted onto glass slides in a home-built chamber and incubated for 10 min. The samples were then gently rinsed at least 5 times by adding 300 µL and taken away with the same amount HEPES buffer. Great care was taken to prevent contact between the bilayer surface and air.

Prior to bilayer formation, the glass coverslips were cleaned using Piranha solution (5:1 v/v concentrated H_2SO_4: 30% H_2O_2) for 30 minutes and rinsed extensively in distilled water. The home-built chambers were cleaned by sonicating in a 2% Hellmanex (Hellma, Müllheim, Germany) solution for 30 min and rinsing extensively with fresh distilled water. The coverslips and chambers were dried under airflow.

Table 5. The Lipid components used in the various bilayer preparations

Number	Components
1.	DOPC
2.	DOPC + 0.1 mol% DOPG
3.	DOPC + 0.1 mol% C_{55}-PP

4.	DOPC + 0.1 mol% C_{55}-P
5.	DOPC + 0.1 mol% lipid II
6.	DOPC + 0.1 mol% DOPG + 0.1 mol% C_{55}-PP
7.	DOPC + 0.1 mol% DOPG + 0.1 mol% C_{55}-P
8.	DOPC + 0.1 mol% DOPG + 0.1 mol% lipid II
9.	DOPC + 0.2 mol% DOPG
10.	DOPC + 0.2 mol% C_{55}-PP
11.	DOPC + 0.2 mol% C_{55}-P
12.	DOPC + 0.2 mol% lipid II

3.2.3.2 Inhibition of DAP binding by specific target molecules

Bacitracin, fruilimicin, and oritavancin were used to treat the bilayers containing 0.1 mol% DOPG + 0.1 mol% C_{55}-PP, 0.1 mol% DOPG + 0.1 mol% C_{55}-P, and 0.1 mol% DOPG + 0.1 mol% lipid II, respectively.

Binding of each antibiotic to the corresponding bilayers was achieved by incubating 300 nM antibiotic with the bilayer (approximate ratio was 100 antibiotic molecules: 1 bactoprenol molecule) for 5 min. Notably, 0.5 mM Zn^{2+} and a final concentration of 0.002% Tween 80 (vol/vol) were presented for the treatment of Bacitracin and oritavancin, respectively.

The excess unbound antibiotics were gently washed off by adding 300 µL and taken away with the same amount HEPES buffer. Great care was taken to prevent contact between the bilayer surface and air.

3.3 Fluorescence imaging methods

3.3.1 Fluorescence microscopy

A culture of *S. aureus* was grown in LB medium at 37 ℃ to an OD_{600} of 0.25. Then, 1-mL cell suspension was pipetted into each of the six Eppendorf centrifuge tubes, and the suspensions were centrifuged, washed with HEPES buffer, and resuspended in 1/10 of the starting volume. Then, 100 µL of the concentrated cell suspension in each tube was incubated with a mixture of 0.1 µM DAP-TMR and 0.5 µM non-labeled DAP. The cells in the six tubes were incubated for 0.5, 5, 10, 15, 20, and 25

min, respectively. The excess unincorporated DAP-TMR and non-labeled DAP were removed by washing the cells in HEPES buffer immediately. A small aliquot (2 µL) of the treated cells was placed on an agarose pad (1% low-melting point agarose in sterile water). The inverted agarose pad was then placed in a microscopy chamber (MatTek, USA) and imaged immediately.

In addition to 0.5 µM non-labeled DAP, cells were also treated with a mixture of 0.1 µM DAP-TMR and 1 µM, 6 µM, and 10 µM non-labeled DAP, in the presence of 1 mM Ca^{2+} and imaged in the same way. Furthermore, where required, the exponentially growing cells of *S. aureus* RN4220 were stained with the membrane dye Nile red (5 µM).

Fluorescence microscopy was performed using HILO to image the binding of low amounts of DAP-TMR with reduced background fluorescence [211]. The oblique illumination beam angle was adjusted by focusing the beams in the back focal plane of the objective and shifting laterally. The schematic of the optical setup is shown in Fig. 14. An inverted microscope was equipped with a 63× objective lens with a numerical aperture (NA) 1.46 (Zeiss, Jena, Germany) and a 4× magnifier (Carl Zeiss MicroImaging GmbH, Göttingen, Germany) onto an electron-multiplying charge-coupled device (EMCCD) camera (iXon DU-897D; Andor Technology, Belfast, Northern Ireland); 2 × 2 binning during acquisition resulted in a pixel size of 127 nm. Images were obtained within 3 min after DAP addition and recorded using transmitted light as well as laser excitation at 532 nm emitted by a solid-state laser (LaNova50 Green, Lasos, Germany) for 5(6)-TAMRA-X, SE. Fluorescence was filtered using the appropriate notch filter (NF03-532E-25, Semrock, USA).

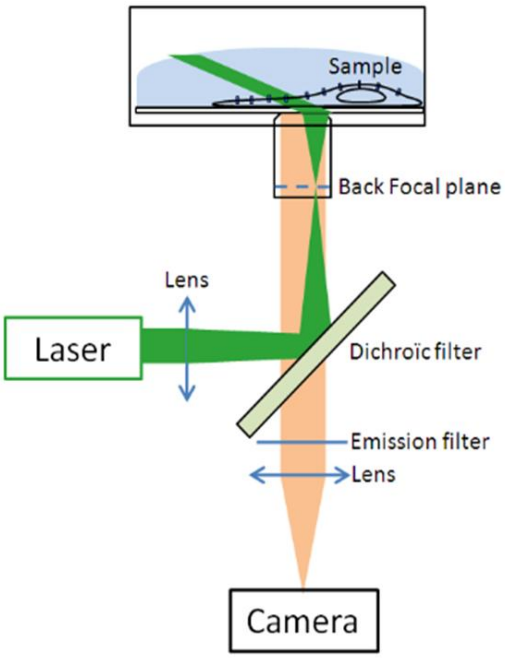

Figure 14: Schematics of the highly inclined and laminated optical sheet (HILO) microscopy optical setup. Picture adopted from Giannone et al. [211].

3.3.2 Super-resolution imaging

We used the uPAINT method to study the binding of DAP-BDP FL to *S. aureus* at the single-molecule level [211].

S. aureus RN4220 was grown in LB medium to exponential phase (OD_{600} = 0.25) at 37 ℃. Cells were centrifuged, washed with HEPES buffer, and resuspended in 1/10 of the starting volume. A small aliquot (2 µL) of cells was placed on an agarose pad (1% low-melting point agarose in sterile water). The inverted agarose pad was then placed in a microscopy chamber (MatTek), and the chamber was placed under microscope. Before imaging, a mixture of 1 nM DAP-BDP FL and 6 µM non-labeled DAP was added into the chamber.

Super-resolution imaging techniques comprise a rapidly emerging new field of microscopy that enhances the spatial resolution of light microscopy, allowing the observation of biological processes at the molecular level. Various super-resolution imaging methods have been devised, and they can be further categorized as illumination-based methods such as stimulated emission by depletion (STED) fluorescence microscopy and single-molecule localization-based methods such as

stochastic optical reconstruction microscopy (STORM), photoactivated localization microscopy (PALM), and PAINT. uPAINT, one of the single-molecule localization based super-resolution methods, can be implemented on any wide-field fluorescence microscope operating in oblique illumination [212]. uPAINT is based on real-time imaging of fluorescently labeled target biomolecules on the cell membrane at the single-molecule level [211]. A low concentration of fluorescent ligands for the targets of interest is introduced in the extracellular medium to ensure that a constant number of membrane molecules is being labeled during a imaging sequence. Oblique illumination is critical, as it allows to image fluorescent ligands bound to the cell surface without exciting the molecules in the solution above (Fig. 15). Thus, the uPAINT method is ideally suited for studies of membrane-bound molecules.

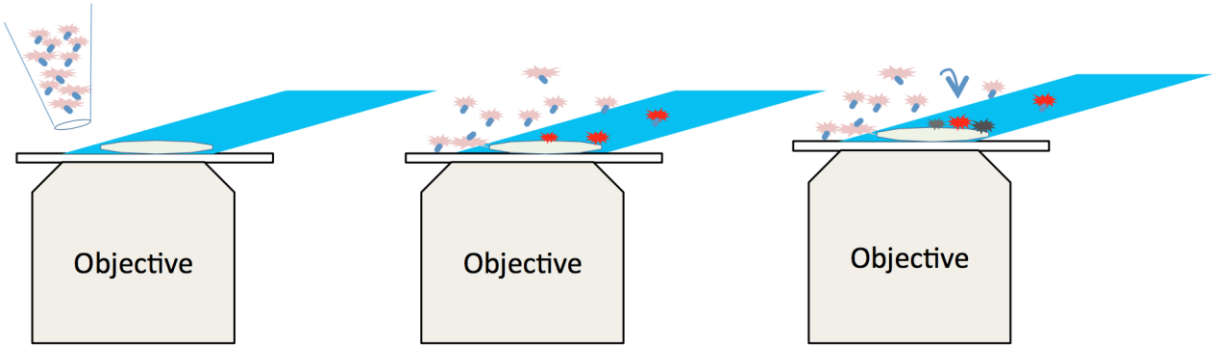

Figure 15: The principle of universal point accumulation imaging in the nanoscale topography (uPAINT). Low concentrations of labeled ligands are added to the cell medium. Non-illuminated dye molecules are displayed in pink, fluorescent ones in red, and photobleached ones in brown; the oblique illumination is marked in blue.

uPAINT acquisitions were performed on an inverted microscope operated in the HILO mode (Fig. 14). The tilting angle between the sample and the illumination beam was set to 5 °to obtain an illumination thickness of ~2 µm in the center of the field. It allowed the imaging of individual DAP-BDP FL molecules bound to the cell surface. The microscope was equipped with a 100× objective lens with an NA of 1.46. And a 4× magnifier was inserted before an EMCCD camera; 2 × 2 binning during acquisition resulted in a pixel size of 80 nm. A built-in C-Focus™ system (Mad City Labs Inc., USA) was used to eliminate any possible microscope focus drift over long data collection periods.

BDP FL dyes were excited by a 488-nm laser (Sapphire-100; Coherent, USA); the illumination intensity was adjusted to 1-3 kW/cm^2. Fluorescence was filtered using the appropriate notch filter (NF03-488E-25, Semrock). Images were acquired with an integration time of 20 ms and EM gain of 280. Two-image stacks of 9,000 images were recorded for the first 3 min and the second (subsequent) 3 min after DAP addition. Images were reconstructed with the software thunderSTORM [213].

3.3.3 Dual color imaging

We examined the colocalization of DAP-TMR with the cell division protein FtsW and lipid II by combining HILO microscopy with dual-color imaging. For this, we inserted a dual-emission image splitter (OptoSplit II; Cairn Research Ltd, Faversham, UK) in front of the camera (Fig. 16).

S. aureus expressing FtsW-GFP were grown in LB medium to an OD of 0.25 at 37 ℃. Cells were centrifuged, washed with HEPES buffer, and resuspended in 1/10 of the starting volume. Then, 100 µL of the concentrated cell suspension in each tube was incubated with a mixture of 0.1 µM DAP-TMR and 1 µM non-labeled DAP for 0.5 min. Excess unincorporated DAP-TMR and non-labeled DAP were removed by washing the cells in HEPES buffer immediately. A small aliquot (2 µL) of the treated cells was placed on an agarose pad. The inverted agarose pad was then placed into a MatTek chamber and imaged with a microscope immediately.

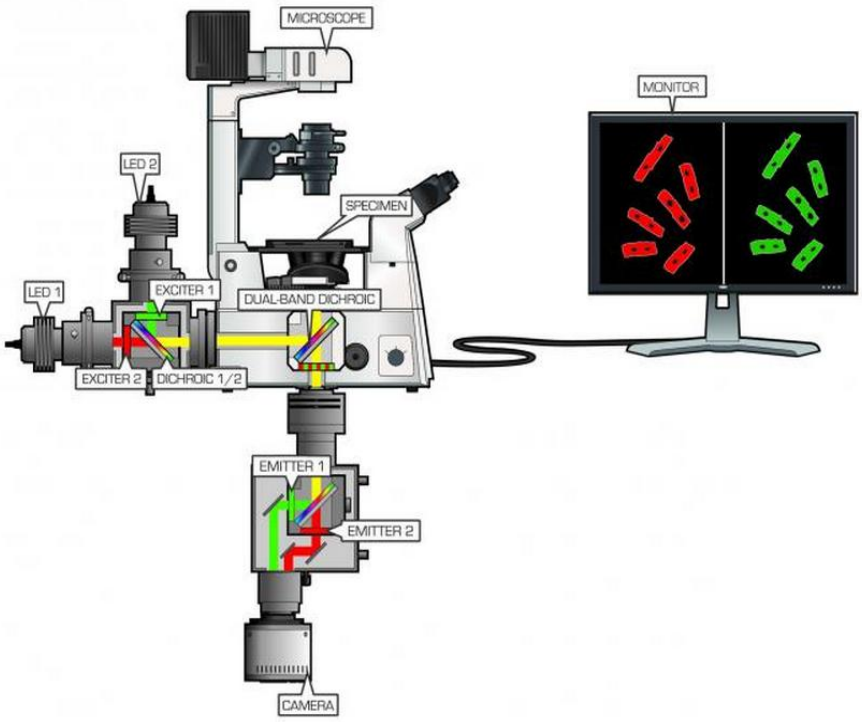

Figure 16: Schematics of the dual-color imaging system. The OptoSplit II system was inserted in the light path between microscope and the electron-multiplying charge-coupled device (EMCCD; Schematic produced by Cairn Research).

Fluorescence images were acquired using HILO microscopy. An inverted microscope was equipped with a 63× objective lens with an NA of 1.46. A 4× magnifier was inserted in front of an EMCCD camera (iXon X-1170; Andor Technology); 1×1 binning during acquisition resulted in a pixel size of 63.5 nm. The OptoSplit II system was placed in the light path between the microscope and EMCCD to visualize the two color channels in two spectrally separated images on the camera. A dichroic mirror (FF509-FDi01-25x36; Semrock) and a band-pass emission filter (LP02-561RE-25, Semrock) were used to separate the emission channels. Image separation was adjusted such that the camera chip was fully illuminated and the two spectrally separated images covered equal areas. FtsW-GFP fusion proteins were excited by a 488 nm laser (Sapphire-100), and the TMR dyes were excited by a 532 nm laser (LaNova50 Green, Lasos). Two laser lines were guided to an acousto-optical tunable filter (AOTF; nC 1001, Opto-Electronics, France). The AOTF selected laser lines and defined illumination durations and intensity. Fluorescence was filtered using the appropriate notch filters (NF03-488E-25 and NF03-532E-25; Semrock).

Z-stacks were acquired for the two fluorescence color channels. A step size of 50 nm was used for acquiring z-stacks and 61 images were acquired for each stack. This covered a distance of 3 μm, which is larger than the axial extension of the bacteria. μ-Manager [214] was used as the main program to control most of the components in the setup, including lasers, AOTF, motorized and piezo stages, EMCCD camera, and shutters.

3.3.4 Total internal reflection microscopy

Binding of DAP-BDP FL to lipid bilayers was studied using total internal reflection fluorescence (TIRF) microscopy.

TIRF microscopy is a wide-field microscopy technique that allows selective excitation of samples just near the coverslip, with a thickness of approximately 100 nm. An evanescent field is produced by a light beam passing through the coverslip with a large incident angle, which must be larger than the critical angle to ensure total internal reflection (TIR) of the beam at the glass/medium interface. Such TIR generates a very thin electromagnetic field above the coverslip. The intensity of this field decays exponentially with an increase in the distance from the surface [215]. This field can illuminate fluorescent molecules near the surface while avoiding excitation of the surrounding bulk molecules present further in the liquid. Thus, TIRF microscopy provides better contrast and reduced background signal from surfaces. The thin volume of excitation near the coverslip makes this technique ideal for investigating supported lipid bilayers.

TIRF microscopy was performed using an inverted microscope equipped with a 63× oil immersion objective lens with an NA 1.46. A 4× magnifier was placed in front of onto an EMCCD camera; 2 × 2 binning during data acquisition resulted in a pixel size of 127 nm. For fluorescence excitation, a 488 nm laser (Sapphire-100) was used for BDP FL, and the excitation light was blocked using a notch filter (NF03-488E-25).

After the supported lipid bilayers were formed on glass coverslips in the custom-built chamber, 1 mM Ca^{2+} was added into the chamber and the bilayers were incubated for 5 min. Then, a mixture of 50 nM DAP-BDP FL and 1 μM non-labeled DAP was added into the chamber and imaged within 2 min.

For each condition, data were collected from at least 20 different areas on the bilayers. Movies with 100 frames were recorded at a frame rate of 60 Hz within 2 min after DAP addition.

4. Results and Discussion

4.1 DAP binding behavior on the membrane of *S. aureus*

4.1.1 Susceptibility testing of native DAP and fluorescently labeled DAP derivatives

The MIC of native DAP, which was determined by serial dilution, for the strain RN4200 used in this study was 1 μM. DAP-TMR and DAP-BDP FL, the two fluorescent derivatives of DAP, were shown to retain antimicrobial activity. Both of them are 3 to 5 times less active than the ummodified DAP. Their reduced activity may not be attributed to modification of the ornithine residue because DAP variants with N-acylated ornithine show only minor differences in MIC [216]. Therefore, a mixture of labeled DAP and a varying concentration of unlabeled DAP was used in the subsequent fluorescence microscopy measurements.

4.1.2 Effect of calcium on the bactericidal activity of DAP

DAP has previously been described to inhibit bacterial growth by disrupting normal cell membrane or cell wall function. It has been clearly established that calcium ions are essential for the DAP activity against gram-positive bacteria [137,139] and that the activity is diminished in the presence of alternative divalent ions. The peptide moiety of DAP is anionic, and it has a net charge of -3 at pH 7. The calcium-DAP complex acts as a cationic peptide and approaches the cell membrane by an electrostatic interaction. To reconfirm the effect of Ca^{2+} on the activity of DAP against cultures of *S. aureus*, we compared the cell growth rates during DAP treatment with supra-MIC doses (2 μM) and sub-MIC doses (0.5 μM) in the presence of varying Ca^{2+} concentration: no Ca^{2+} (0.1 mM EDTA was used to chelate divalent cations in LB medium); physiological level of Ca^{2+} (1 mM); and low Ca^{2+} level (0.1 mM). The untreated culture was considered as control. Culture density (OD_{600}) was measured periodically during DAP treatment.

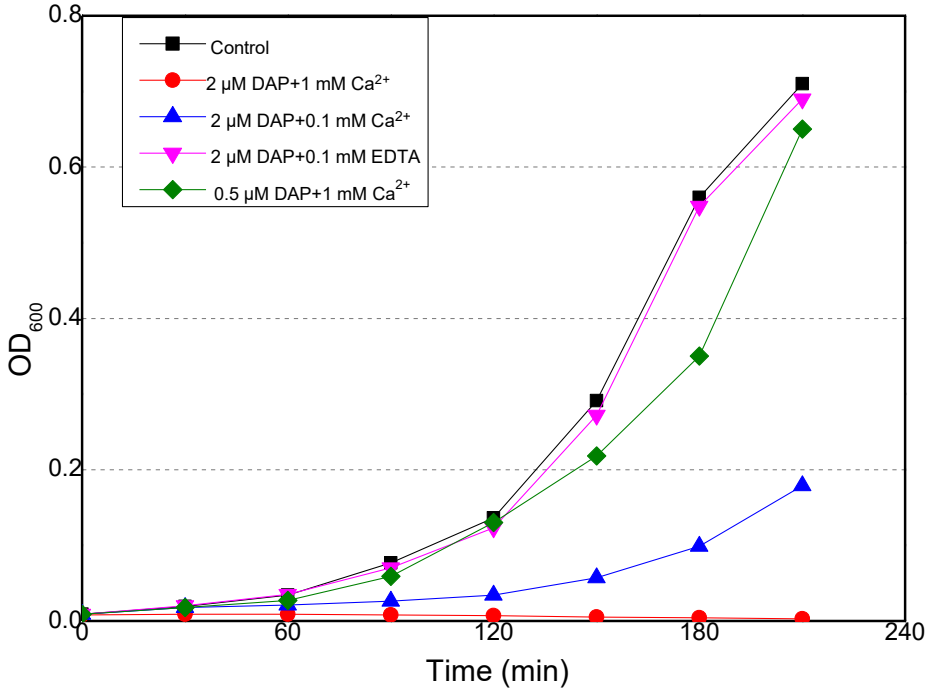

Figure 17: Growth dependence of *Staphylococcus aureus* cells on the concentration of daptomycin and Ca^{2+}. Cells were grown in the presence of different concentrations of DAP and Ca^{2+}, and the growth was monitored by measuring the optical density at 600 nm (OD_{600}). This is a qualitative test for verification only.

Cells treated with a supra-MIC dose (2 µM) with 0.1 mM EDTA and sub-MIC dose (0.5 µM) with 1 mM Ca^{2+} showed growth rates identical to those in the control, whereas cells treated with supra-MIC doses with insufficient concentration of Ca^{2+} (0.1 mM) showed considerably slow growth. In contrast, the bacterial growth was completely inhibited under the treatment with supra-MIC doses with 1 mM Ca^{2+}. These findings confirm that the bactericidal activity of DAP on *S. aureus* cultures is calcium-dependent.

4.1.3 Fluorescence microscopy of *S. aureus* treated with DAP

S. aureus is a gram-positive bacterium and a prominent pathogen in the community and healthcare settings, and is therefore widely used as a model organism. To investigate the binding behavior of DAP to *S. aureus*, we used DAP-TMR, fluorescently labeled DAP with antimicrobial activity. By using HILO microscopy,

we imaged the binding of low amounts of DAP-TMR to *S. aureus* cells with reduced background fluorescence.

Cells were grown to exponential phase (OD_{600} = 0.25) in LB medium. One hundred microliters of cells were incubated with a mixture of 0.1 µM DAP-TMR and increasing concentrations of non-labeled DAP: sub-MIC (0.5 µM), in the range of MIC (1 µM), and supra-MIC (6 and 10 µM). The cells were imaged at different time points (0.5, 5, 10, 15, 20, and 25 min; Fig. 18). The same contrast settings were used for all images in Fig. 18A. However, to visualize the fluorescence distribution on cells at different times and concentrations, the contrast and brightness of each image was set to an optimal value in Fig. 18B.

DAP-TMR accumulated at the cell membrane (Fig.18) and there were several noticeable findings: 1) cell intensity and cell size were considerably different after treatment with different concentrations of DAP; 2) spotty pattern cells (red arrows) and "very bright" cells (yellow arrows) appeared at DAP concentrations above the MIC; 3) DAP-TMR bound to the septum at sub-MIC DAP concentrations and around the MIC, but to the complete membrane at supra-MIC DAP concentrations. Next, we quantitatively analyzed the amount of cell-bound DAP in correlation to cell size and spotty pattern formation and DAP location on the cell membrane.

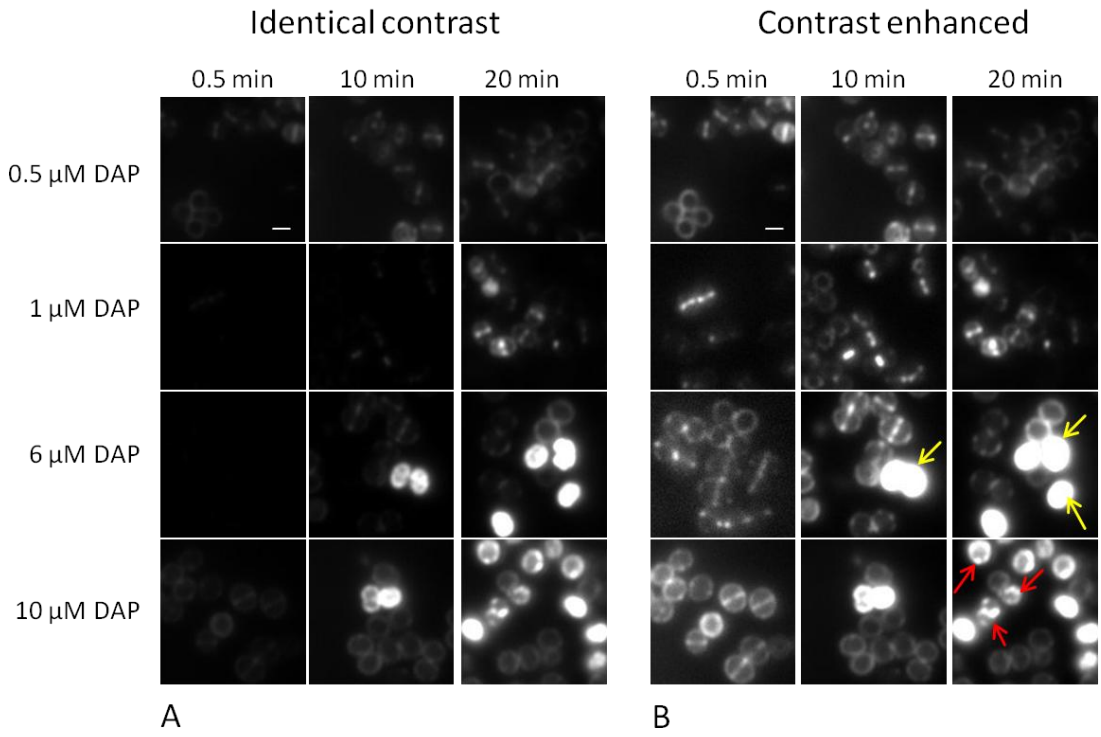

Figure 18: Representative images for localization of 5(6)-TAMRA-X, SE-labeled daptomycin (DAP-TMR) in *Staphylococcus aureus*. One hundred microliters of cells were incubated with a mixture of 0.1 µM DAP-TMR and increasing concentrations of non-labeled DAP in presence of 1 mM Ca^{2+}. Each sample was then imaged at different time points (0.5, 5, 10, 15, 20, and 25 min). Panel A: raw images with the same contrast setting; panel B: Image contrast and brightness were adjusted to visualize each cell. Red arrows: cells with spotty patterns; yellow arrows: "very bright" cells. Scale bar: 1 µm.

4.1.3.1 Correlation between DAP-TMR intensity and cell size

First, we analyzed the mean fluorescence intensity and size of each cell at each time point using the ImageJ program [217]. Cell sizes were calculated from the measured cell diameter assuming round cell shapes. As shown in Fig. 19, for cells treated with sub-MIC DAP concentration (0.5 µM), the mean intensity and size per cell remained constant. However, for cells treated with DAP concentrations around the MIC (1 µM), the mean intensity and cell size were constant for the first 10 min of incubation. At longer incubation times, the intensity increased whereas the cell size decreased. Cells treated with DAP concentration higher than the MIC (6 µM and 10 µM) exhibited more drastic increase in the mean fluorescence intensity and decrease in cells size in an incubation time-dependent manner.

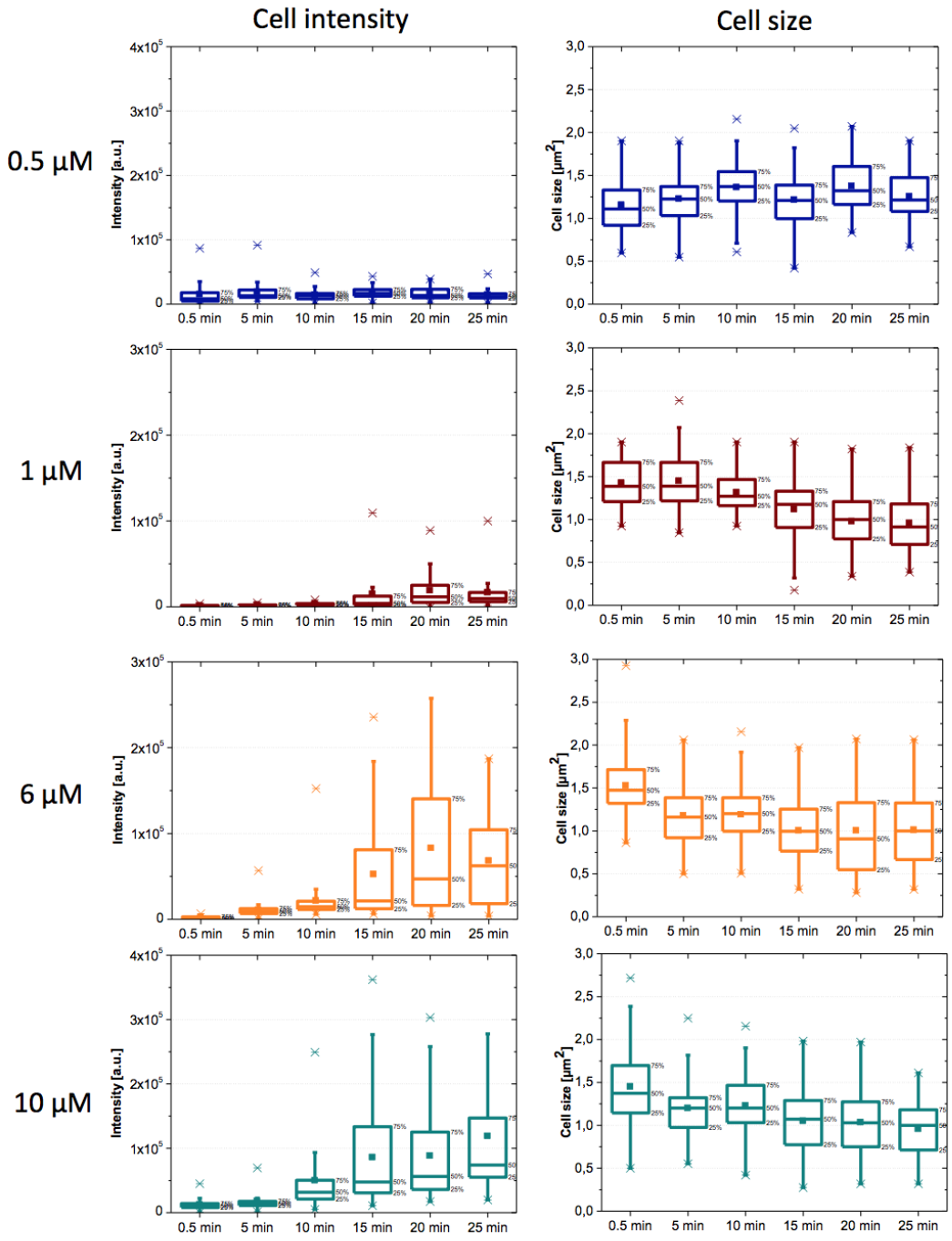

Figure 19: Quantitative analysis of fluorescence intensity and cell size. Mean fluorescence intensity and cell size at each time point were evaluated. The box represents 25th and 75th percentiles, the median is denoted by middle horizontal line, and the mean is indicated by small squares. Whiskers show 5-95 percentile and asterisks represent minimum and maximum values. Approximately 80 cells were analyzed at each time point.

The correlation between mean fluorescence intensity and cell size was further analyzed; the mean intensity per cell was plotted against cell size, for each

concentration (Fig. 20). The data for the various time points were color-coded. For 0.5 μM DAP, most data points distributed compactly in the area of low intensity and a cell size of 1-1.5 μm^2. For 1 μM DAP, the points were more scattered at incubation time of 15, 20, and 25 min, implying that more points were located at higher intensity but smaller cell size (0.3-1.0 μm^2). For 6 μM and 10 μM DAP, a negative correlation between fluorescence intensity and cell size was observed after 0.5 min.

It has been reported that DAP does not induce cell lysis in *S. aureus*, and transmission electron microscopy (TEM) showed that cell membranes remained intact but the cells formed aberrant division septa [130]. Studies of *B. subtilis* cells treated with sub-MIC DAP concentrations showed bent and elongated shapes [131]. Our results indicate that strong DAP binding to the cell membrane results in reduction of the cell size in *S. aureus*. Interestingly, Chen and coworkers [218] proposed a lipid extracting mechanism, they found that DAP removed lipid molecules from giant unilamellar vesicles (GUVs) by forming lipid-peptide aggregates, resulting in a reduction of GUV size. The lipid extracting effect is dependent on the DAP concentration (around or supra-MIC) and in the presence of Ca^{2+} and PG, the same conditions required for DAP antibacterial acitivity. This indicates that a correlation may exist between the lipid extracting effect and the antibacterial activity of DAP. This mechanism by which DAP may remove lipids from the cell membrane that we observed can probably explain the reduction of cell size.

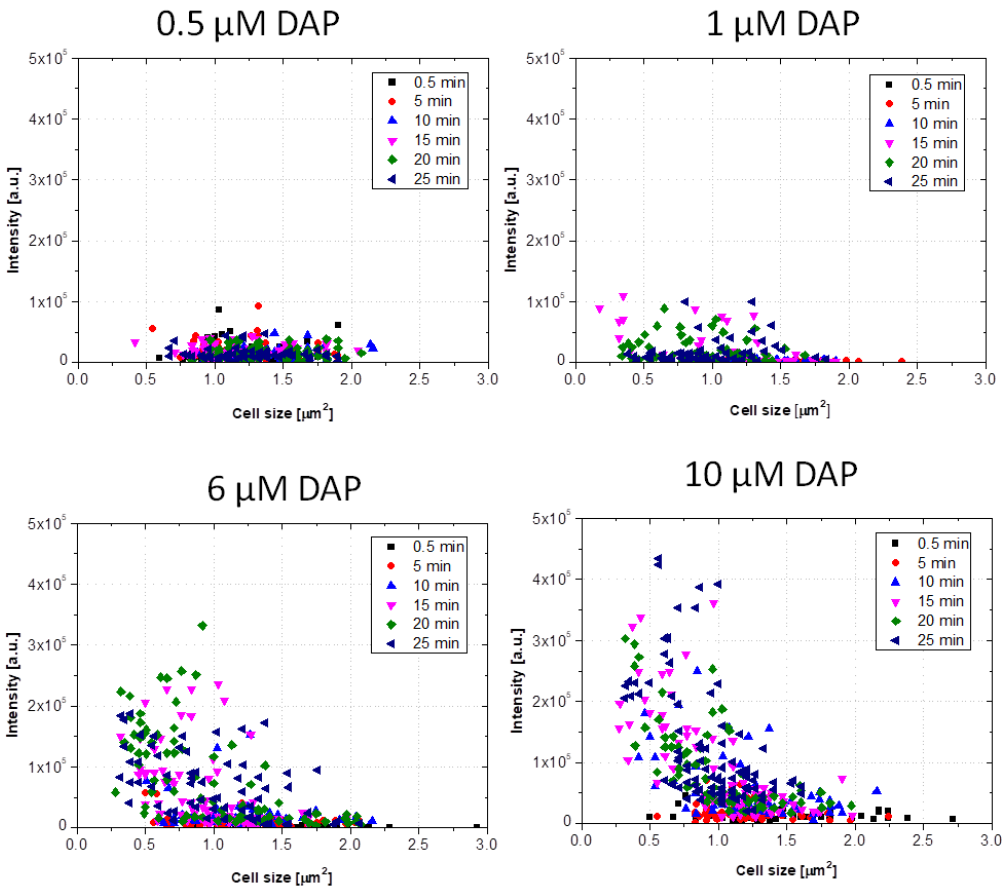

Figure 20: Correlation between 5(6)-TAMRA-X, SE-labeled daptomycin (DAP-TMR) intensity and cell size for different DAP concentrations. The mean fluorescence intensity of cells was plotted against cell size. Incubation time has been color-coded as indicated.

4.1.3.2 Analysis of formation of spotty pattern cells and "very bright" cells

As shown in Fig. 18, spotty pattern cells and cells that accumulated DAP-TMR densely, which we termed as "very bright" cells, appeared at supra-MIC DAP concentrations. Therefore, we calculated the percentages these two types of cells at each time point for each concentration (Fig. 21). The "very bright" cells were defined as cells with a mean fluorescence intensity value > 1×10^5. Neither the "very bright" nor the spotty patterns cells were observed when cells were treated with sub-MIC DAP concentration (0.5 µM); only a few "very bright" and spotty pattern cells were observed at longer incubation times (after 15 min) for cells treated with 1 µM DAP; and the percentages of both cell types increased steadily from 0.5 min to 25 min of the incubation time at supra-MIC DAP concentrations (6 µM and 10 µM). This indicated a positive correlation between DAP accumulation and spotty pattern formation.

Spotty patterns were also reported in the studies of *B. subtilis* by Poliano et al. [131] and Müller et al. [140]. Poliano demonstrated that DAP generates randomly positioned membrane patches at both lethal and sublethal doses and that such patches specifically recruit the cell division protein DivIVA, which can bind to negatively curved membranes; thus, DAP induces negative membrane curvature. However, Müller showed that such DAP-induced membrane patches do not cause membrane curvature and that DAP clusters fluid lipid (lipids with short, branched or unsaturated fatty acyl chains) domains by forming large DAP-fluid lipid complexes, thus affecting the overall membrane fluidity. A DAP-BDP FL labeled spiral pattern along the cell wall was reported in *B. subtilis*; this pattern is due to a preferential interaction with the membrane in PG-enriched regions. Studies of lipid vesicles showed that DAP molecules form oligomers on liposomes and that the oligomerization is dependent on Ca^{2+} and the presence of PG in the target membrane [143,219,220].

Our results demonstrate that DAP induces spotty patterns in *S. aureus* only at concentrations around (1 µM) and above MIC (6 µM and 10 µM); this result is consistent with the report that DAP induces lipid-peptide aggregates on the surface of GUVs at concentrations of 1 µM and 5 µM but does not induce aggregates at concentration of 0.3 µM [218]. This suggests that the spotty pattern and the bactericidal activity of DAP are correlated.

Whether DAP targets on cell division proteins and how DAP acts on artificial membranes were further investigated in the following measurements.

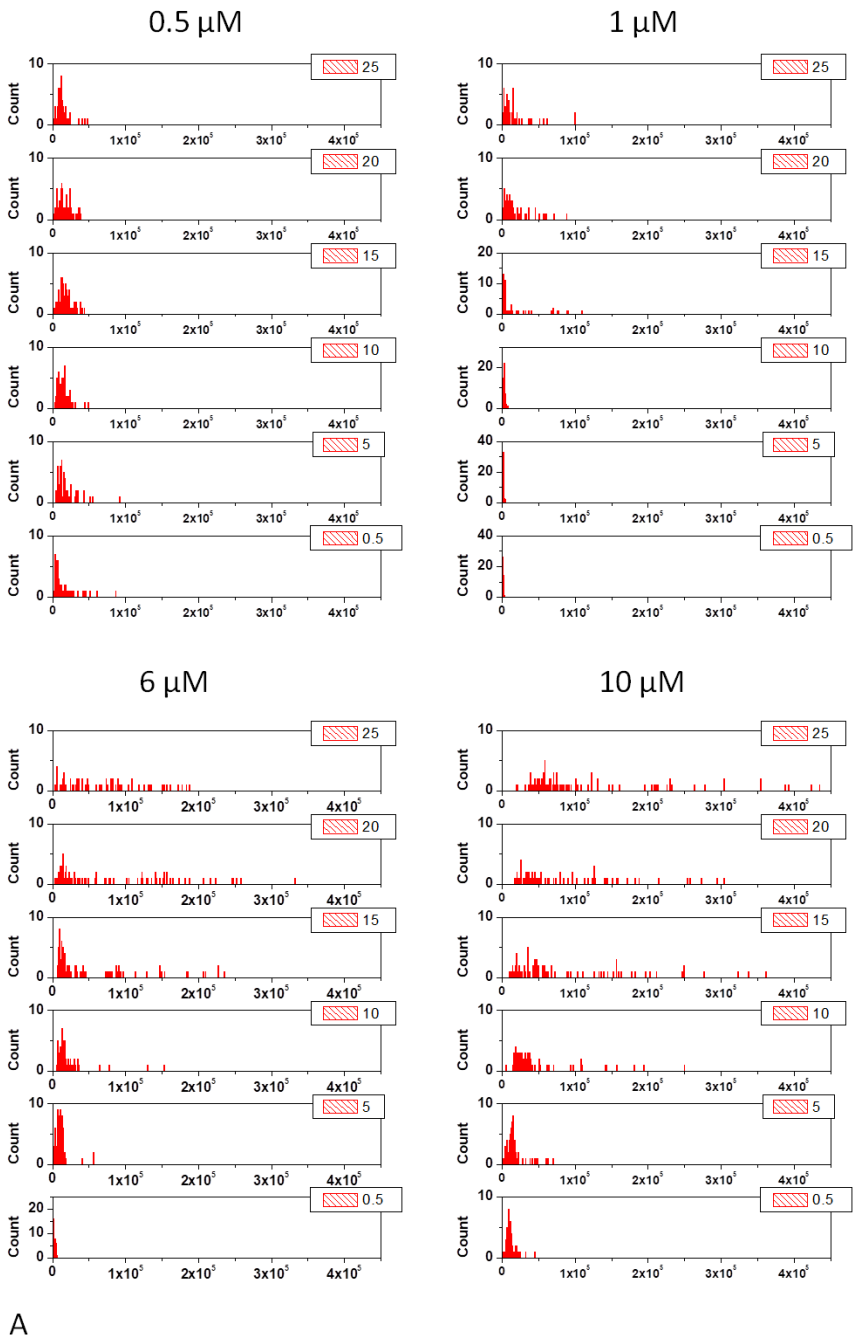
0.5 µM
1 µM
6 µM
10 µM
Count
25
20
15
10
5
0.5
1x10^5
2x10^5
3x10^5
4x10^5

A

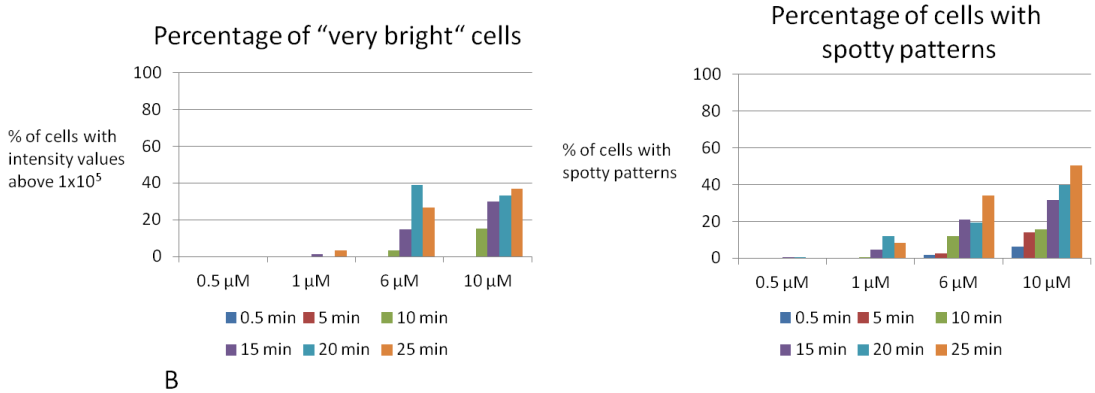
Percentage of "very bright" cells
% of cells with intensity values above 1x10^5
Percentage of cells with spotty patterns
% of cells with spotty patterns
100
80
60
40
20
0
0.5 µM
1 µM
6 µM
10 µM
0.5 min
5 min
10 min
15 min
20 min
25 min

B

Figure 21: Quantitative analysis of the “very bright” cells and spotty pattern cells. A: the counts of cells versus mean fluorescence intensity per cell at each time point. “Very bright” cells were defined as showing a mean fluorescence intensity value above 1×10^5; B: percentage of “very bright” cells and spotty pattern cells at each time point. Incubation time has been color-coded as indicated. More than 300 cells were analyzed at each time point.

4.1.3.3 Quantitative analysis of septum binding

DAP is known to act at the cell membrane. However, as shown in Fig. 18, the distribution of DAP-TMR on the cell membrane is non-uniform for cells treated with different concentrations of native DAP or even for the same concentration at different incubation times. As mentioned earlier, DAP-TMR bound to the septum at sub-MIC concentrations and concentrations equal to the MIC, but to the complete membrane at supra-MIC concentrations. Hence, we quantitatively analyzed the distribution of DAP-TMR on the cell membrane as a function of time.

The idea of our DAP-TMR distribution analysis is shown in Fig. 22. We analyzed the linear profile of cells with closed septum and the fluorescence intensity distribution along the red box (Fig. 22). The fluorescence profiles that showed one peak at septum with a ratio of septum/membrane ≈ 4, were characterized as septum binding (Fig 22. 1), whereas the profiles that showed 3 peaks with a ratio of septum/membrane ≈ 2 were characterized as membrane binding (Fig 22. 3).

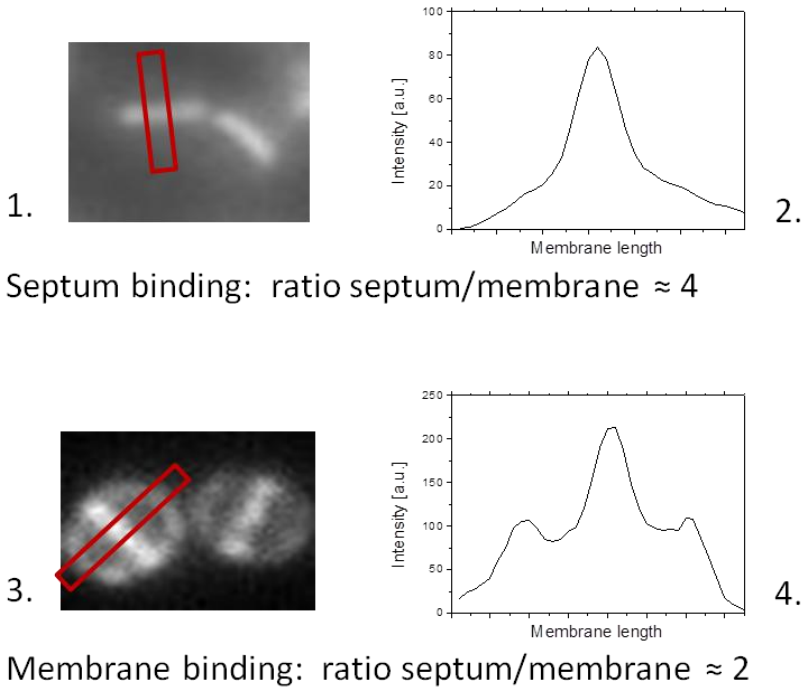

Figure 22: Analysis of linear fluorescence profiles. Fluorescence images of cells stained with 5(6)-TAMRA-X, SE-labeled daptomycin (DAP-TMR) and profiles of fluorescence intensity along the red box in the corresponding images. Analysis of linear fluorescence profiles for cells with closed septum. One peak (1) indicates septum binding, and yielded as a septum/membrane ratio ≈ 4; three peaks (4) indicate membrane binding, and yielded as a septum/membrane ratio of around 2.

To demonstrate the discrimination between septum binding and membrane binding, we introduced the septum fusion protein FtsW-GFP and the membrane dye Nile red as controls (Fig. 21A). FtsW is an essential cell division protein that translocates lipid II to the extracellular side of the cell membrane and is localized to the septum; Genetic fusion of GFP (green fluorescent protein) to cell division proteins, such as FtsZ and FtsW have been widely used to visualize the division ring in situ [221].

As shown in Fig. 23A, FtsW-GFP specifically accumulated at the division septum, and the ratio of fluorescence at the septum versus the lateral membrane is around 4. Nile red is a membrane dye that is homogeneously distributed over the entire cell membrane. The intensity of the fluorescent signal at the septum was about 1.5-fold higher than at the lateral membrane.

As shown in Fig. 23B, septum binding was observed at sub-MIC DAP concentration (0.5 µM) for all incubation times tested, with median values above 2. However, for

cells treated with DAP concentration around the MIC (1 µM), septum binding was dominant for the first 10 min incubation with fluorescence ratios > 4; after 10 min of incubation, DAP was found to bind to the complete membrane with a fluorescence ratio approaching 2. Furthermore, for cells treated with supra-MIC DAP concentrations (6 µM and 10 µM), the overall membrane binding of DAP occurred for all incubation times with ratios around or below 2. Notably, at the concentration of 6 µM, for the first 5 min incubation, the ratios are higher than those at other incubation time points.

DAP has been reported to be rapidly bactericidal against both exponentially growing and stationary-phase *S. aureus*, suggesting that its bactericidal activity does not require cell division [222]. However, our results strongly suggest that DAP initially binds to the division septum, which indicates a specific interaction with septum-localized membrane components, and that the binding then extends to the complete membrane. In *S. aureus*, the septum is the only place where cell wall synthesis occurs [223]; therefore, our findings indicate that DAP may interfere with the cell division and affect cell wall and lipid synthesis.

These findings are in general agreement with those from early *B. subtilis* studies [131,150] , which reported that fluorescently labeled DAP preferentially binds to division septa and PG-enriched regions in a helical pattern along the long axis of the cell. Binding of DAP causes membrane distortions that alter the cell morphology and recruits cell division proteins. Defects in cell membrane and cell wall synthesis damage cell integrity, causing cell death. Additionally, *B. subtilis* cells treated with sub-MIC DAP concentration appeared bent and elongated, suggesting the inhibition of cell division [131]. Aberrant division septa and multilobate morphology were also observed in *S. aureus* cells treated with supra-MIC DAP concentration [224]. More recently, *B. subtilis* studies showed that DAP preferred to insert into the fluid membrane domains and clustered the fluid lipids, thus interfering with cell wall and lipid synthesis [140].

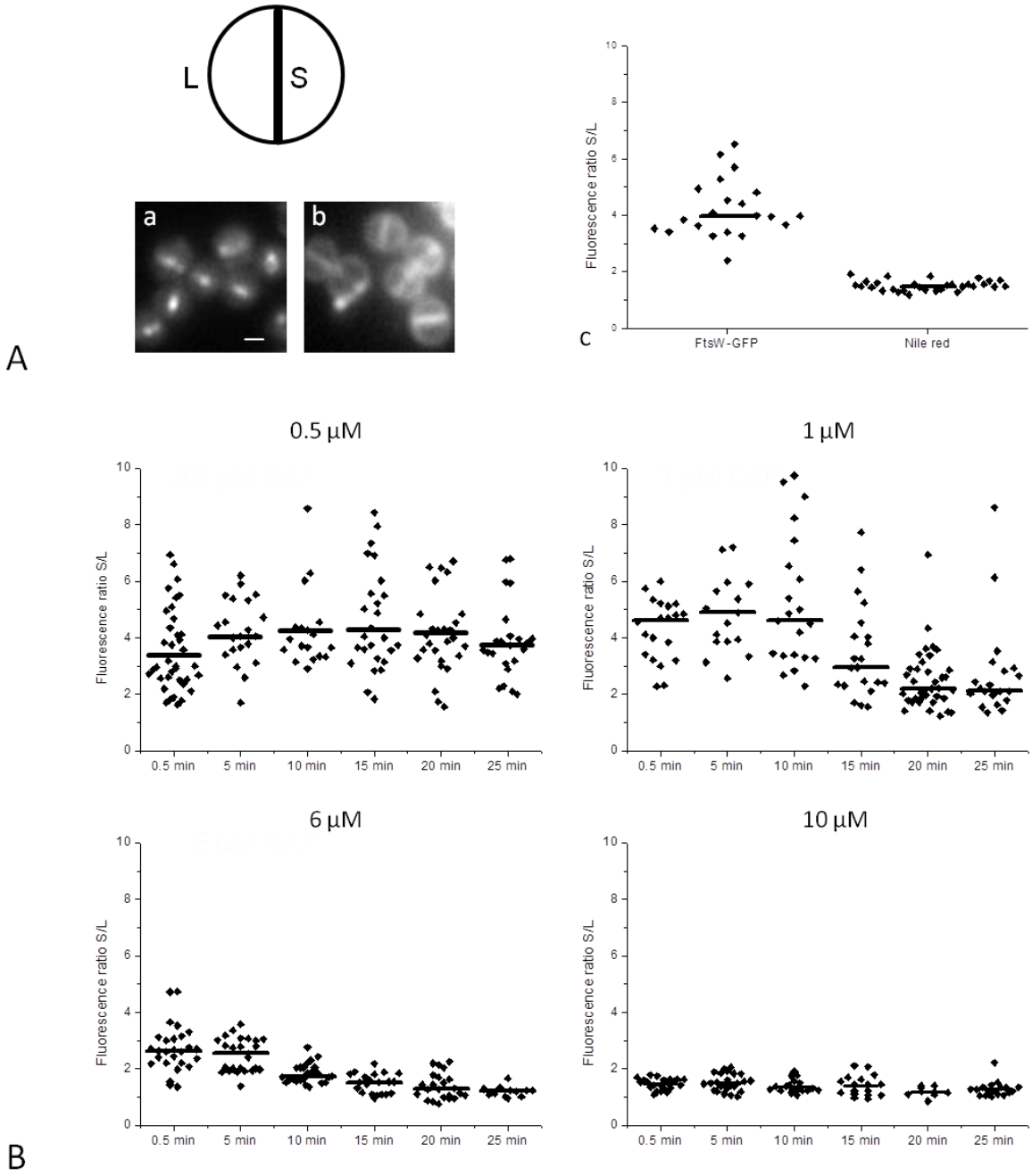

Figure 23: Quantitative analysis of septum binding. Septum binding was characterized by ratio of fluorescence intensities measured at the septum and the lateral membrane. A. Fluorescence microscopy images (a and b) showing controls with septum binding (FtsW-GFP) of median values ≈ 4 and homogeneous binding (Nile red) of median values ≤ 2, respectively. B. Fluorescence ratios for cells treated with different DAP concentrations for different time points. For each time point, quantification was performed in at least 30 cells that displayed a closed septum. Horizontal lines correspond to median fluorescence ratio. Scale bar: 1 µm.

4.1.4 Super-resolution imaging of DAP-BDP FL molecules on *S. aureus* cells

Although the specific target molecule of DAP is uncertain, it is well established that DAP target the cell membrane. uPAINT is a super-resolution imaging method that is ideally suited for studies of membrane-bound molecules. Therefore, uPAINT can be used to study the DAP binding behavior to the membrane of *S. aureus* at the single-molecule level with high spatial precision. We thus implemented uPAINT on HILO microscopy to investigate the localization of single DAP-BDP FL molecules on the membrane of *S. aureus* cells. A mixture of 6 μM native DAP and 1 nM DAP-BDP FL and 1 mM Ca^{2+} was added onto exponential phase *S. aureus* cells immediately before image acquisition.

Movies with 9,000 frames were recorded at a frame rate of 60 Hz within two time intervals $0 < t < 3$ min and $3 \text{ min} < t < 6$ min after DAP addition. Representative images obtained in the first time interval (upper panel) and the second time interval after DAP addition (lower panel) are shown in Fig. 24. Fluorescence images at different time points indicate different DAP-BDP FL molecules that localized on the membrane of *S. aureus*. The positions of single DAP-BDP FL molecules in each frame were determined by curve fitting and plotted together to construct super-resolution images using the software thunderSTORM (Fig. 24B, D).

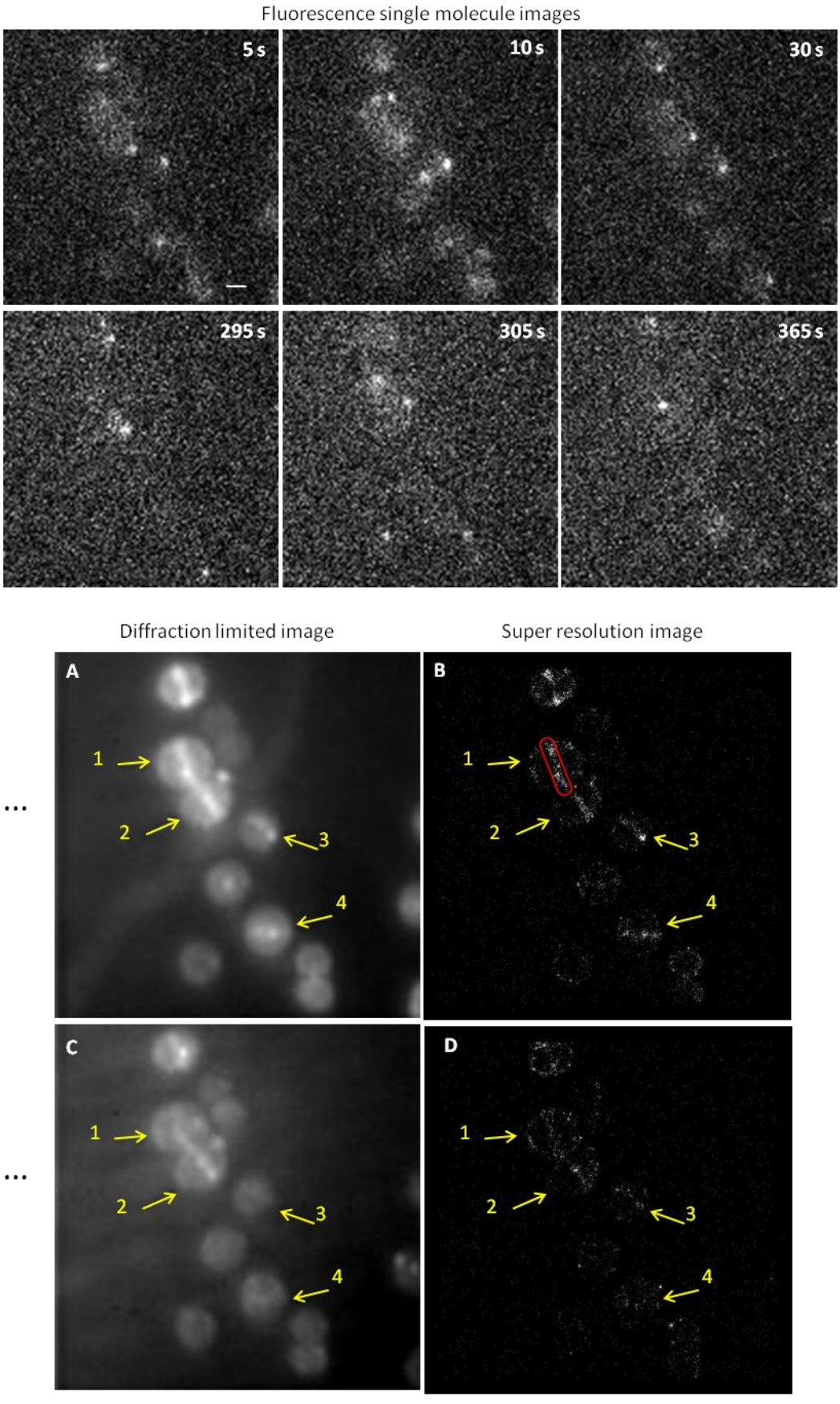

Figure 24: Fluorescence images and super-resolution images of BODIPY FL-labeled daptomycin

(DAP-BDP FL) molecules on the membrane of *Staphylococcus aureus* cells. Upper panel: representative images for the first 3 min after DAP addition; lower panel: representative images for the second 3 min after DAP addition. A and C: the corresponding summed up diffraction limited images; B and D: super-resolution images. Four cells were chosen for comparison. The number of molecules on septum (red box) and periphery of each cell were counted with the ImageJ program.

We observed that DAP-BDP FL molecules constantly bound to the surface of cell membrane. Super-resolution images (Fig. 24B and D) showed that DAP-BDP FL molecules bound to both the septum and the periphery. We selected four cells that displayed a closed septum, analyzed the super-resolution images, and counted the number of molecules that bound to the septum and the periphery using ImageJ. Then, we compared the ratios of the numbers of molecules that localized on the septum to those localized on the periphery in the first 3 min (Table 7) and the second 3 min (Table 8) after DAP addition. In the first 3 min, more DAP-BDP FL molecules localized on the septum, and the ratios were either around 2 (cell 1 and cell 2) or above 2 (cell 3 and cell 4). However, in the second 3 min after DAP addition, more localizations were found on the periphery, and the ratios were below 1 for all the cells; for the cell 4, no septal localization was found.

Table 7: Number of DAP-BDP FL molecules on the septum and periphery of each cell in the first 3 min after DAP addition.

Cell	Septum	Periphery	Ratio
1	596	331	1.8
2	368	207	1.8
3	330	93	3.6
4	382	50	7.6

Table 8: Number of DAP-BDP FL molecules on the septum and periphery of each cell in the second 3 min after DAP addition.

Cell	Septum	Periphery	Ratio

1	225	270	0.8
2	163	232	0.7
3	86	116	0.7
4	0	38	0

These results further support our previous conclusion that DAP initially binds to the septum and then extends to the overall membrane at the single-molecule level.

Furthermore, this also verifies that uPAINT is an ideal super-resolution imaging method to study the mechanism of other membrane-targeting antibiotics if the antibiotics can be labeled with a suitable fluorescent marker.

On the basis of all the results presented above, we conclude that three phases of DAP binding to *S. aureus* exist (Fig. 25): (I) initial binding to the division septum, (II) extended binding to the envelope, and (III) finally, strong accumulation of DAP accompanied by formation of multiple spotty pattern cells and cell size reduction. The preferential binding of DAP to the division septum indicates that DAP might interact with septum-localized membrane components, thus interfering with cell wall and lipid synthesis.

DAP exerts rapid bactericidal activity against both exponentially growing and stationary-phase *S. aureus* cells; this activity is superior to other antibiotics such as vancomycin, nafcillin, and linezolid [225]. This effective bactericidal action may be attributed to the combination of effects on the division septum and membrane.

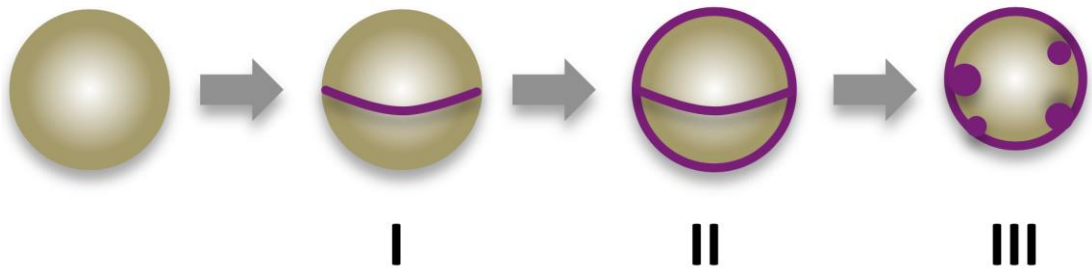

Figure 25: Schematic representation of three different phases of daptomycin binding to cells of *Staphylococcus aureus*. Purple color demonstrates the distribution of DAP on the surface. This

model was suggested by Dr. Fabian Grein.

4.2 Colocalization of DAP with septum localized membrane components in *S. aureus*

Although our studies clarified the phases of DAP binding, the existence of specific target molecules for DAP has not yet been confirmed. The quantitative analysis in section 1.4.3.3 proved the initial septum binding of DAP, indicating that DAP may specifically interact with septum-localized membrane components and interfere with cell wall and lipid synthesis. Therefore, we next examined the colocalization of fluorescently labeled DAP with two septum-localized membrane components: cell division protein FtsW and the cell wall precursor lipid II.

4.2.1 Colocalization of DAP with FtsW

FtsW is an integral membrane protein required for cell division in most bacteria. It belongs to the SEDS protein family, a large family of polytopic membrane proteins present in all bacteria with a PGN cell wall [226,227]. SEDS proteins have been proposed to act as flippases, which function in the translocation of lipid II-linked PGN precursors from the inner to the outer leaflet of the cytoplasmic membrane. FtsW has been shown to localize to the division septum, and it is essential to recruit other division protein such as FtsI and interact with other proteins such as FtsZ and FtsI at the division site. As our previous results demonstrate that DAP preferentially binds to septum, the division protein could be a potential target of DAP. Therefore, we first investigated the colocalization of DAP with FtsW in *S. aureus*.

To observe the localization of FtsW, we expressed FtsW-GFP fusion protein in *S. aureus*. For DAP localization, we incubated cells with a mixture of 1 μM DAP and 0.1 μM DAP-TMR for 0.5 min in the presence of 1 mM Ca^{2+}. This concentration of DAP is similar to the MIC mentioned earlier. Excess DAP-TMR and non-labeled DAP were removed by washing the cells in HEPES buffer immediately. Then, the colocalization of DAP-TMR with FtsW-GFP was investigated by combining HILO microscopy with dual-color imaging using a dual-emission image splitter.

Two color images indicating the locations of FtsW-GFP and DAP-TMR on the cell membrane are shown in Fig. 26. Both FtsW-GFP and DAP-TMR were found to

localize at the septum.

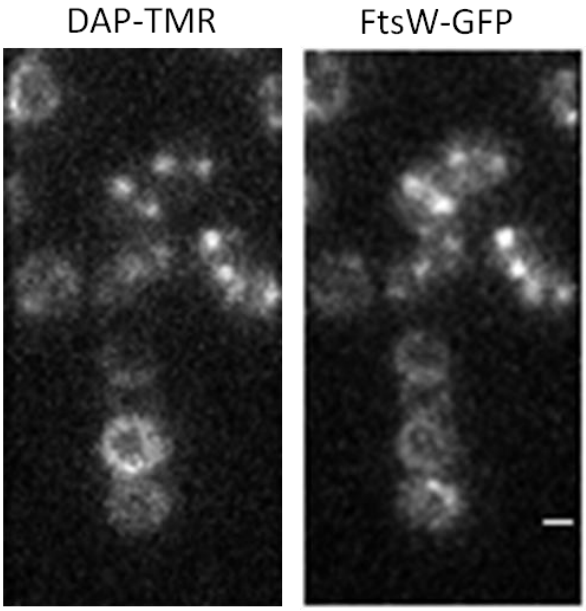

Figure 26: Two-color fluorescence images of 5(6)-TAMRA-X, SE-labeled daptomycin (DAP-TMR) and FtsW-GFP fusion protein at the middle focal plane. *Staphylococcus aureus* cells expressing FtsW-GFP fusion protein were incubated with a mixture of 0.1 µM DAP-TMR and 1 µM native DAP for 10 min in presence of 1 mM Ca^{2+}. Scale bar: 1 µm.

To acquire three-dimensional fluorescence images of the z-ring, the known localization site of FtsW-GFP, z-stacks were acquired for each of the two fluorescence color channels. A step size of 50 nm was used for acquiring z-stacks, and 61 images were acquired for each stack. This covered a distance of 3 µm, which is larger than the bacteria. Sixty-one images acquired for each color channel were summed up to create z-stack projection images. As shown in Fig. 27A, both DAP-TMR and FtsW-GFP proteins were observed to localize to the cell septa. The stacks were then filtered and reconstructed in three-dimensions by the 3D Hybrid Median Filter function of ImageJ (Fig. 27B), to observe the complete structure of the z-ring. From the rotation images shown in Fig. 27C, we found that DAP-TMR and FtsW-GFP were distributed all over the z-rings. These results demonstrate that at an incubation time of 0.5 min (the first phase of DAP binding), DAP-TMR and FtsW-GFP colocalize to the septal z-ring.

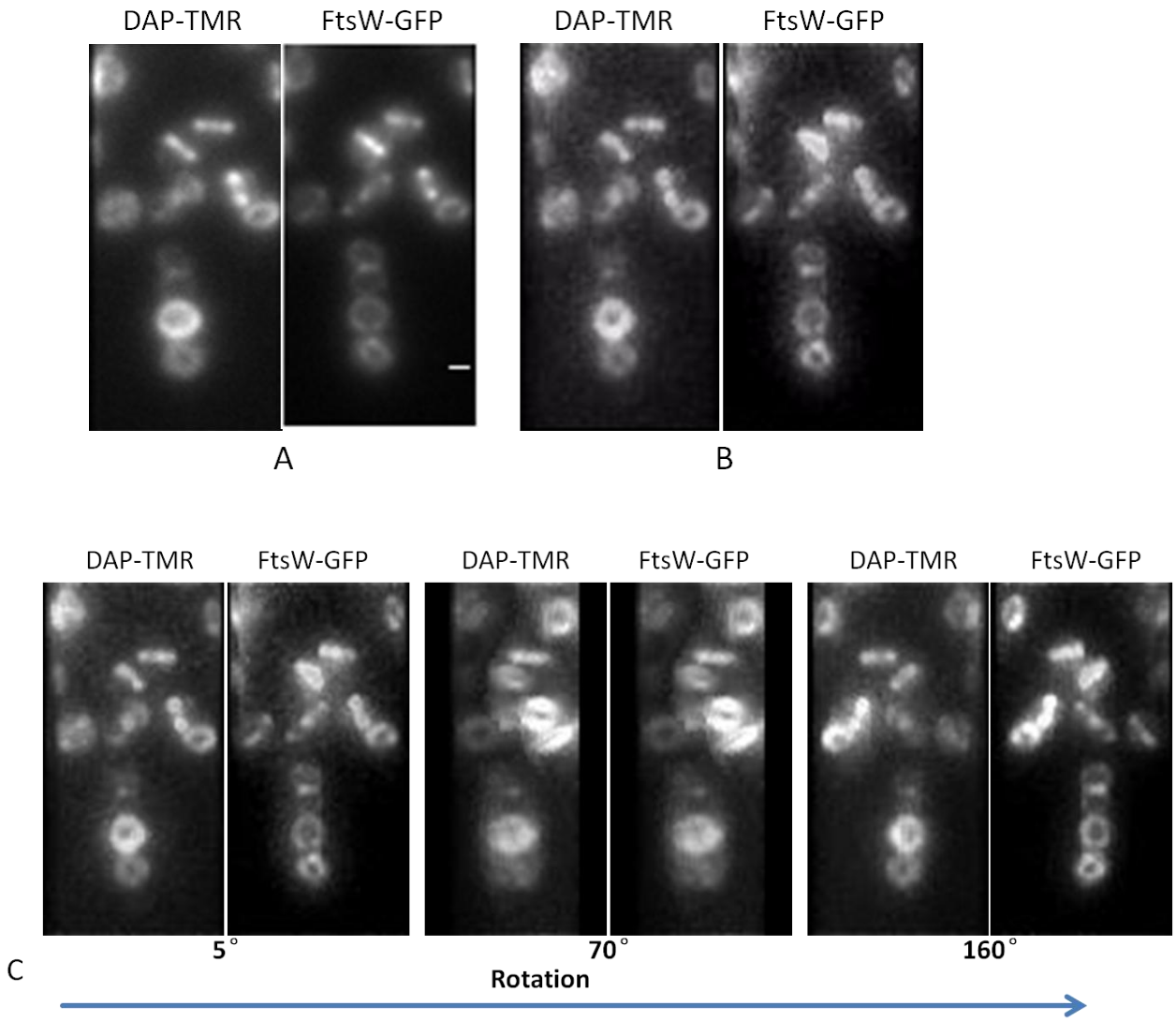

Figure 27: Colocalization of 5(6)-TAMRA-X, SE-labeled daptomycin (DAP-TMR) and FtsW-GFP fusion proteins in the septum. (A) z-stack maximum projection images of the corresponding color channels (B) one of the reconstructed three-dimensional images of each color channel (C) the three-dimensional images rotated through 180 °(from left to right). Scale bar: 1 µm.

According to our previous results, at longer incubation time, DAP binding extends over the envelop (Phase II). Therefore, we further examined the colocalization of DAP-TMR and FtsW-GFP at two different incubation time points (0.5 min and 20 min).

After incubation for 0.5 min, DAP-TMR and FtsW-GFP fusion protein colocalized to the septum as expected (Fig. 28). However, at 20 min, the distribution of FtsW-GFP remained unaffected, whereas DAP-TMR was bound to the complete cell membrane and interestingly, spotty patterns appeared.

It has been reported that the cell division protein DivIVA-GFP colocalized with DAP-induced membrane patches in *B. subtilis* [131]. DivIVA is an essential cell division protein that targets negatively curved membranes and localizes to the midcell region. As DAP was shown to induce membrane curvature, it was concluded that DAP recruits this cell division protein, thus leading to local changes in PGN biosynthesis. However, this conclusion remains controversial because another study reported that the DivIVA-GFP patches were proved to be artifacts due to the formation of GFP dimers [140]. In contrast, DAP delocalizes different cell membrane proteins that are involved in cell wall synthesis, such as MurG, PlsX, and DivIVA in *B. subtilis*. Therefore, it was concluded that DAP does not target one specific protein but rather targets the fluid lipid areas. The fluid lipid domain was assumed to contain lipid II as well, because the long bactoprenol moiety of lipid II prefers a fluid lipid environment. Because FtsW can specifically transport lipid II from the inner to the outer leaflet of the cytoplasmic membrane, we speculate that FtsW might not be the specific target of DAP. Rather, the colocalization of FtsW-GFP and DAP observed at the earlier incubation interval is due to the fact that both of them can interact with lipid II.

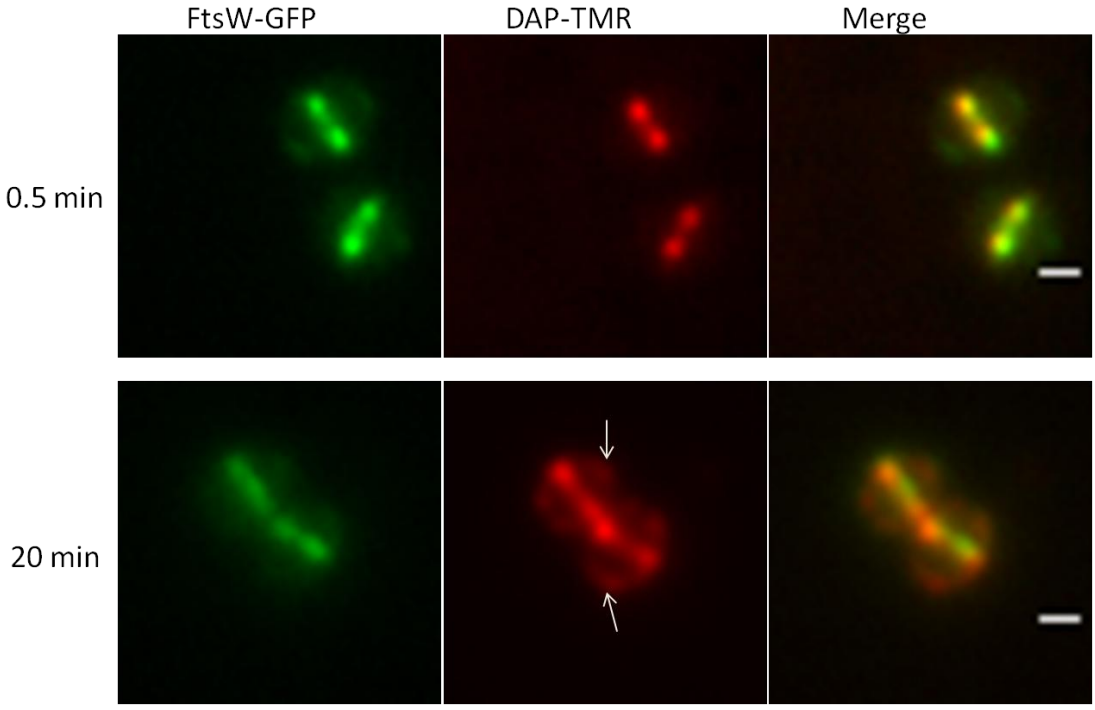

Figure 28: Colocalization of 5(6)-TAMRA-X, SE-labeled daptomycin (DAP-TMR) and FtsW-GFP at different incubation time points. At 0.5 min, both were localized to the septum. At 20 min, DAP binding extended to the overall membrane and spotty pattern appeared (white arrows) whereas FtsW remained localized only to the septum. Scale bars: 1 µm.

4.2.2 Interaction of DAP with lipid II

As our previous experiments suggested that DAP does not target the cell division protein FtsW, we investigated the interaction between DAP and cell wall precursor lipid II. As discussed in chapter 1.2, lipid II is a key component in PGN synthesis. It transports monomeric PGN units across the cell membrane for the cell biosynthesis. Because the structure of lipid II is highly conserved and difficult to modify, it has been a particularly attractive target of many antibiotics, such as nisin [228], plectasin [229] and vancomycin [230].

Vancomycin elicits its bactericidal response by specifically binding to the sequence D-Ala–D-Ala of lipid II [230]; it effectively sequesters lipid II and prevents its normal incorporation into the growing PGN network, ultimately leading to cell death [231]. Therefore, if lipid II is the target molecule of DAP, their interaction should be inhibited in cells pre-treated with vancomycin.

Here, we used Van-BDP FL to label lipid II. In *S. aureus*, D-Ala–D-Ala residues are distributed all over the cell wall, even in the mature PGN [232]; therefore, Van-BDP FL could bind to the complete membrane instead of the septum. Hence, we incubated the cells with D-serine, to promote the incorporation of this amino acid as the C-terminal residue of muropeptides in the cell wall, replacing the usual D-Ala to block the binding of Van-BDP FL. Therefore, Van-BDP FL can only specifically bind to the newly produced D-Ala–D-Ala residues at the septum [223]. *S. aureus* RN4200 was grown to an OD_{600} of 0.25 in TSB containing 0.125 M D-serine. Cells were then pre-incubated with 1 µM Van-BDP FL for 2 min, excess Van-BDP FL was removed, and the cells were incubated with a mixture of 0.1 µM DAP-TMR and 1 µM unlabeled DAP for 10 min in the presence of 1 mM Ca^{2+}. Cells were washed again and immobilized on an agarose pad and observed by fluorescence microscopy. Cells without Van-BDP FL pre-incubation and treated only with a mixture of 0.1 µM DAP-TMR and 1 µM unlabeled DAP were considered as the control.

As expected, for cells pre-incubated with Van-BDP FL, Van-BDP FL mostly localized to the septum (Fig. 29A, left panel), whereas DAP-TMR binding to the same cells was very faint (Fig. 29A, middle panel). The differences between cells with and without Van-BDP FL pre-incubation could be clearly observed and have

been indicated using circles with dashed yellow lines in the figure. Normal septum binding of DAP-TMR was clearly displayed for cells without vancomycin pre-incubation (Fig. 29A, right panel). With vancomycin pre-incubation, the fluorescent intensity of DAP-TMR was almost two-fold lower than that of the control (Fig. 29B). These results indicate that the binding of Van-BDP FL clearly inhibits the interaction between DAP and the septum. As vancomycin specifically binds to lipid II, DAP might also interact with lipid II.

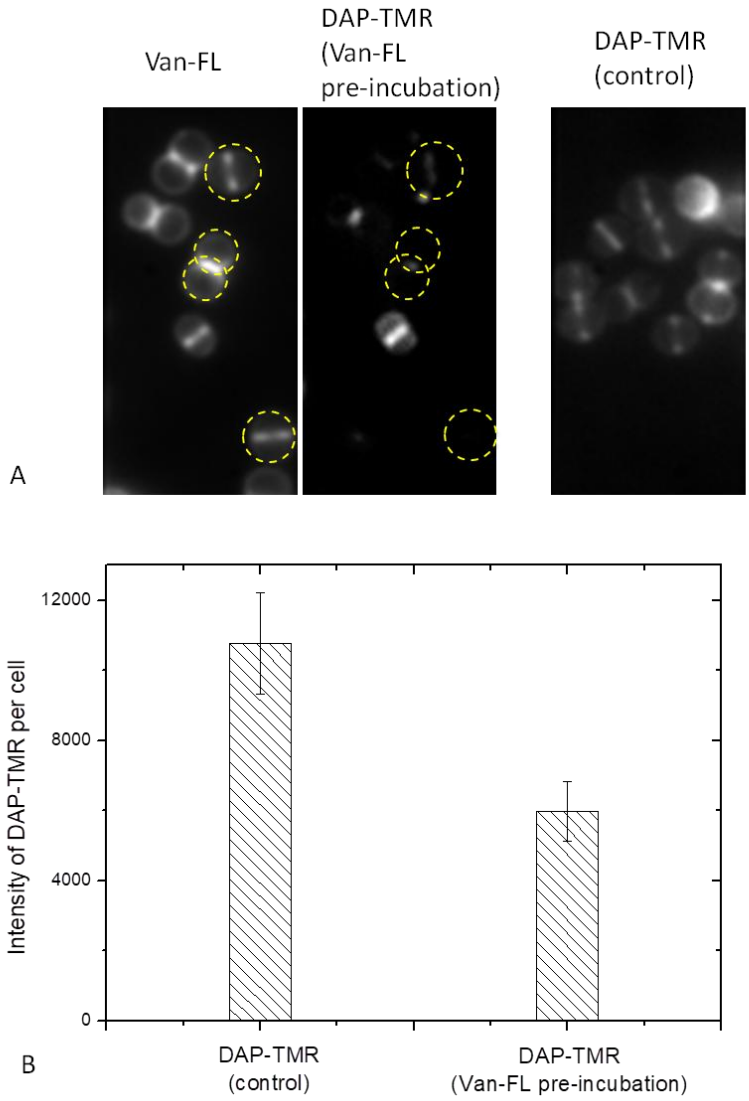

Figure 29: BODIPY FL fluorescent vancomycin (Van-BDP FL) inhibits the interaction between daptomycin and lipid II. A: Two-color images of cells treated with Van-BDP FL and 5(6)-TAMRA-X, SE-labeled DAP (DAP-TMR; left and middle) and cells treated with DAP-TMR only (control, right); B: quantitative analysis of intensity of DAP-TMR per cell. For each condition, quantification was performed in at least 100 cells. Standard errors of the mean are given by error

bars.

Thus, we concluded that DAP might directly interact with lipid II at the septum, thereby interfering with the process of the cell wall biosynthesis. However, the precise interaction between DAP and lipid II and the precise binding site remain unclear. Lipid II has a large hydrophilic head group linked via a pyrophosphate to a long bactoprenol chain. Several lantibiotics and antimicrobial peptides, such as nisin, plectasin, and mersacidin have been reported to specifically bind to the pyrophosphate structure of lipid II. However, the interaction between lipid II and DAP might be simply considered as unspecific and driven by electrostatic attraction. The DAP-Ca^{2+} complex functions as a cationic peptide and can easily attach to the pyrophosphate linked head group of lipid II. As vancomycin has a net charge of around 1 at pH 7, the binding of vancomycin may neutralize the negative charge, thus blocking the binding of the DAP-Ca^{2+} complex. Alternatively, vancomycin may occupy the binding site of DAP on the lipid II.

A positive correlation between vancomycin and DAP susceptibilities in *S. aureus* has been reported, suggesting the existence of a cross-resistance machinery between these two antibiotics [233]. Furthermore, it was proposed that such correlation is due to cell wall thickening, and the thickened cell wall may act as a physical barrier to DAP and vancomycin penetration; however, this explanation remains controversial [234]. The recent report showed that fluorescently labeled vancomycin localizes to DAP-induced membrane patches and bent regions in *Bacillus subtilis* cells treated with a sublethal dose of DAP [131]. This implies that the DAP-induced patches contains lipid II and that DAP may interfere with cell wall synthesis. More recently, DAP was found to prevent PGN synthesis by delocalizing the peripheral membrane protein MurG, which is responsible for the synthesis of lipid II. Moreover, DAP targets fluid lipid domains, which may contain lipid II as well, because the long bactoprenol moiety of lipid II prefers a fluid lipid environment [140]. Collectively, these reports suggest that DAP may bind to one of the substrate or protein involved in cell wall synthesis and are in good agreement with our finding that DAP may interact with lipid II.

4.3 Specific interaction of DAP with lipid components in supported planar lipid bilayer

Supported lipid bilayers are popular cell membrane models and are ideal for studying peptide binding. To visualize the binding of DAP to bilayers, we examined the interaction of fluorescently labeled DAP (DAP-BDP FL) with pure DOPC bilayer, and DOPC bilayer containing DOPG and/or several bactoprenol lipids by TIRF microscopy. TIRF microscopy is an established excellent method to study planar supported membranes because of its thin excitation depth.

4.3.1 Interaction of DAP with different membranes lipid components

We observed the preferential binding of DAP to the septum of *S. aureus* and identified that the cell wall precursor lipid II as a probable target. Next, we studied the binding behavior of DAP with respect to further membrane lipid components, including PG, lipid II, and its bactoprenol precursors C_{55}-P and C_{55}-PP.

We integrated DOPG or/and C_{55}-P, C_{55}-PP, and lipid II into the DOPC bilayers. The negatively charged phospholipid PG has been shown to interact with DAP directly [219], and reduction of PG content leads to DAP resistance in *B. subtilis* [194]. Therefore, we first studied the interaction of DAP with DOPG-containing bilayers. Bactoprenol lipids C_{55}-P, C_{55}-PP, and lipid II are the key components in cell wall biosynthesis and are all negatively charged phospholipids. Furthermore both lipid II and C_{55}-PP contain a pyrophosphate group, which is a binding site of many antibiotics. Therefore, we assumed that these bactoprenol lipids could be the potential targets of DAP. All lipid chemical structures are shown in Fig. 30. Notably, the negatively charged head group of these lipids could increase affinity for DAP-Ca^{2+} complexes.

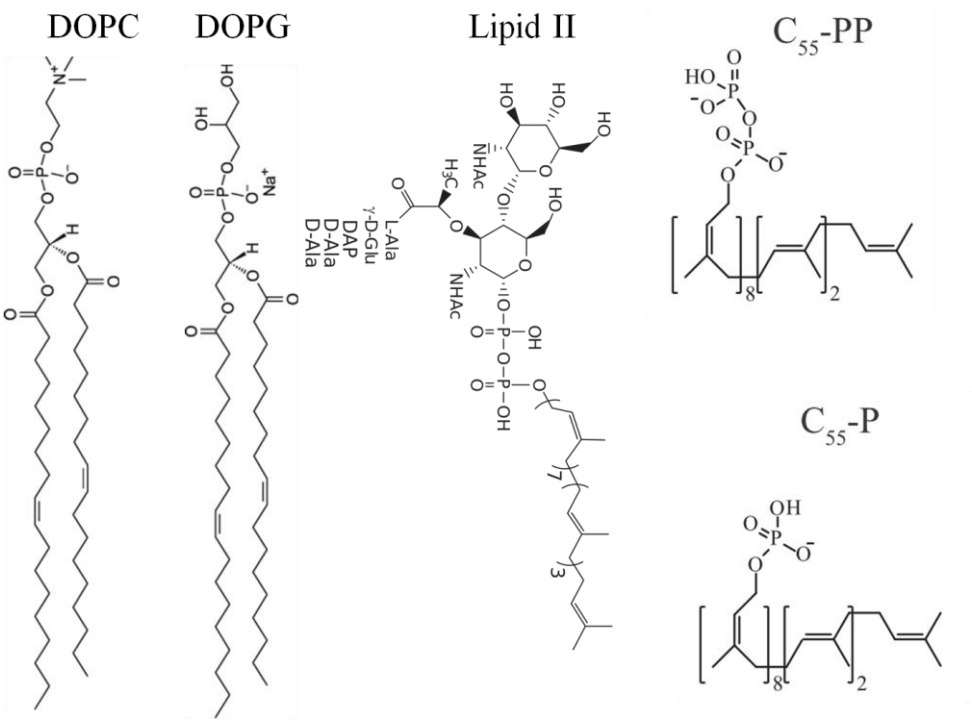

Figure 30: Chemical structures of lipids used in this study.

Bilayers were prepared on coverslips by fusion of VSUVs. The neutral lipid DOPC was used as matrix to which PG or/and bactoprenol lipids (C_{55}-P, C_{55}-PP, and lipid II) with an amount of 0.1 mol% or 0.2 mol% were added. It has been reported that DAP destabilizes and induces fusion of lipid bilayers at higher concentrations [135]. Hence, we added a mixture of 1 µM native DAP (MIC observed in susceptible bacteria) and 50 nM DAP-BDP FL onto the lipid membranes in HEPES buffer in the presence of 1 mM Ca^{2+}.

To ensure that the membranes were intact and fluid, FRAP assays were performed for the DOPC bilayer. We integrated 0.1 mol% TopFluor PC into the DOPC bilayer to make it visible. Fluorescent lipids were photobleached by exposing a part of the bilayer to a high-intensity laser beam, followed by a recovery monitoring with a low-intensity laser beam. The fluorescence images and representative fluorescence recovery curves from the bleached region of interest (ROI) indicate that the DOPC bilayer remains intact and fluid (Fig. 31).

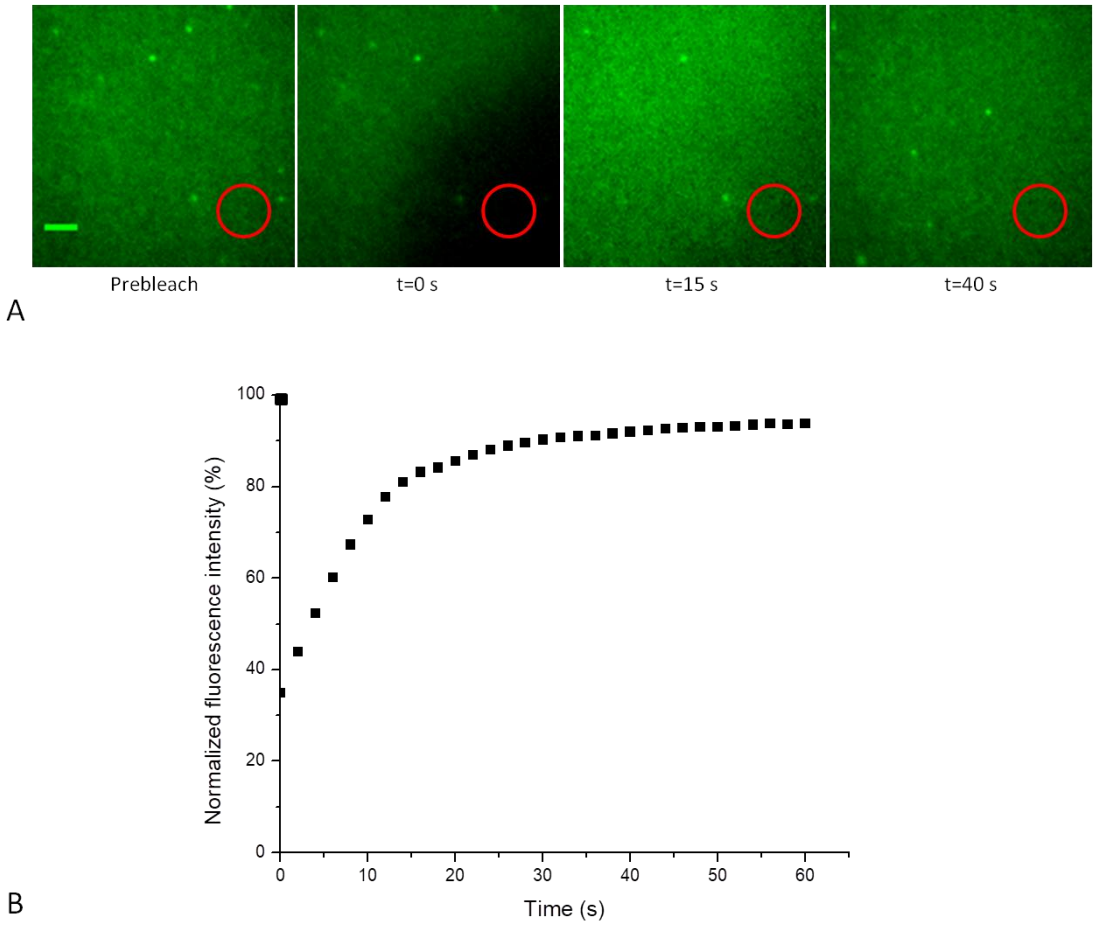

Figure 31: Fluorescence recovery after photobleaching (FRAP) analysis to examine the integrity of the supported lipid bilayer. A: Fluorescent images of a region of TopFluor PC-containing bilayers before and after local bleaching as well as the subsequent recovery. B: Representative fluorescence recovery curve from the bleached region (red circle). The photobleaching and recovery of a specific area shows that the bilayer remains intact and fluid. Lipid mixture: DOPC and 0.1 mol% TopFluor PC. Scale bar: 2 µm.

Twelve types of bilayers with different lipid components were prepared, a mixture of 50 nM DAP-BDP FL and 1 µM DAP was added onto each bilayer, and the layers were imaged using a TIRF microscope within 2 min after DAP addition. Movies with 100 frames were recorded at a frame rate of 60 Hz. The differences of the amount of bound DAP-BDP FL molecules for each bilayer were determined by comparing the fluorescence intensity of the images. The mean values of average fluorescence intensity of each image for each sample was calculated. Representative images of each bilayer and quantified data are shown in Fig. 32.

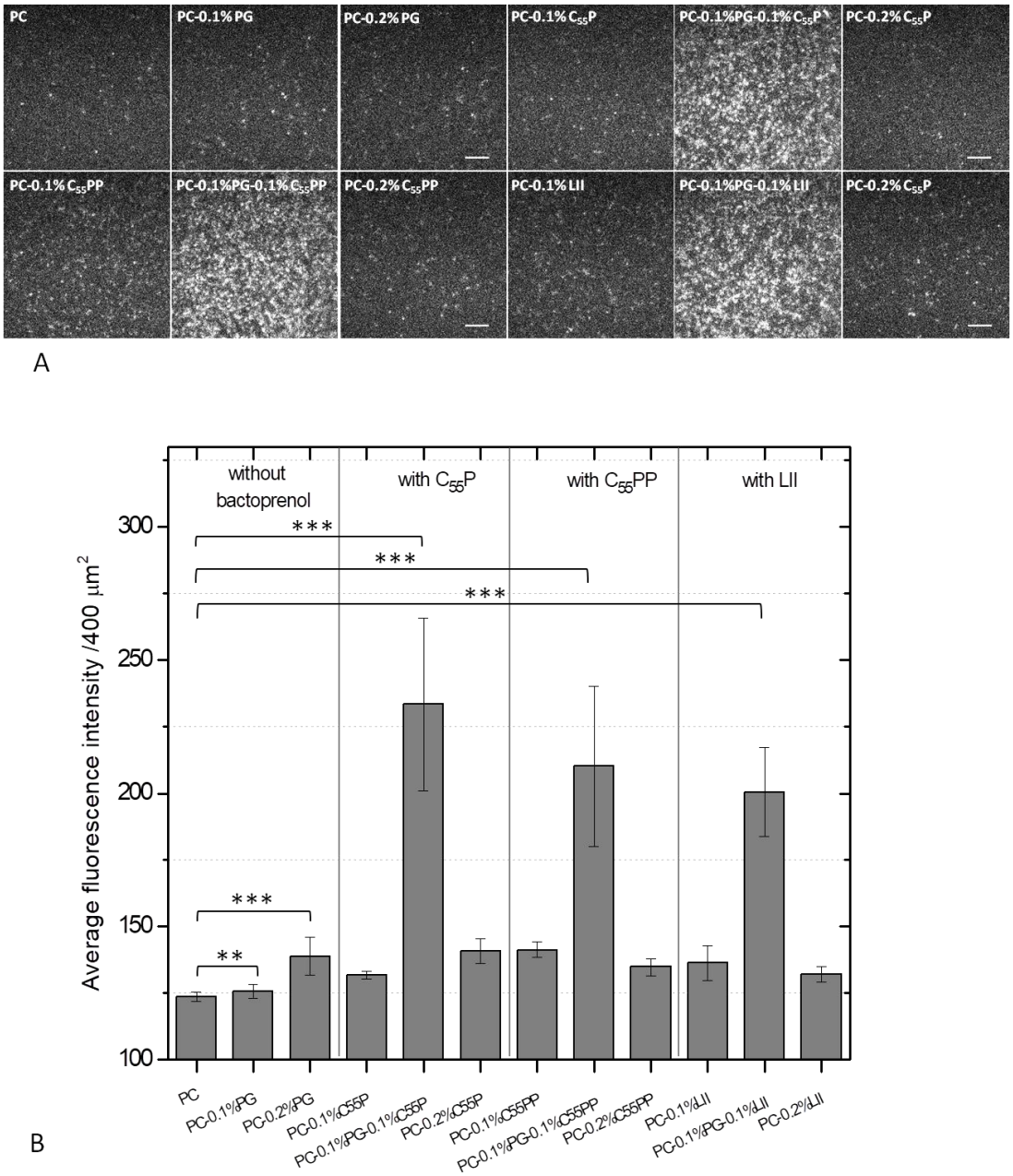

Figure 32: Binding of BODIPY FL-labeled daptomycin (DAP-BDP FL) to fluid supported bilayers containing different molecular components. A: Representative total internal reflection fluorescence microscopy images of the binding of DAP to each bilayer. Movies with 100 frames were recorded at a frame rate of 60 Hz within 2 min after addition of DAP; B: Data were plotted as mean values of the time-averaged intensity of each movie. The data shown were obtained from at least 20 movies for each bilayer. The measurement was repeated three times and was reproducible. Standard errors of the mean are given by error bars. Significance of the differences between the values of the respective bilayers and the values determined for the DOPC bilayer was tested using Origin's independent, two-sample *t*-test. *** indicates $p < 0.001$ and ** indicates $p < 0.01$. Scale bar: 5 μm.

As illustrated in Fig. 31, depending on the bilayer composition, the numbers of binding DAP-BDP FL molecules (average fluorescence intensity) strongly varied. For pure, electrically neutral DOPC membrane, only a low amount of DAP was observed. This is in agreement with a previous study showing that less DAP bound to the electrically neutral pure PC membranes compared to PC/PG membranes [218, 235]. The binding of DAP-Ca^{2+} complexes to PC bilayers can occur because calcium leads to an increased exposure of the N-terminal acyl chain of the DAP molecule, allowing binding to the uncharged PC membrane [235].

As expected, the presence of PG in the membrane enhanced the binding of DAP, and higher amounts of PG (0.2 mol%) induced higher amount of accumulations, resulting in a higher fluorescence intensities (0.1 mol% PG: p-value < 0.01; 0.2 mol% PG: p-value < 0.001), compared to that in the DOPC membrane. The binding to PG-containing membrane is considered as non-specific binding driven by the attractive electrostatic forces between the negatively charged PG and the positively charged DAP-Ca^{2+} complex. It has been reported that PG also triggers a conformation change of DAP molecules, enabling in deeper membrane penetration and oligomer formation [235]. When the PG contents increased to 1 mol%, DAP-BDP FL strongly and homogeneously accumulated on the entire membrane, resulting in a very high fluorescence intensity, which was difficult to quantify (data not shown); hence, only 0.1 mol% and 0.2 mol% PG-containing membranes were studied.

The fluorescence intensity for membranes with 0.1 mol% of three bactoprenol lipids (C_{55}-P, C_{55}-PP, and lipid II) was higher than that of pure PC membranes. This was not surprising, as all these three bactoprenol lipids are negatively charged and increase the affinity for DAP-Ca^{2+} complexes. The intensity of the 0.1 mol% lipid II-containing membrane was higher than that of the 0.1 mol% PG-containing membrane, implying that DAP binds to lipid-II-containing membrane more strongly than to PG-containing membranes. This confirms our speculation that lipid II might be a target of DAP. Interestingly, the intensities of membranes containing 0.1 mol% C_{55}-PP and 0.1 mol% C_{55}-P were also higher than that of 0.1 mol% PG-containing membrane, indicating that these bactoprenol lipids are more attractive to DAP than PG is. However, the nature of interactions between DAP and bactoprenol lipids by hydrogen bonding or attractive electrostatic forces remains unclear.

Surprisingly, membranes containing 0.1 mol% PG and 0.1 mol% of each bactoprenol lipids (C_{55}-P, C_{55}-PP, and lipid II) triggered significantly stronger binding of DAP, indicating that the presence of PG considerably enhanced the binding of DAP to the bactoprenol lipids. The images showed dense accumulations of DAP on the membranes, resulting in evidently higher fluorescence intensity. The corresponding quantification revealed that these three types membrane showed significantly higher fluorescence intensities, compared to those of the other membranes tested (Fig. 32B). Such results were not observed when we increased the contents of each lipid from 0.1 mol% to 0.2 mol%, suggesting that the dramatic increase in intensity was not simply due to a higher amount of negative charges.

Collectively, these results demonstrate that DAP preferably binds to membranes containing both PG and bactoprenol lipids, compared to those containing only PG or only bactoprenol lipids. We concluded that DAP binding to the septum is not alone driven by opposite charges attracting each other, but rather by a more complex combinatorial effect of PG and bactoprenol lipids.

4.3.2 Inhibition of DAP binding to bactoprenol precursors

To further verify the specificity of DAP binding to membranes containing the bactoprenol precursors C_{55}-P, C_{55}-PP, and lipid II along with PG, these membranes were incubated with fruilimicin, bacitracin, and oritavancin, the antibiotics acting against these bactoprenol lipids, respectively (as discussed in 1.3.2.1) before DAP addition. If the binding of DAP-Ca^{2+} complex to the bactoprenol lipids is specific, such interactions should be inhibited by these competitive antibiotics.

Fruilimicin is a cyclic lipopeptide that interrupts the cell wall precursor cycle by specifically forming of a complex with C_{55}-P [160]. Bacitracin inhibits PGN synthesis by sequestering C_{55}-PP, thereby inducing the loss of cell integrity, leading to cell death [236]. Oritavancin is an amphiphilic derivative of vancomycin, and it specifically binds to the D-Ala–D-Ala terminus of lipid II to inhibit PGN biosynthesis [237].

Therefore, we pre-incubated the membranes containing 0.1 mol% PG and 0.1 mol% bactoprenol lipids (C_{55}-P, C_{55}-PP, and lipid II) with fruilimicin, bacitracin, and oritavancin, respectively (antibiotic to bactoprenol lipids ratio, 100:1) for 5 min. The excess unbound antibiotics was washed away, and the membranes were incubated

with a mixture of 50 nM DAP-BDP FL and 1 μM native DAP in the presence of 1 mM Ca^{2+}. The membranes were observed and imaged by TIRF microscopy within 2 min after DAP addition.

DAP-BDP FL molecules showed markedly decreased affinities for the membranes treated with the corresponding antibiotics, compared to the membranes without the antibiotic treatment, resulting in significant lower fluorescence intensity (Fig. 33A). The quantitative evaluation clearly showed a drastic decrease in the average fluorescence intensity in antibiotic-treated membranes, compared to that in the membranes without antibiotic pre-treatment (Fig. 33B). These results demonstrate that the binding of DAP to each bactoprenol lipid-containing membrane was inhibited by the corresponding specific antibiotics, thus proving the specificity in the interaction between DAP and the respective target molecules.

Based on these observations, we conclude that the combination of PG and each of these three bactoprenol lipids (C_{55}-P, C_{55}-PP, and lipid II) in the membrane is crucial for DAP binding. However, the driving force for these interactions remains unclear. We suggest that the presence of negatively charged PG provides a more suitable environment for the interaction between DAP-Ca^{2+} complexes and bactoprenol lipids. Alternatively, PG may serve as scaffold and induce a confirmation change in DAP, thereby enabling the easy attachment of DAP to these bactoprenol lipids.

In *S. aureus*, the septum is the only place where cell wall synthesis occurs, and all the three bactoprenol precursors are located at the septum and play key roles in teichoic acid biosynthesis. DAP preferably binds to C_{55}-P, C_{55}-PP, and lipid II in the presence of PG, probably locks these cell wall precursors by complex formation, thereby inhibiting PGN biosynthesis. This may explain the preferable binding of DAP to the septum in *S. aureus* cells during the first phase of DAP binding.

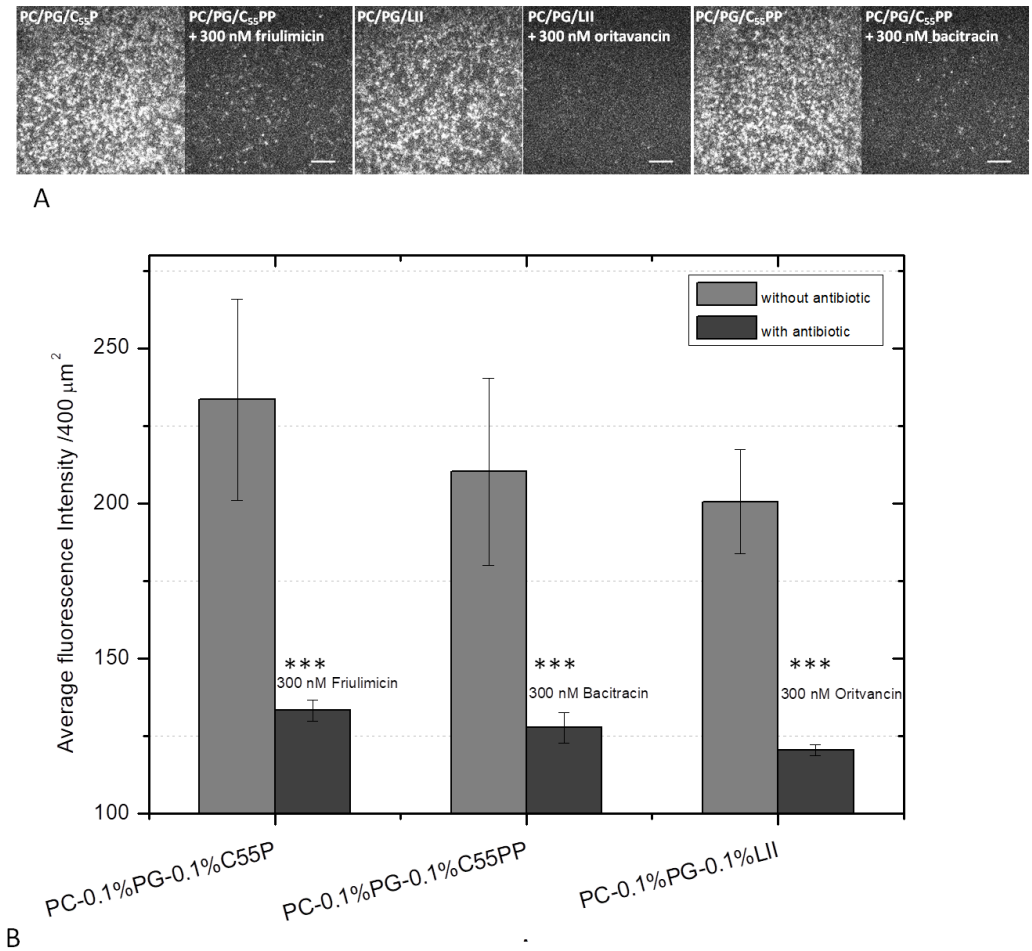

Figure 33: Inhibition of daptomycin (DAP) binding to the membranes containing the three bactoprenol lipids and phosphatidylglycerol (PG). A: TIRF images of DAP binding to each membrane. B: Data were plotted as mean values of the time-averaged intensity of each movies. The data shown were obtained from at least 20 movies for each membrane type. Standard errors of the mean are given by error bars. Significance was tested (independent, two-sample *t*-test) for the same membrane with and without antibiotic treatment; *** indicates $p < 0.001$.

On the basis of the collective findings from this work, we propose a model for the action of DAP in *S. aureus* (Fig. 34). The binding of DAP to the membrane of *S. aureus* can be classified as specific septum binding (Fig. 34A) and non-specific peripheral membrane binding (Fig. 34B). Both the types of binding are crucial to its bactericidal activity against *S. aureus*.

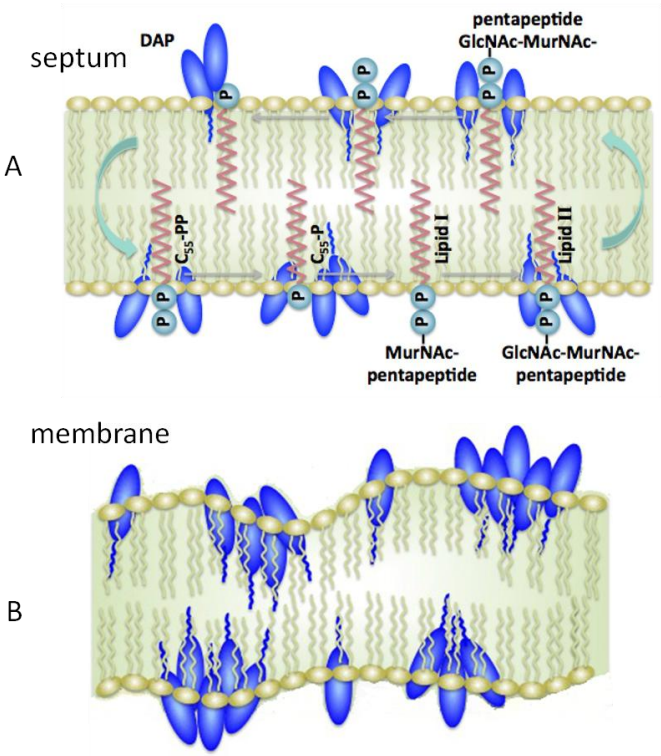

Figure 34: Proposed model for daptomycin (DAP) action. A: Specific septum binding. DAP (blue) preferably binds to bactoprenol precursors [undecaprenyl phosphate (C_{55}-P), undecaprenyl pyrophosphate (C_{55}-PP), and lipid II] in the presence of phosphatidylglycerol (PG) at septum. B: Non-specific peripheral membrane binding. DAP causes membrane distortion, aggregate formation, and cell size reduction.

Initially, the DAP-Ca^{2+} complex specifically binds to the bactoprenol precursors (C_{55}-P, C_{55}-PP, and lipid II) in the presence of PG at the septum. As DAP has been reported to flip between the two membrane leaflets [156], we suggest that DAP binds to these bactoprenol precursors on both leaflets of the membrane, forming DAP-bactoprenol lipid-PG complexes to block the PGN synthesis cycles. Such complexes might inhibit certain enzymatic steps that use these bactoprenol precursors as the substrate. This hypothesis is consistent with a recent report that DAP delocalizes MurG, a membrane-associated transferase that catalyzes the synthesis of lipid II in *B. subtilis* [140]. Notably, another important lipid precursor, lipid I, was not included in our studies; however, as lipid I is structurally similar to lipid II, we speculate the DAP might bind to lipid I as well. DAP-Ca^{2+} can directly bind to PG, driven by the attractive electrostatic forces; however, from our results, this binding is not dominant at the septum. It has been shown that fluorescently labeled DAP binds preferentially to the septa and forespore membrane in *B. subtilis*, because these areas are rich in PG

[150, 238]. In contrast to the *B. subtilis* cell membrane, which contains many phospholipids in the membrane, such as LPG, polyglycerol phospholipid, CL, PE, and PG [239], the *S. aureus* cell membrane contains PG as the major phospholipid and it is distributed throughout the membrane. Therefore, if the interaction of DAP and PG is dominant in *S. aureus*, DAP should have bound to all the regions of the membrane, rather than binding preferentially to the septa. Without PG, the DAP-Ca^{2+} complexes can also directly bind to each of the bactoprenol lipids. However, the binding efficiency in membranes containing only the bactoprenol lipids is remarkably lower than that in membranes containing both bactoprenol lipids and PG, indicating that PG plays a key role in the interaction of DAP with bactoprenol lipids.

After the binding sites at the septa are saturated, DAP binding extends to the peripheral membrane, thereby causing membrane distortion, aggregate formation, and cell size reduction. The interactions between DAP and PG both *in vivo* and on the artificial membrane have been well investigated in many studies. Generally, the interaction is considered as non-specific binding driven by attractive electrostatic forces. DAP reaches the membrane in the presence of Ca^{2+} and inserts its short lipid tail into the membrane. PG triggers a conformation change and enables the deeper insertion of DAP and promotes oligomer formation, thus inducing membrane distortion and aggregate (spotty pattern) formation [235]. We also observed cell size reduction caused by DAP; this finding is consistent with a previous report that DAP removed lipid molecules from GUVs by forming lipid-peptide aggregates, resulting in a reduction of GUV size [218]. Because spotty pattern formation and cell size reduction were dependent on DAP concentration and incubation time, we speculate that these effects are associated with the bactericidal activity of DAP.

Thus, we suggest both septum binding and peripheral membrane binding of DAP can eventually induce cell death. Septum binding contributes to inhibition of cell wall synthesis, whereas peripheral membrane binding contributes to membrane distortion and lipid removal from the membrane.

5. Summary

DAP is a clinically important lipopeptide antibiotic, its bactericidal activity has been reported to be Ca^{2+} and PG dependent [240,75,137]. Reduced PG content or increased conversion of PG to lysyl-PG promotes bacterial resistance to DAP [154,152]. Despite a large number of studies, the exact mechanism of action of DAP is still incompletely understood.

In this study, the mechanism of action of DAP was investigated. We studied the DAP binding behavior in *S. aureus* cells and attempted to identify its target molecule using several fluorescence imaging techniques.

First, we studied the distribution of fluorescently labeled DAP on *S. aureus* cell membranes. We analyzed the distribution of DAP on *S. aureus* cell membranes as well as its correlation with cell size and spotty pattern formation in a time- and concentration-dependent manner. HILO microscopy was used to reduce background fluorescence. *S. aureus* cells were incubated with mixtures of DAP-TMR (100 nM) and native DAP at sub-MIC (0.5 µM), around MIC (1 µM), or supra-MIC (6 and 10 µM) for varying time intervals. Septum binding was quantified in terms of the fluorescence ratio of DAP binding at the septum to lateral membrane. Septum binding was characterized by mean values of FR ≈ 4, whereas homogeneous membrane binding yielded mean values of FR ≈ 2. We observed septum binding for the DAP concentrations lower than the MIC for all incubations times tested (max. 25 min) and for the concentration around the MIC after 10 min of incubation. At longer incubation times and higher concentrations, homogeneous membrane binding of DAP occurred. DAP accumulation was negatively correlated with cell size but positively correlated with aggregate formation. The results from the use of a super-resolution imaging method, uPAINT, to study the binding of DAP-TMR to *S. aureus* at the single-molecule level, further support the conclusion that DAP binds preferentially to the septum. On the basis of these observations, we postulate a three-phase process of DAP binding to *S. aureus* cells: (I) initial binding to the division septum, (II) extended binding to the envelope, and (III) strong accumulation of DAP accompanied by formation of multiple foci cells and cell size reduction.

We further investigated the reason for such preferential binding of DAP to the septa

and attempted to identify a target molecule. For this, we studied the colocalization of DAP-TMR with two septum components, the cell division protein FtsW-GFP and the bactoprenol precursor lipid II by dual-color imaging microscopy. FtsW-GFP colocalized with DAP during the first phase of DAP binding at the septum; however, in the second phase, the distribution of the FtsW proteins remained unaffected, whereas DAP bound to the complete cell membrane. Treatment of *S. aureus* cells containing Van-BDP FL-labeled lipid II with a mixture of DAP-TMR and native DAP, revealed that the binding of DAP to the septum was inhibited by the vancomycin. This suggests that DAP interacts with lipid II.

Finally, we used fluid supported lipid bilayers to study the binding behavior of DAP with respect to the lipid composition of the membrane. DAP binds to membranes in a Ca^{2+}-dependent fashion [141], and it is known that anionic PG lipids are essential for effective DAP binding [149,150]. Bilayers were prepared on coverslips by vesicle fusion. We used neutral PC phospholipids as matrix to which PG or/and bactoprenol lipids (C_{55}-P, C_{55}-PP and lipid II) were added with an amount of 0.1 mol% or 0.2 mol%. As expected, the presence of PG enhanced the DAP binding. Interestingly, the intensity in bactoprenol lipid-containing membranes was higher than that in 0.1 mol% PG-containing membrane, indicating that DAP preferentially binds to these bactoprenol lipids rather than to PG. Notably, the addition of PG in each of bactoprenol-containing membrane further strengthened the binding of DAP. To further verify the specificity of DAP binding to each of bactoprenol precursors, membranes containing C_{55}-P, C_{55}-PP, and lipid II along with PG, were pre-treated with fruilimicin [160], bacitracin [236], and oritavancin [237], respectively to block the DAP binding. The results confirmed the specificity in the interaction between DAP and bactoprenol lipids and PG. In fact, bactoprenol lipids affect the binding of DAP, and the combination of PG and bactoprenol lipids play a key role in the bactericidal mechanism of DAP.

Further, as DAP was reported to form aggregates in solution, we studied aggregate formation in a mixture of varying concentrations of native DAP and fluorescently labeled DAP (DAP-BDP FL and DAP-TMR) in presence of Ca^{2+} by using fluorescence correlation spectroscopy (FCS). We did not observed any aggregates (data not shown); this result is contradictory to those from other studies. This

discrepancy may be attributed to DAP conformational changes induced by the covalently attached fluorescent labels.

In conclusion, we propose a new model for the binding of DAP to the septum of *S. aureus*, thereby providing important insights into the mechanism of action of DAP. However, the molecular mechanism of DAP binding to bactoprenol lipids in the presence of PG needs to be further investigated in the future studies.

6. Reference

[1] R. I. Aminov, A brief history of the antibiotic era: lessons learned and challenges for the future. Frontiers in Microbiology, 1 (2010) 134.

[2] R. Bentley, Different roads to discovery; Prontosil (hence sulfa drugs) and penicillin (hence β-lactams). Journal of Industrial Microbiology and Biotechnology, 36 (2009) 775-786.

[3] A. Fleming, On the antibacterial action of cultures of a penicillium, with special reference to their use in the isolation of B. influenza, British Journal of Experimental Pathology, 10 (1929) 226-236.

[4] S. Waksman, What is an antibiotic or an antibiotic substance? Mycologia, 39 (1947) 565-569.

[5] A. L. Demain, S. Sanchez, Microbial drug discovery: 80 years of progress. Journal of Antibiotics, 62 (2009) 5-16 (2009).

[6] L. I. Rothfield, Biological membranes: An overview at the molecular level. In structure and function of biological membranes, Academic Press, New York, (1971) 3-9.

[7] F. E. Frerman, D. C. White, Membrane lipid changes during the formation of a functional electron transport system in *Staphylococcus aureus*. Journal of Bacteriology, 94 (1967) 1868-1874.

[8] G. H. Joyce, R. K. Hammond, D. C. White, Changes in membrane lipid composition in exponentially growing *Staphylococcus aureus* during the shift from 37 to 25 C. Journal of Bacteriology, 104 (1970) 323-330.

[9] W. Dowhan, Molecular basis for membrane phospholipid diversity: why are there so many lipids? Annual Review of Biochemistry, 66 (1997) 199-232.

[10] H. Goldfine, M. E. Ellis, N-methyl groups in bacterial lipids. Journal of Bacteriology, 87 (1964) 8-15.

[11] T. G. Tornabene, Lipid composition of selected strains of Yersinia pestis and Yersinia pseudotuberculosis. Biochimica et Biophysica Acta, 306 (1973) 173-185.

[12] H. Roy, K. Dare, M. Ibba, Adaptation of the bacterial membrane to changing environments using aminoacylated phospholipids. Molecular Microbiology, 71 (2009) 547-550.

[13] H. Roy, M. Ibba, Broad range amino acid sppecificity of RNA-dependent lipid remodeling by multiple peptide resistance factors. Journal of Biological Chemistry, 284 (2009) 29677-29683.

[14] J. A. F. Op den Kamp, I. Redai, L. L. M. van Deenen, Phospholipid composition of *Bacillus subtilis*. Journal of Bacteriology, 99 (1969) 298-303.

[15] M. R. Nahaie, M. Goodfellow, D. E. Minnikin, V. Hajek, Polar lipid and isoprenoid quinone composition in the classification of Staphylococcus. Journal of General Microbiology, 130 (1984) 2427-2437.

[16] W. Fischer, K. Leopold, Polar lipids of four Listeria species containing L-lysylcardiolipin, a novel lipid structure, and other unique phospholipids. International Journal of Systematic Bacteriology, 49 (1999) 653-662.

[17] C. Sohlenkamp, K. A. Galindo-Lagunas, Z. Guan, P. Vinuesa, S. Robinson, J. Thomas-Oates, C. R. Raetz, O. Geiger, The lipid lysyl-phosphatidylglycerol is present in membranes of Rhizobium tropici CIAT899 and confers increased resistance to polymyxin B under acidic growth conditions. Molecular Plant-Microbe Interactions, 20 (2007) 1421-1430.

[18] S. Klein, C. Lorenzo, S. Hoffmann, J. M. Walther, S. Storbeck, T. Piekarski, B. J. Tindall, V. Wray, M. Nimtz, J. Moser, Adaptation of Pseudomonas aeruginosa to various conditions includes tRNA-dependent formation of alanyl-phosphatidylglycerol. Molecular Microbiology, 71 (2009) 551-565.

[19] S. Hebecker, W. Arendt, I. U. Heinemann, J. H. Tiefenau, M. Nimtz, M. Rohde, D. Soll, J. Moser, Alanyl-phosphatidylglycerol synthase: mechanism of substrate recognition during tRNA-dependent lipid modification in Pseudomonas aeruginosa. Molecular Microbiology, 80 (2011) 935-950.

[20] N. A. Nguyen, L. Sallans, E. S. Kaneshiro, The major glycerophospho-lipids of the predatory and parasitic bacterium Bdellovibrio bacteriovorus HID5. Lipids, 43 (2008) 1053-1063.

[21] P. Lata, D. Lal, R. Lal, Flavobacterium ummariense sp. nov., isolated from hexachlorocyclohexane-contaminated soil, and emended description of Flavobacterium ceti Vela et al. 2007. International Journal of Systematic and Evolutionary Microbiology, 62 (2012) 2674-2679.

[22] C. R. Raetz, W. Dowhan, Biosynthesis and function of phospho-lipids in Escherichia coli. Journal of Biological Chemistry, 265 (1990) 1235-1238.

[23] C. Benning, Z. H. Huang, D. A. Gage, Accumulation of a novel glycolipid and a betaine lipid in cells of Rhodobacter sphaeroides grown under phosphate limitation. Archives of Biochemistry and Biophysics, 317 (1995) 103-111.

[24] O. Geiger, V. Rohrs, B. Weissenmayer, T. M. Finan, J. E. Thomas-Oates, The regulator gene phoB mediates phosphate stress-controlled synthesis of the membrane lipid diacylglyceryl-N,N,N-trimethylhomoserine in Rhizobium (Sinorhizobium) meliloti. Molecular Microbiology, 32 (1999) 63-73.

[25] R. Anderson, K. Hansen, Structure of a novel phosphoglycolipid from Deinococcus radiodurans. Journal of Biological Chemistry, 260 (1985) 12219-12223.

[26] O. Geiger, N. Gonzalez-Silva, I. M. Lopez-Lara, C. Sohlenkamp, Amino acid-containing membrane lipids in bacteria. Progress in Lipid Research, 49 (2010) 46-60.

[27] M. A. Vences-Guzman, O. Geiger, C. Sohlenkamp, Ornithine lipids and their structural modications: from A to E and beyond. FEMS Microbiology Letters, 335 (2012) 1-10.

[28] K. Zhang, S. M. Beverley, Phospholipid and sphingolipid metabolism in Leishmania. Molecular and Biochemical Parasitology, 170 (2010) 55-64.

[29] R. Austrian, The Gram Stain and the etiology of lobar pneumonia, an historical note. Bacteriological Reviews, 24 (1960) 261-265.

[30] R. M. Epand, R. F. Epand, Domains in bacterial membranes and the action of antimicrobial agents. Molecular BioSystems, 5 (2009) 580-587.

[31] G. D. Shockman, J. F. Barrett, Structure, function, and assembly of cell walls of Gram-positive bacteria. Annual Review of Microbiology, 37 (1983) 501-527.

[32] J. R. Scott, T. C. Barnett, Surface proteins of Gram-positive bacteria and how they get there. Annual Review of Microbiology, 60 (2006) 397-423.

[33] A. Wright, D. J. Tipper, The outer membrane of gram-negative bacteria. In The Bacteria, J. R. Sokatch, L. N. Ornston, editors. Academic Press, New York, VII (1979) 427-485.

[34] H. Nikaido, Outer membrane. In Escherichia coli and Salmonella: Cellular and Molecular Biology; F. C. Neidhardt, editors, ASM Press, Washington DC, I (1996) 29-47.

[35] O. Ciofu, T. J. Beveridge, J. Kadurugamuwa, J. Walther-Rasmussen, N. Hoiby, Chromosomal betalactamase is packaged into membrane vesicles and secreted from Pseudomonas aeruginosa. Journal of Antimicrobial Chemotherapy, 45 (2000) 9-13.

[36] S. S. Thompson, Y.M. Naidu, J. J. Pestka, Ultrastructural localization of an extracellular protease in Pseudomonas fragi by using the peroxidase-antiperoxidase reaction. Applied and Environment Microbiology, 50 (1985) 1038-1042.

[37] K. Sankaran, H. C. Wu, Lipid modification of bacterial prolipoprotein. Transfer of diacylglyceryl moiety from phosphatidylglycerol. Journal of Biological Chemistry, 269 (1994) 19701-19706.

[38] H. Nikaido, M. Vaara, Molecular basis of bacterial outer membrane permeability. Microbiological Reviews, 49 (1985) 1-32.

[39] T. J. Silhavy, D. Kahne, S. Walker, The bacterial cell envelope. Cold Spring Harbor Perspectives in biology, 2 (2010) a000414

[40] M. R. Salton, Structure and function of bacterial cell membranes. Annual Review of Microbiology, 21 (1967) 417-442.

[41] J. W. Costerton, J. M. Ingram, K. J. Cheng, Structure and function of the cell envelope of gram-negative bacteria. Bacteriological reviews, 38 (1974) 87-110.

[42] Y. M. Zhang, C. Rock. Membrane lipid homeostasis in bacteria. Nature Reviews Microbiology, 6 (2008) 222-233.

[43] A. Typas, M. Banzhaf, C. A. Gross, W. Vollmer, From the regulation of peptidoglycan synthesis to bacterial growth and morphology. Nature Reviews Microbiology, 10 (2012) 123-136.

[44] J. van Heijenoort, Assembly of the monomer unit of bacterial peptidoglycan. Cellular and Molecular Life Sciences, 54 (1998) 300-304.

[45] J. van Heijenoort, Recent advances in the formation of the bacterial peptidoglycan monomer unit. Natural Products Reports, 18 (2001) 503-519.

[46] J. van Heijenoort, Lipid intermediates in the biosynthesis of bacterial peptidoglycan. Microbiology and Molecular Biology Reviews, 71 (2007) 620-635.

[47] H. Barreteau, A. Kovac, A. Boniface, M. Sova, D. Blanot, Cytoplasmic steps of peptidoglycan biosynthesis. FEMS Microbiology Review, 32 (2008) 168-207.

[48] A. L. Lovering, S. S. Safadi, N. C. J. Strynadka, Structural perspective of peptidoglycan biosynthesis and assembly. Annual Review of Biochemistry, 81 (2012) 451-478.

[49] A. J. Meeske, E. P. Riley, W. P. Robins, T. Uehara, J. J. Mekalanos, D. Kahne, S. Walker, A. C. Kruse, T. G. Bernhardt, D. Z. Rudner, SEDS proteins are a widespread family of bacterial cell wall polymerases. Nature, 537 (2016) 634-638.

[50] H. Cho, C. N. Wivagg, M. Kapoor, Z. Barry, P. D. A. Rohs, H. Suh, J. A. Marto, E. C. Garner, T. G. Bernhardt, Bacterial cell wall biogenesis is mediated by SEDS and PBP polymerase families functioning semi-autonomously. Nature Microbiology, 1 (2016) 16172.

[51] D. J. Scheffers, M. G. Pinho, Bacterial cell wall synthesis: new insights from localization studies. Microbiology and Molecular Biology Reviews, 69 (2005) 585-607.

[52] K. Ehlert, J. V. Holtje, Role of precursor translocation in coordination of murein and phospholipid synthesis in Escherichia coli. Journal of Bacteriology, 178 (1996) 6766-6771.

[53] F. Ishino, M. Matsuhashi, Peptidoglycan synthetic enzyme activities of highly purified penicillin-binding protein 3 in Escherichia coli: a septum-forming reaction sequence. Biochemical and Biophysical Research Communications, 101 (1981) 905-911.

[54] F. Ishino, W. Park, S. Tomioka, S. Tamaki, I. Takase, K. Kunugita, H. Matsuzawa, S. Asoh, T. Ohta, B. G. Spratt, M. Matsuhashi, Peptidoglycan synthetic activities in membranes of Escherichia coli caused by overproduction of penicillin-

binding protein 2 and RodA protein. Journal of Biological Chemistry, 261 (1986) 7024-7031.

[55] R. J. Watkinson, H. Hussey, J. Baddiley, Shared lipid phosphate carrier in the biosynthesis of teichoic acid and peptidoglycan. Nature New Biology, 229 (1971) 57-59.

[56] M. Scher, W. J. Lennarz, C. C. Sweeley, The biosynthesis of mannosyl-1-phosphoryl-polyisoprenol in Micrococcus lysodeikticus and its role in mannan synthesis. Proceedings of the National Academy of Sciences of the United States of America, 59 (1968) 1313-1320.

[57] T. E. Rohr, G. N. Levy, N. J. Stark, J. S. Anderson, Initial reactions in biosynthesis of teichuronic acid of Micrococcus lysodeikticus cell walls. Journal of Biological Chemistry, 252 (1977) 3460-3465.

[58] F. A. Troy, F. E. Frerman, E. C. Heath, The biosynthesis of capsular polysaccharide in Aerobacter aerogenes. Journal of Biological Chemistry, 246 (1971) 118-133.

[59] A. Wright, M. Dankert, P. Fennessey, P. W. Robbins, Characterization of a polyisoprenoid compound functional in O-antigen biosynthesis. Proceedings of the National Academy of Sciences of the United States of America, 57 (1967) 1798-1803.

[60] P. R. Reeves, M. Hobbs, M. A. Valvano, M. Skurnik, C. Whitfield, D. Coplin, N. Kido, J. Klena, D. Maskell, C. R. Raetz, P. D. Rick, Bacterial polysaccharide synthesis and gene nomenclature. Trends in Microbiology, 4 (1996) 495-503.

[61] A. Bouhss, A. E. Trunkfield, T. D. H. Bugg, D. Mengin-Lecreulx, The biosynthe sis of peptidoglycan lipid-linked intermediates. FEMS Microbiology Reviews, 32 (20 08) 208-233.

[62] K. Ogura, T. Koyama, Enzymatic aspects of isoprenoid chain elongation. Chemical Reviews, 98 (1998) 1263-1276.

[63] S. S. Richter, D. E. Kealey, C. T. Murray, K. P. Heilmann, S. L. Coffman, G. V. Doern, The in vitro activity of daptomycin against *Staphylococcus aureus* and Enterococcus species. Journal of Antimicrobial Chemotherapy, 52 (2003) 123-127.

[64] M. J. Rybak, E. Hershberger, T. Moldovan, R. G. Grucz, In vitro activities of daptomycin, vancomycin, linezolid, and quinupristin–dalfopristin against staphylococci and enterococci, including vancomycin-intermediate and-resistant strains. Antimicrobial Agents and Chemotherapy, 44 (2000) 1062-1066.

[65] D. R. Snydman, N. V. Jacobus, L. A. McDermott, J. R. Lonks, J. M. Boyce, Comparative in vitro activities of daptomycin and vancomycin against resistant Gram-positive pathogens. Antimicrobial Agents and Chemotherapy, 44 (2000) 3447-3450.

[66] F. P. Tally, M. Zeckel, M. M. Wasilewski, C. Carini, C. L. Berman, G. L. Drusano, F. B. Oleson, Daptomycin: a novel agent for gram-positive infections. Expert Opinion on Investigational Drugs, 8 (1999) 1223-1238.

[67] F. P. Tally, M. F. DeBruin, Development of daptomycin for gram-positive infections. Journal of Antimicrobial Chemotherapy, 46 (2000) 523-526.

[68] A. H. Mutnick, D. J. Biedenbach, R. N. Jones, Geographic variations and trends in antimicrobial resistance among *Enterococcus faecalis* and *Enterococcus faecium* in the SENTRY Antimicrobial Surveillance Program (1997–2000). Diagnostic Microbiology and Infectious Disease, 46 (2003) 63-68.

[69] Cubicin (daptomycin for injection), Lexington, MA: Cubist Pharaceuticals, 2003.

[70] L. A. Mortara, A. S. Bayer, *Staphylococcus aureus* bacteremia and endocarditis. New diagnostic and therapeutic concepts. Infectious Disease Clinics of North America, 7 (1993) 53-68.

[71] J. K. Hobbs, K. Miller, A. J. O'Neill, I. Chopra, Consequences of daptomycin-mediated membrane damage in *Staphylococcus aureus*. Journal of Antimicrobial Chemotherapy, 62 (2008) 1003-1008.

[72] G. Sakoulas, G. M. Eliopoulos, J. Alder, C. T. Eliopoulos, Efficacy of daptomycin in experimental endocarditis due to methicillin-resistant *Staphylococcus aureus*. Antimicrobial Agents and Chemotherapy, 47 (2003) 1714-1718.

[73] R. H. Baltz, Lipopeptide antibiotics produced by Streptomyces roseosporus and Streptomyces fradiae. In Biotechnology of Antibiotics Second Edition, (1997) 415-435.

[74] R. H. Baltz, V. Miao, S. K. Wrigley, Natural products to drugs: daptomycin and related lipopeptide antibiotics. Natural Product Reports, 22 (2005) 717-741.

[75] J. A. Silverman, N. G. Perlmutter, H. M. Shapiro, Correlation of daptomycin bactericidal activity and membrane depolarization in *Staphylococcus aureus*. Antimicrobial Agents and Chemotherapy, 47 (2003), 2538-2544.

[76] L. Robbel, A. M. Mohamed, Daptomycin, a bacterial lipopeptide synthesized by a non-ribosomal machinery. Journal of Biological Chemistry, 285 (2010) 27501-27508.

[77] M. Debono, B. J. Abbott, R. M. Molloy, D. S. Fukuda, A. H. Hunt, V. M. Daupert, F. T. Counter, J. L. Ott, C. B. Carrell, L. C. Howard, Enzymatic and chemical modifications of lipopeptide antibiotic A21978C: the synthesis and evaluation of daptomycin (LY146032). Journal of Antibiotics, 41 (1988) 1093-1105.

[78] K. Nguyen, D. Ritz, J. Q. Gu, D. Alexander, M. Chu, V. Miao, P. Brian, R. H. Baltz, Combinatorial biosynthesis of novel antibiotics related to daptomycin. Proceedings of the National Academy of Sciences, 103 (2006) 17462-17467.

[79] M. Debono, M. Barnhart, C. B. Carrell, J. A. Hoffmann, J. L. Occolowitz, B. J. Abbott, D. S. Fukuda, R. L. Hamill, K. Biemann, W. C. Herlihy, A21978C, a complex of new acidic peptide antibiotics: isolation, chemistry, and mass spectral structure elucidation. Journal of Antibiotics, 40 (1987) 761-777.

[80] J. H. Lakey, E. J. Lea, B. A. Rudd, H. M. Wright, D. A. Hopwood, A new channel-forming antibiotic from Streptomyces coelicolor A3(2) which requires calcium for its activity. Journal of General Microbiology, 129 (1983) 3565-3573.

[81] Z. Hojati, C. Milne, B. Harvey, L. Gordon, M. Borg, F. Flett, B. Wilkinson, P. J. Sidebottom, B. A. Rudd, M. A. Hayes, C. P. Smith, J. Micklefield, Structure, biosynthetic origin, and engineered biosynthesis of calcium-dependent antibiotics from Streptomyces coelicolor. Chemistry and Biology, 9 (2002) 1175-1187.

[82] L. D. Boeck, H. R. Papiska, R. W. Wetzel, J. S. Mynderse, D. S. Fukuda, F. P. Mertz, D. M. Berry, A54145, a new lipopeptide antibiotic complex: discovery, taxonomy, fermentation and HPLC. Journal of Antibiotics, 43 (1990) 587-593.

[83] R. Benne, P. Sloof, Evolution of the mitochondrial protein synthetic machinery. BioSystems, 21 (1987) 51-68.

[84] K. E. Bushley, B. G. Turgeon, Phylogenomics reveals subfamilies of fungal nonribosomal peptide synthetases and their evolutionary relationships. BMC Evolutionary Biology, (2010) 10:26.

[85] E. A. Felnagle, E. E. Jackson, Y. A. Chan, A. M. Podevels, A. D. Berti, M. D. McMahon, M. G. Thomas, Nonribosomal peptide synthetases involved in the production of medically relevant natural products. Molecular Pharmaceutics, 5 (2008) 191-211.

[86] M. A. McHenney, T. J. Hosted, B. S. Dehoff, P. R. Rosteck, R. H. Baltz, Molecular cloning and physical mapping of the daptomycin gene cluster from Streptomyces roseosporus. Journal of Bacteriology, 180 (1998) 143-151.

[87] D. Schwarzer, R. Finking, M. A. Marahiel, Nonribosomal peptides: from genes to products. Natural Products Reports, 20 (2003) 275-287.

[88] M. A. Marahiel, T. Stachelhaus, H. D. Mootz, Modular peptide synthetases involved in nonribosomal peptide synthesis. Chemical Reviews, 97 (1997) 2651-2674.

[89] P. H. Nakhate, V. K. Yadav, A. N. Pathak, A review on daptomycin; the first US-FDA approved lipopeptide antibiotics. Journal of Scientific and Innovative Research, 2 (2013) 970-980.

[90] G. H. Yu, X. Q. Jia, J. P. Wen, G. Y. Wang, Y. L. Chen, Enhancement of daptomycin production in Streptomyces roseosporus LC-51 by manipulation of cofactors concentration in the fermentation culture‖. World Journal of Microbiology and Biotechnology, 27 (2011) 1859-1868.

[91] V. Miao, M. F. Coeeffet-Legal, P. Brian, R. Brost, J. Penn, A. Whiting, S. Martin, R. Ford, R. Parr, M. Bouchard, C. J. Silva, S. K. Wrigley, R. H. Baltz, Daptomycin biosynthesis in Streptomyces roseosporus: cloning and analysis of the gene cluster and revision of peptide stereochemistry. Microbiology, 151 (2005) 1507-1523.

[92] F. M. Huber, R. L. Pieper, A. J. Tietz, The formation of daptomycin by supplying decanoic acid to Streptomyces roseosporus cultures producing the antibiotic complex A21978C. Journal of Biotechnology, 7 (1998) 283-292.

[93] R. H. Baltz, Biosynthesis and genetic engineering of lipopeptide antibiotics related to daptomycin. Current Topics in Medicinal Chemistry, 8 (2008) 618-638.

[94] S. Y. Lee, H. U. Kim, J. H. Park, J. M. Park, T. Y. Kim, Metabolic engineering of microorganisms: general strategies and drug production. Drug Discovery Today, 14 (2009) 78-88.

[95] V. Miao, M. F. Coeeffet-Legal, K. Nguyen, P. Brian, J. Penn, A. Whiting, J. Steele, D. Kau, S. Martin, R. Ford, T. Gibson, M. Bouchard, S. K. Wrigley, R. H. Baltz, Genetic Engineering in Streptomyces roseosporus to produce hybrid lipopeptide antibiotics. Chemistry and Biology, 13 (2006) 269-276.

[96] A. D. Russell, I. Chopra. Antiseptics, disinfectants, and preservatives: their properties, mechanisms of action and uptake into bacteria. In: Understanding Antibacterial Action and Resistance, Ellis Horwood, Hertfordshire, (1996) 96-149.

[97] J. A. Sutcliffe, J. P. Mueller, E. A. Utt, Antibiotic resistance mechanisms of bacterial pathogens. In: Manual of Industrial Microbiology and Biotechnology, ASM Press, Washington, (1999) 759-775.

[98] H. C. Neu, The crisis in antibiotic resistance. Science, 257 (1992) 1064-1073.

[99] S. P. Chakraborty, P. Pramanik, S. Roy, A review on emergence of antibiotic resistant *Staphylococcus aureus* and role of chitosan nanoparticle in drug delivery. Pharmaceutical Sciences, Novel drug delivery system, 2 (2012) L96 - L115.

[100] T. D. Bugg, D. Braddick, C. G. Dowson, D. I. Roper, Bacterial cell wall assembly: still an attractive antibacterial target. Trends in Biotechnology, 29 (2011) 167-173.

[101] T. Schneider, H.-G. Sahl, An oldie but a goodie-cell biosynthesis as antibiotic target pathway. International Journal of Medical Microbiology, 300 (2011) 161-169.

[102] K. G. Gunetileke, R. A. Anwar, Biosynthesis of uridine diphospho-N-acetyl muramic acid. Journal of Biological Chemistry, 241 (1966) 5740-5743.

[103] D. H. Kim, W. J. Lees, K. E. Kempsell, W. S. Lane, K. Duncan, C. T. Walsh, Characterization of a Cys115 to Asp substitution in the Escherichia coli cell wall biosynthetic enzyme UDP-GlcNAc enolpyruvyl transferase (MurA) that confers

resistance to inactivation by the antibiotic fosfomycin. Biochemistry, 35 (1996) 4923-4928.

[104] J. L. Marquardt, E. D. Brown, W. S. Lane, T. M. Haley, Y. Ichikawa, C. H. Wong, C. T. Walsh, Kinetics, stoichiometry, and identification of the reactive thiolate in the inactivation of UDP-GlcNAc enolpyruvoyl transferase by the antibiotic fosfomycin. Biochemistry, 33 (1994) 10646-10651.

[105] E. Ito, J. L. Strominger, Enzymatic synthesis of the peptide in bacterial uridine nucleotides. III. Purification and properties of L-lysine- adding enzyme. Journal of Biological Chemistry, 239 (1964) 210-214.

[106] S. G. Nathensen, J. L. Strominger, E. Ito, Enzymatic synthesis of the peptide in bacterial uridine nucleotides. IV. Purification and properties of D-glutamic acid-adding enzyme. Journal of Biological Chemistry, 239 (1964) 1773-1776.

[107] Z. Feng, R. G. Barletta, Roles of mycobacterium smegmatis D-alanine: D-alanine ligase and D-alanine racemase in the mechanisms of action of and resistance to the peptidoglycan inhibitor D-cycloserine. Antimicrobial Agents and Chemotherapy, 47 (2003) 283-291.

[108] M. Noda, Y. Kawahara, A. Ichikawa, Y. Matoba, H. Matsuo, D. G. Lee, T. Kumagai, M. Sugiyama, Self-protection mechanism in D-cycloserine-producing Streptomyces lavendulae. Gene cloning, characterization, and kinetics of its alanine racemase and D-alanyl-D-alanine ligase, which are target enzymes of D-cycloserine. Journal of Biological Chemistry, 279 (2004) 46143-46152.

[109] M. Winn, R. J. M. Goss, K. Kimura, T. D. H. Bugg, Antimicrobial nucleoside antibiotics targeting cell wall assembly: recent advances in structure-function studies and nucleoside biosynthesis. Natural Product Reports, 27 (2010) 279-304.

[110] P. E. Brandish, K. I. Kimura, M. Inukai, R. Southgate, J. T. Lonsdale, T. D. Bugg, Modes of action of tunicamycin, liposidomycin B, and mureidomycin A: inhibition of phosphor-N-acetylmuramyl-pentapeptide translocase from Escherichia coli. Antimicrobial Agents and Chemotherapy, 40 (1996) 1640-1644.

[111] B. C. Chung, J. Zhao, R. A. Gillespie, D. Y. Kwon, Z. Guan, J. Hong, P. Zhou, S. Y. Lee, Crystal structure of MraY, an essential membrane enzyme for bacterial cell wall synthesis. Science, 341 (2013) 1012-1016.

[112] H. Tanaka, R. Oiwa, S. Matusukura, S. Omura, Amphomycin inhibits phospho-N-acetylmuramyl-pentapeptide translocase in peptidoglycan synthesis of Bacillus. Biochemical and Biophysical Research Communications, 86 (1979) 902-908.

[113] K. D. Young, Microbiology. A flipping cell wall ferry. Science, 345 (2014) 139-140.

[114] S. T. Hsu, E. Breukink, E. Tischenko, M. A. Lutters, B. de Kruijff, R. Kaptein, A. M. Bonvin, N. A. van Nuland, The nisin-lipid II complex reveals a pyrophosphate cage that provides a blueprint for novel antibiotics. Nature Structural and Molecular Biology, 11 (2004) 963-967.

[115] B. Ostash, S. Walker, Moenomycin family antibiotics: chemical synthesis, biosynthesis, and biological activity. Natural Product Reports, 27 (2010) 1594-1617.

[116] Y. Yuan, S. Fuse, B. Ostash, P. Sliz, D. Kahne, S. Walker, Structural analysis of the contacts anchoring moenomycin to peptidoglycan glycosyltransferases and implications for antibiotic design. ACS Chemical Biology, 3 (2008) 429-436.

[117] J. M. Ghuysen, Serine beta-lactamases and penicillin-binding proteins. Annual Review of Microbiology, 45 (1991) 37-67.

[118] P. E. Reynolds, Studies on the mode of action of vancomycin. Biochimica et Biophysica Acta, 52 (1961) 403-405.

[119] H. R. Perkins, Specificity of combination between mucopeptide precursors and vancomycin or ristocetin. Biochemical Journal, 111 (1969) 195-205.

[120] D. J. Tipper, J. L. Strominger, Mechanism of action of penicillins: a proposal based on their structural similarity to acyl-D-alanyl-D-alanine. Proceedings of the National Academy of Sciences, 54 (1965) 1133-1141.

[121] G. Manat, S. Roure, R. Auger, A. Bouhss, H. Barreteau, D. Mengin-Lecreulx, T. Touze, Deciphering the metabolism of undecaprenyl-phosphate: the bacterial cell-wall unit carrier at the membrane frontier. Microbial Drug Resistance, 20 (2014) 199-214.

[122] K. J. Stone, J. L. Strominger, Mechanism of action of bacitracin: complexation with metal ion and C55-isoprenyl pyrophosphate. Proceedings of the National Academy of Sciences, 68 (1971) 3223-3227.

[123] K. J. Stone, J. L. Strominger, Inhibition of sterol biosynthesis by bacitracin. Proceedings of the National Academy of Sciences, 69 (1972) 1287-1289.

[124] P. C. Fuchs, A. L. Barry, S. D. Brown. In vitro bactericidal activity of daptomycin against staphylococci. Journal of Antimicrobial Chemotherapy, 49 (2002) 467-470.

[125] N. E. Allen, J. N. Hobbs, W. E. Alborn. Inhibition of peptidoglycan biosynthesis in gram-positive bacteria by LY146032. Antimicrobial agents and chemotherapy, 31 (1987) 1093-1099.

[126] N. E. Allen, W. E. J. Alborn, J. N. J. Hobbs. Inhibition of membrane potential-dependent amino acid transport by daptomycin. Antimicrobial Agents and Chemotherapy, 35(1991) 2639-2642.

[127] P. Canepari, M. Boaretti, M. M. Lleo, G. Satta. Lipoteichoic acid as a new target for activity of antibiotics: mode of action of daptomycin (ly146032). Antimicrobial Agents and Chemotherapy, 34 (1990) 1220-1226.

[128] M. Boaretti, P. Canepari, M. M. Lleo, G. Satta. The activity of daptomycin on enterococcus faecium protoplasts: indirect evidence supporting a novel mode of action on lipoteichoic acid synthesis. Antimicrobial Agents and Chemotherapy, 31 (1993) 227-235.

[129] V. Laganas, J. Alder, J. A. Silverman. In vitro bactericidal activities of daptomycin against *Staphylococcus aureus* and *Enterococcus faecalis* are not mediated by inhibition of lipoteichoic acid biosynthesis. Antimicrobial Agents and Chemotherapy, 47 (2003) 2682-2684.

[130] N. Cotroneo, R. Harris, N. Perlmutter, T. Beveridge, J. A. Silverman. Daptomycin exerts bactericidal activity without lysis of *Staphylococcus aureus*. Antimicrobial Agents and Chemotherapy, 52 (2008) 2223-2225.

[131] J. Pogliano, N. Pogliano, J. A. Silverman. Daptomycin-mediated reorganization of membrane architecture causes mislocalization of essential cell division proteins. Journal of Bacteriology, 194 (2012) 4494-4504.

[132] R. H. Baltz. Daptomycin: mechanisms of action and resistance, and biosyntethis engineering. Current Opinion in Chemical Biology, 13 (2009) 144-151.

[133] S. K. Straus, R. E. W. Hancock. Mode of action of the new antibiotic for Gram-positive pathogens daptomycin: comparison with cationic antimicrobial peptides and lipopeptides. Biochimica et Biophysica Acta, 1758 (2006) 1215-1223.

[134] W. R. P. Scott, S. B. Baek, D. Jung, R. E. W. Hancock, S. K. Straus. NMR structural studies of the antibiotic lipopeptide daptomycin in DHPC micelles. Biochimica et Biophysica Acta, 1768 (2007) 3116-3146.

[135] D. Jung, J. P. Powers, S. K. Straus, R. E. W. Hancock. Lipid-specific binding of the calcium-dependent antibiotic daptomycin leads to changes in lipid polymorphism of model membranes. Chemistry and Physics of Lipids, 154 (2008) 120-128.

[136] J. N. Steenbergen, J. Alder, G. M. Thorne, F. P. Tally. Daptomycin: a lipopeptide antibiotic for the treatment of serious Gram-positive infections. Journal of Antimicrobial Chemotherapy, 55 (2005) 283-288.

[137] D. Jung, A. Rozek, M. Okon, R. E. W. Hancock. Structural transitions as determinants of the action of the calcium-dependent antibiotic daptomycin. Chemistry and Biology, 11 (2004) 949-957.

[138] N. Woodford. Novel agents for the treatment of resistant gram-positive infections. Expert Opinion on Investigational Drugs, 12 (2003) 117-137.

[139] S. W. Ho, D. Jung, J. R. Calhoun, J. D. Lear, M. Okon, W. R. Scott, R. E. Hancock, S. K. Straus. Effect of divalent cations on the structure of the antibiotic daptomycin. European Biophysics Journal, 37 (2008) 421-433.

[140] A. Müller, M. Wenzel, H. Strahl, F. Grein, T. N. Saaki, B. Kohl, T. Siersma, J. E. Bandow, H.-G. Sahl, T. Schneider, L. W. Hamoen, Daptomycin inhibits cell envelope synthesis by interfering with fluid membrane microdomains. Proceedings of the National Academy of Sciences of the United States of America, (2016) E7077-E7086.

[141] J. H. Andrew, M. C. Wale, L. J. Wale, D. Greenwood, The effect of cultural conditions on the activity of LY146032 against *staphylococci* and *streptococci*. Journal of Antimicrobial Chemotherapy, 20 (1987) 213-221.

[142] A. W. Chow, N. Cheng, In vitro activities of daptomycin (LY146032) and paldimycin (U-70, 138F) against anaerobic gram-positive bacteria. Antimicrobial Agents and Chemotherapy, 32 (1988) 788-790.

[143] J. K. Muraih, A. Pearson, J. A. Silverman, M. Palmer, Oligomerization of daptomycin on membranes. Biochimica et Biophysica Acta, 1808 (2011) 1154-1160.

[144] K. S. Rotondi, L. M. Gierasch, A well-defined amphipathic conformation for the calcium-free cyclic lipopeptide antibiotic, daptomycin, in aqueous solution. Biopolymers, 80 (2005) 374-385.

[145] L. J. Ball, C. M. Goult, J. A. Donarski, J. Micklefield, V. Ramesh, NMR structure determination and calcium binding effects of lipopeptide antibiotic daptomycin. Organic and Biomolecular Chemistry, 2 (2004) 1872-1878.

[146] P. Garidel, A. Blume, 1,2-Dimyristoyl-sn-glycero-3-phosphoglycerol (DMPG) monolayers: influence of temperature, pH, ionic strength and binding of alkaline earth cations. Chemistry and Physics of Lipids, 138 (2005) 50–59.

[147] J. H. Lakey, E. J. Lea, The role of acyl chain character and other determinants on the bilayer activity of A21978C an acidic lipopeptide antibiotic. Biochimica et Biophysica Acta, 859 (1986) 219-226.

[148] J. H. Lakey, M. Ptak, Fluorescence indicates a calcium-dependent interaction between the lipopeptide antibiotic LY146032 and phospholipid membranes. Biochemistry, 27 (1988) 4639-4645.

[149] R. M. Epand, S. Rotem, A. Mor, B. Berno, R. F. Epand, Bacterial membranes as predictors of antimicrobial potency. Journal of the American Chemical Society, 130 (2008) 14346-14352.

[150] A. B. Hachmann, E. R. Angert, J. D. Helmann, Genetic analysis of factors affecting susceptibility of *Bacillus subtilis* to daptomycin. Antimicrobial Agents and Chemotherapy, 53 (2009) 1598-1609.

[151] K. L. Palmer, A. Daniel, C. Hardy, J. Silverman, M. S. Gilmore, Genetic basis for daptomycin resistance in *enterococci*. Antimicrobial Agents and Chemotherapy, 55 (2011) 3345-3356.

[152] N. N. Mishra, S. J. Yang, A. Sawa, A. Rubio, C. C. Nast, M. R. Yeaman, A. S. Bayer, Analysis of cell membrane characteristics of in vitro-selected daptomycin-resistant strains of methicillin-resistant *Staphylococcus aureus*. Antimicrobial Agents and Chemotherapy, 53 (2009) 2312-2318.

[153] N. N. Mishra, G. Y. Liu, M. R. Yeaman, C. C. Nast, R. A. Proctor, J. Mckinnell, A. S. Bayer, Carotenoid-related alteration of cell membrane fluidity impacts *Staphylococcus aureus* susceptibility to host defense peptides. Antimicrobial Agents and Chemotherapy, 55 (2011) 526-531.

[154] L. Friedman, J. D. Alder, J. A. Silverman, Genetic changes that correlate with reduced susceptibility to daptomycin in *Staphylococcus aureus*. Antimicrobial Agents and Chemotherapy, 50 (2006) 2137-2145.

[155] S. J. Yang, Y. Q. Xiong, P. M. Dunman, J. Schrenzel, P. Francois, A. Peschel, A. S. Bayer, Regulation of mprF in daptomycin-nonsusceptible *Staphylococcus aureus* strains. Antimicrobial Agents and Chemotherapy, 53 (2009) 2636-2637.

[156] T. Zhang, J. K. Muraih, N. Tishbi, J. Herskowitz, R. L. Victor, J. Silverman, S. Uwumarenogie, S. D. Taylor, M. Palmer, E. Mintzer, Cardiolipin prevents membrane translocation and permeabilization by daptomycin. Journal of Biological Chemistry, 289 (2014) 11584-11591.

[157] T. T. Tran, D. Panesso, N. N. Mishra, E. Mileykovskaya, Z. Guan, J. M. Munita, J. Reyes, L. Diaz, G. M. Weinstock, B. E. Murray, Y. Shamoo, W. Dowhan, A. S. Bayer, C. A. Arias, Daptomycin-resistant *Enterococcus faecalis* diverts the antibiotic molecule from the division septum and remodels cell membrane phospholipids. mBio, 4 (2013) 4.

[158] D. Mengin-Lecreulx, N. E. Allen, J. N. Hobbs, J. van Heijenoort, Inhibition of peptidoglycan biosynthesis in *Bacillus megaterium* by daptomycin. FEMS Microbiology Letters, 57 (1990) 245-248.

[159] K. Bush, Antimicrobial agents targeting bacterial cell walls and cell membranes. Revue Scientifique Et Technique, 1 (2012) 43-56.

[160] T. Schneider, K. Gries, M. Josten, I. Wiedemann, S. Pelzer, H. Labischinski, H.-G. Sahl, The lipopeptide antibiotic Friulimicin B inhibits cell wall biosynthesis

through complex formation with bactoprenol phosphate. Antimicrobial Agents and Chemotherapy, 53 (2009) 1610-1618.

[161] E. Rubinchik, T. Schneide, M. Elliott, W. R. P. Scott, J. Pan, C. Anklin, H. Yang, D. Dugourd, A. Muller, K. Gries, S. K. Straus, H.-G. Sahl, R. E. W. Hancock, Mechanism of action and limited cross-resistance of new lipopeptide MX-2401. Antimicrobial Agents and Chemotherapy, 55 (2011) 2743-2754.

[162] M. Singh, J. Chang, L. Coffman, S. J. Kim, Solid-state NMR characterization of amphomycin effects on peptidoglycan and wall teichoic acid biosyntheses in *Staphylococcus aureus*. Scientific Reports, 6 (2016) 31757.

[163] T. Wecke, D. Zuhlke, U. Mader, S. Jordan, B. Voigt, S. Pelzer, H. Labischinski, G. Homuth, M. Hecker, T. Mascher, Daptomycin versus friulimicin B: in-depth profiling of *Bacillus subtilis* cell envelope stress responses, Antimicrobial Agents and Chemotherapy, 53 (2009) 1619-1623.

[164] D. M. Livermore, Bacterial resistance: origins, epidemiology and impact. Clinical Infectious Diseases, 36 (2003) 11-23.

[165] J. Davies, Inactivation of antibiotics and the dissemination of resistance genes. Science, 264 (1994) 375-382.

[166] F. C. Tenover, Development and spread of bacterial resistance to antimicrobial agents: An overview. Clinical Infectious Diseases, 33 (2001) 108-115.

[167] J. A. Karlowsky, D. C. Draghi, M. E. Jones, C. Thornsberry, I. R. Friedl, D. F. Sahm, Surveillance for antimicrobial susceptibility among clinical isolates of Pseudomonas aeruginosa and Acinetobacter baumannii from hospitalized patients in the United States, 1998 to 2001. Antimicrobial Agents and Chemotherapy, 47 (2003) 1681-1688.

[168] E. H. Ibrahim, G. Sherman, S. Ward, V. J. Fraser, M. H. Kollef, The influence of inadequate antimicrobial treatment of bloodstream infections on patient outcomes in the ICU setting. Chest, 118 (2000) 146-155.

[169] M. N. Alekshun, S. B. Levy, Molecular mechanisms of antibacterial multidrug resistance. Cell, 128 (2007) 1037-50.

[170] J. E. Jr. McGowan, Economic impact of antimicrobial resistance. Emerging Infectious Dieseases, 7 (2001) 286-292.

[171] C. I. Kang, S. H. Kim, W. B. Park, K. D. Lee, H. B. Kim, E. C. Kim, M. D. Oh, K. W. Choe, Bloodstream infections caused by antibiotic-resistant gram-negative bacilli: risk factors for mortality and impact of inappropriate initial antimicrobial therapy on outcome. Antimicrobial Agents and Chemotherapy, 49 (2005) 760-766.

[172] K. B. Stevenson, Methicillin-resistant *Staphylococcus aureus* and vancomycin-resistant enterococci in rural communities, Western United States. Emerging Infectious Dieseases, 11 (2005) 895-903.

[173] N. Woodford, M. E. Ward, M. E. Kaufmann, J. Turton, E. J. Fagan, D. James, A. P. Johnson, R. Pike, M. Warner, T. Cheasty, A. Pearson, S. Harry, J. B. Leach, A. Loughrey, J. A. Lowes, R. E. Warren, D. M. Livermore, Community and hospital spread of Escherichia coli producing CTX-M extended-spectrum beta-lactamases in the UK. J. Antimicrobial Agents and Chemotherapy, 54 (2004) 735-743.

[174] D. W. Isenbarger, C. W. Hoge, A. Srijan, C. Pitarangsi, N. Vithayasai, L. Bodhidatta, K. W. Hickey, P. D. Cam, Comparative antibiotic resistance of diarrheal pathogens from Vietnam and Thailand, 1996–1999. Emerging Infectious Dieseases, 8 (2002) 175-180.

[175] I. Nachamkin, H. Ung, M. Li, Increasing fluoroquinolone resistance in Campylobacter jejuni, Pennsylvania, USA, 1982–2001. Emerging Infectious Dieseases, 12 (2002) 1501-1503.

[176] L. Fernandez, R. E. W. Hancock, Adaptive and mutational resistance: role of porins and efflux pumps in drug resistance. Clinical Microbiology Reviews, 25 (2012) 661-681.

[177] H. Nikaido, Multidrug resistance in bacteria. Annual Review of Biochemistry, 78 (2009) 119-146.

[178] G. D. Wright, Molecular mechanisms of antibiotic resistance, Chemical Communications, 47 (2011) 4055-4061.

[179] D. Senka, S. Jagoda, K. Blazenka, Antibiotic resistance mechanisms in bacteria: biochemical and genetic aspects. Food Technology and Biotechnology, 46 (2008) 11-21.

[180] A. Louie, A. L. Baltch, W. J. Ritz, R. P. Smith, M. Asperilla, Comparison of in vitro inhibitory and bactericidal activities of daptomycin (LY 146032) and four reference antibiotics, singly and in combination, against gentamicin-susceptible and high-level-gentamicin-resistant enterococci. Chemotherapy, 39 (1993) 302-310.

[181] A. Mangili, I. Bica, D. R. Snydman, D. H. Hamer, Daptomycin-resistant, methicillin-resistant *Staphylococcus aureus* bacteremia. Clinical Infectious Diseases, 40 (2005) 1058-1060.

[182] J. Vouillamoz, P. Moreillon, M. Giddey, J. M. Entenza, Efficacy of daptomycin in the treatment of experimental endocarditis due to susceptible and multidrug-resistant enterococci. Journal of Antimicrobial Chemotherapy, 58 (2006) 1208-1214.

[183] M. K. Hayden, K. Rezai, R. A. Hayes, K. Lolans, J. P. Quinn, R. A. Weinstein, Development of daptomycin resistance in vivo in methicillin-resistant *Staphylococcus aureus*. Journal of Clinical Microbiology, 43 (2005) 5285-5287.

[184] F. M. Marty, W. W. Yeh, C. B. Wennersten, L. Venkataraman, E. Albano, E. P. Alyea, H. S. Gold, L. R. Baden, S. K. Pillai, Emergence of a clinical daptomycin-resistant *Staphylococcus aureus* isolate during treatment of methicillin-resistant *Staphylococcus aureus* bacteremia and osteomyelitis. Journal of Clinical Microbiology, 44 (2006) 595-597.

[185] J. S. Lewis, A. Owens, J. Cadena, K. Sabol, J. E. Patterson, J. P. Jorgensen, Emergence of daptomycin resistance in Enterococcus faecium during daptomycin therapy. Antimicrobial Agents and Chemotherapy, 49 (2005) 1664-1665.

[186] L. Munoz-Price, K. Lolans, J. P. Quinn, Emergence of resistance to daptomycin during treatment of vancomycin-resistant *Enterococcus faecalis* infection. Clinical Infectious Diseases, 41 (2005) 565-566.

[187] M. R. Green, C. Anasetti, R. L. Sandin, N. E. Rolfe, J. N. Greene, Development of daptomycin resistance in a bone marrow transplant patient with vancomycin-resistant Enterococcus durans. Journal of Oncology Pharmacy Practice, 12 (2006) 179-181.

[188] J. A. Silverman, N. Oliver, T. Andrew, T. Li, Resistance studies with daptomycin. Antimicrobial Agents and Chemotherapy, 45 (2001) 1799-1802.

[189] H. W. Boucher, G. Sakoulas, Perspectives on daptomycin resistance, with emphasis on resistance in aureus. Clinical Infectious Diseases, 45 (2007) 601-608.

[190] L. Z. Cui, E. Tominaga, H. M. Neoh, K. Hiramatsu, Correlation between reduced daptomycin susceptibility and vancomycin resistance in vancomycin-intermediate *Staphylococcus aureus*. Antimicrobial Agents and Chemotherapy, 50 (2006) 1079-1082.

[191] D. A. Enoch, J. M. Bygott, M. L. Daly, J. A. Karas, Daptomycin. Journal of Infection, 55 (2007) 205-213.

[192] C. M. Ernst, A. Peschel, Broad spectrum antimicrobial peptide resistance by MprF mediated aminoacylation and flipping of phospholipids. Molecular Microbiology, 80 (2011) 290-299.

[193] T. Jones, M. R. Yeaman, G. Sakoulas, S. J. Yang, R. A. Proctor, H.-G. Sahl, J. Schrenzel, Y. Q. Xiong, A. S. Bayer, Failures in clinical treatment of *Staphylococcus aureus* infection with daptomycin are associated with alterations in surface charge, membrane phospholipid asymmetry, and drug binding. Antimicrobial Agents and Chemotherapy, 52 (2008) 269-278.

[194] A. B. Hachmann, E. Sevim, A. Gaballa, D. L. Popham, H. Antelmann, J. D. Helmann, Reduction in membrane phosphatidylglycerol content leads to daptomycin resistance in *Bacillus subtilis*. Antimicrobial Agents and Chemotherapy, 55 (2011) 4326-4337.

[195] D. R. Cameron, L. I. Mortin, A. Rubio, E. Mylonakis, R. C. Moellering Jr, G. M. Eliopoulos, A. Y. Peleg, Impact of daptomycin resistance on *Staphylococcus aureus* virulence. Virulence, 6 (2015) 127-131.

[196] C. M. Ernst, P. Staubitz, N. N. Mishra, S. J. Yang, G. Hornig, H. Kalbacher, A. S. Bayer, D. Kraus, A. Peschel, The bacterial defensin resistance protein MprF consists of separable domains for lipid lysinylation and antimicrobial peptide repulsion. PLoS pathogens, 11 (2009) 1000660.

[197] A. Peschel, R. W. Jack, M. Otto, L. V. Collins, P. Staubitz, G. Nicholson, H. Kalbacher, W. F. Nieuwenhuizen, G. Jung, A. Tarkowski, K. P. M. van Kessel, J. A. G. van Strijp, *Staphylococcus aureus* resistance to human defensins and evasion of neutrophil killing via the novel virulence factor MprF is based on modification of membrane lipids with L-lysine. Journal of Experimental Medicine, 193 (2001) 1067-1076.

[198] M. E. Winkler, J. A. Hock, Essentiality, bypass, and targeting of YycFG (VicRK) two-component regulatory system in Gram-positive bacteria. Journal of Bacteriology, 190 (2008) 2645-2648.

[199] B. P. Howden, C. R. McEvoy, D. L. Allen, K. Chua, W. Gao, P. F. Harrison, J. Bell, G. Coombs, V. Bennett-Wood, J. L. Porter, R. Robins-Browne, J. K. Davies, T. Seemann, T. P. Stinear, Evolution of multidrug resistance during *staphylococcus aureus* infection involves mutation of the essential two component regulator walkr. PLoS pathogens, 7 (2011) 1002359.

[200] S. Dubrac, I. G. Boneca, O. Poupel, T. Msadek, New insights into the WalK/WalR (YycG/YycF) essential signal transduction pathway reveal a major role in controlling cell wall metabolism and biofilm formation in *Staphylococcus aureus*. Journal of Bacteriology, 189 (2007) 8257-8269.

[201] L. Cui, T. Isii, M. Fukuda, T. Ochiai, H. Neoh, I. L. B. da Cunha Camargo, Y. Watanabe, M. Shoji, T. Hishinuma, K. Hiramatsu, An rpoB mutation confers dual heteroresistance to daptomycin and vancomycin in *Staphylococcus aureus*. Antimicrobial Agents and Chemotherapy, 54 (2010) 5222-5233.

[202] Y. Watanabe, L. Cui, Y. Katayama, K. Kozue, K. Hiramatsu, Impact of rpoB mutations on reduced vancomycin susceptibility in *Staphylococcus aureus*. Journal of Clinical Microbiology, 49 (2011) 2680-2684.

[203] M. Saito, Y. Katayama, T. Hishinuma, A. Iwamoto, Y. Aiba, K. Kuwahara-Arai, L. Cui, M. Matsuo, N. Aritaka, K. Hiramatsu, “Slow VISA,” a novel phenotype of vancomycin resistance, found in vitro in heterogeneous vancomycin-intermediate *Staphylococcus aureus* strain Mu3. Antimicrobial Agents and Chemotherapy, 58 (2014) 5024-5035.

[204] M. Matsuo, T. Hishinuma, Y. Katayama, L. Cui, M. Kapi, K. Hiramatsu, Mutation of RNA polymerase b subunit (rpoB) promotes hVISA-to-VISA phenotypic conversion of strain Mu3. Antimicrobial Agents and Chemotherapy, 55 (2011) 4188-4195.

[205] S. Jordan, A. Junker, J. D. Helmann, T. Mascher, Regulation of LiaRS-dependent gene expression in *Bacillus subtilis*: identification of inhibitor proteins, regulator binding sites, and target genes of a conserved cell envelope stress-sensing two-component system. Journal of Bacteriology, 188 (2006) 5153-5166.

[206] K. Schrecke, S. Jordan, T. Mascher, Stoichiometry and perturbation studies of the LiaFSR system of *Bacillus subtilis*. Molecular Microbiology, 87 (2013) 769-788.

[207] S. Kesel, A. Mader, C. Hofler, T. Mascher, M. S. Leisner, Immediate and heterogeneous response of the LiaFSR two-component system of *Bacillus subtilis* to the peptide antibiotic bacitracin. PLoS One, 8 (2013) e53457.

[208] National committee for clinical laboratory standards. Methods for dilution antimicrobial susceptibility tests for bacteria that grow aerobically- Fourth edition: Approved standard M7-A4. NCCLS, Wayne, PA, USA, 1997.

[209] M. Pinho, J. Errington, Dispersed mode of *Staphylococcus aureus* cell wall synthesis in the absence of the division machinery. Molecular Microbiology, 50 (2003) 871-881.

[210] F. Roder, S. Waichman, D. Paterok, R. Schubert, C. Richter, B. Liedberg, J. Piehler, Reconstitution of membrane proteins into polymer-supported membranes for probing diffusion and interactions by single molecule techniques. Analytical Chemistry, 83 (2011) 6792-6799.

[211] G. Giannone, E. Hosy, Sibarita, J. B. Choquet D, L. Cognet, High content Super-Resolution Imaging of Live Cell by uPAINT. Methods in Molecular Biology, 950 (2013) 95-110.

[212] A. Sharonov, R. M. Hochstrasser, Wide-field subdiffraction imaging by accumulated binding of diffusing probes. Proceedings of the National Academy of Sciences, 103 (2006) 18911-18916.

[213] M. Ovesný, P. Křížek, J. Borkovec, Z. Svindrych, G. M. Hagen, ThunderSTORM: a comprehensive ImageJ plug-in for PALM and STORM data analysis and super-resolution imaging. Bioinformatics, 30 (2014) 2389-2390.

[214] A. Edelstein, N. Amodaj, K. Hoover, R. Vale, N. Struurman, Computer control of microscopes using μmanager. Current Protocols in Molecular Biology, 14 (2012) 20.1-20.17.

[215] D. Axelrod, Total internal reflection fluorescence microscopy in cell biology. Traffic, 2 (2001) 764-774.

[216] J. Hill, J. Siedlecki, I. Parr, et al., Synthesis and biological activity of N-Acylated ornithine analogues of daptomycin. Bioorganic and Medicinal Chemistry Letters, 13 (2003) 4187-4191.

[217] M. D. Abramoff, P. J. Magalhaes, S. J. Ram, Image processing with ImageJ. Biophotonics International, 11 (2004) 36-42

[218] Y. F. Chen, T. L. Sun, Y. Sun, H. W. Huang, Interaction of daptomycin with lipid bilayers: a lipid extracting effect. Biochemistry, 53 (2014) 5384-5392.

[219] T. Zhang, J. K. Muraih, B. MacCormick, M. Palmer, Daptomycin forms cation- and size-selective pores in model membranes, 1838 (2014) 2425-2430.

[220] M. A. Kreutzberger, A. Pokorny, P. Almeida, Daptomycin–Phosphatidylglycero l Domains in Lipid Membranes. Langmuir, 33 (2017) 13669-13679.

[221] R. Yuste, Fluorescence microscopy today. Nature Methods, 2 (2005) 902-904.

[222] C. T. M. Mascio, J. D. Alder, J. A. Silverman, Bactericidal Action of Daptomycin against Stationary-Phase and Nondividing *Staphylococcus aureus* Cells. Antimicrobial Agents and Chemotherapy, 51 (2007) 4255-4260.

[223] M. G. Pinho, J. Errington, Dispersed mode of *Staphylococcus aureus* cell wall synthesis in the absence of the division machinery. Molecular Microbiology, 50 (2003) 871-881.

[224] L. J. Wale, A. P. Shelton, D. Greenwood, Scanning electronmicroscopy of *Staphylococcus aureus* and *Enterococcus faecalis* exposed to daptomycin. Journal of Medical Microbiology, 30 (1987) 45-49.

[225] L. Mortin, T. Li, A. D. Van Praagh, S. Zhang, X. X. Zhang, J. D. Alder, Rapid bactericidal activity of daptomycin against methicillin-resistant and methicillin-susceptible *Staphylococcus aureus* peritonitis in mice as measured with bioluminescent bacteria. Antimicrob Agents Chemother, 51 (2007) 1787-1794.

[226] K. N. Mercer, D. S. Weiss, The *Escherichia coli* Cell Division Protein FtsW Is Required To Recruit Its Cognate Transpeptidase, FtsI (PBP3), to the Division Site. Journal of Bacteriology, 184 (2002) 902-912.

[227] A. O. Henriques, P. Glaser, P. J. Piggot, and C. P. Moran, Control of cell shape and elongation by the *rodA* gene in *Bacillus subtilis*. Molecular Microbiology, 28 (1998) 235-247.

[228] K. Scherer, I. Wiedemann, C. Ciobanasu, H.-G. Sahl, U. Kubitscheck, Aggregates of nisin with various bactoprenol-containing cell wall precursors differ in size and membrane permeation capacity. Biochimica et Biophysica Acta 1828 (2013) 2628–2636.

[229] T. Schneider, T. Kruse, R. Wimmer, I. Wiedemann, V. Sass, U. Pag, A. Jansen, A. K. Nielsen, P. H. Mygind, D. S. Raventós, S. Neve, B, Ravn, A. M. J. J. Bonvin, L. De Maria, A. S. Andersen, L. K. Gammelgaard, H.-G. Sahl, H.-H. Kristensen, Plectasin, a fungal Defensin, targets the bacterial cell wall precursor Lipid II. Science 328 (2010) 1168–72.

[230] H. R. Perkins, M. Nieto, The chemical basis for the action of the vancomycin group of antibiotics. Annals of the New York Academy of Sciences, 235 (1974) 348-363.

[231] N. I. Martin, E. Breukink, The espanding role of lipid II as a target for lantibiotics. Future Microbiology, 2 (2007) 513-525.

[232] B. L. de Jonge, Y. S. Chang, D. Gage, A. Tomasz, Peptidoglycan composition in heterogeneous Tn551 mutants of a methicillin-resistant *Staphylococcus aureus* strain. Journal of Biological Chemistry, 267 (1992) 11255-11259.

[233] L. Cui, E. T. Tominaga, H. M. Neoh, K. Hiramatsu, Correlation between reduced daptomycin susceptibility and vancomycin resistance in vancomycin-intermediate *Staphylococcus aureus*. Antimicrobial Agents and Chemotherapy, 50 (2006) 1079-1082.

[234] S. J. Yang, C. C. Nast, N. N. Mishra, M. R. Yeaman, P. D. Fey, A. S. Bayer, Cell wall thickening is not a universal accompaniment of the daptomycin nonsusceptibility phenotype in *Staphylococcus aureus*: Evidence for Multiple Resistance Mechanisms. Antimicrobial Agents and Chemotherapy, 50 (2010) 3079-3085.

[235] J. K. Murailh, A. Pearson, J. Sliverman, M. Palmer, Oligomerization of daptomycin on membranes. Biochimica et Biophysica Acta, 1808 (2011) 1154-1160.

[236] B. D. Cain, P. J. Norton, W. Eubanks, H. S. Nick, M. A. Charles, Amplification of the bacA Gene Confers Bacitracin Resistance to *Escherichia coli*. Journal of Bacteriology, 175 (1993) 3784-3789.

[237] S. J. Kim, L. Cegelski, D. Stueber, M. Singh, E. Dietrich, K. S. E. Tanaka, A. R. Far, J. Schaefer, Oritavancin exhibits dual mode of action to inhibit cell-wall biosynthesis in *Staphylococcus aureus*. Journal of Molecular Biology, 377 (2008) 281-293

[238] A. B. Hachmann, E. R. Angert, J. D. Helmann, Genetic analysis of factors affecting susceptibility of *Bacillus subtilis* to daptomycin. Antimicrobial Agents and Chemotherapy, 53 (2009) 1598-1609.

[239] J. A. F. Op den Kamp, L. L. M. Van Deenen, Phospholipid composition of Bacillus subtilis. Journal of Bacteriology, 99 (1969) 298-303

[240] G. M. Eliopoulos, C. Thauvin, B. Gerson and R. C. Moellering Jr, In vitro activity and mechanism of action of A21978C1, a novel cyclic lipopeptide antibiotic. Antimicrobial Agents and Chemotherapy, 27 (1985) 357-362